

Functionalized quinolizinium-based fluorescent reagents for modification of cysteine-containing peptides and proteins

Karen Ka-Yan Kung,^{a,b} Cai-fung Xu,^a Wa-Yi O,^{a,b} Qiong Yu,^a Sai-Fung Chung,^c Suet-Ying Tam,^c
Yun-Chung Leung,^{*c} and Man-Kin Wong^{*a,b}

^a The Hong Kong Polytechnic University Shenzhen Research Institute, Shenzhen, 518057,
China.

^b State Key Laboratory of Chemical Biology and Drug Discovery, and Department of Applied
Biology and Chemical Technology, The Hong Kong Polytechnic University, Hung Hom,
Hong Kong, China.

^c Henry Cheng Research Laboratory for Drug Development and Lo Ka Chung Centre for
Natural Anti-Cancer Drug Development, The Hong Kong Polytechnic University,
Hung Hom, Hong Kong, China.

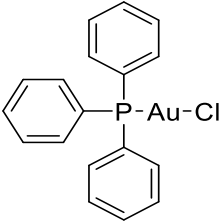
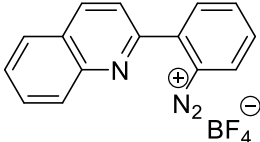
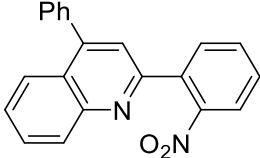
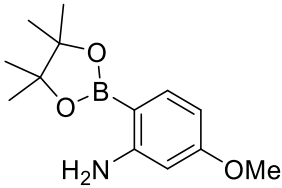
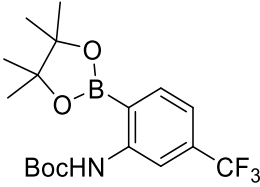
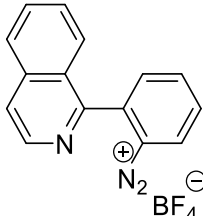
E-mail: mankin.wong@polyu.edu.hk;
thomas.yun-chung.leung@polyu.edu.hk

Supporting Information

Table of Content

Literature References	S3
General Procedures	S4
ESI-MS Analysis of Peptide Modification	S5
ESI-MS Analysis of Protein Modification	S5
Calculation of Peptide Conversion	S5
Calculation of Protein Conversion	S8
Synthesis of Compounds	S13
Photophysical Properties of Compounds	S17
Procedure of Peptide Modification	S18
Procedure of Protein Modification.....	S18
Procedure for SDS-PAGE Analysis	S18
Procedure for Trypsin Digestion	S18
Procedure for Site-Directed Mutagenesis of BCArg	S19
Mutated BCArg Peptide Sequence	S21
Enzyme Activity	S21
Inhibition of <i>in vitro</i> Cancer Cell Proliferation	S21
¹ H and ¹³ C NMR Spectra	S22
LC-MS and LC-MS/MS of Peptides	S36
LC-MS and LC-MS/MS of Proteins	S64
UV/Visible Absorption Spectra of Quinolizinium Compounds	S82
Supplementary References	S90

Literature References

 <p style="text-align: center;">AuPPh₃Cl</p>	<p>K. Nunokawa, S. Onaka, T. Tatematsu, M. Ito and J. Sakai, <i>Inorg. Chim. Acta</i>, 2001, 322, 56-64.</p>
 <p style="text-align: center;">3a</p>	<p>J.-R. Deng, W.-C. Chan, N. Chun-Him Lai, B. Yang, C.-S. Tsang, B. Chi-Bun Ko, S. Lai-Fung Chan, M.-K. Wong, <i>Chem. Sci.</i>, 2017, 8, 7537–7544.</p>
 <p style="text-align: center;">3b'</p>	<p>J. Tang, L.-M. Wang, D. Mao, W.-B. Wang, L. Zhang, S.-Y. Wu, Y.-S. Xie, <i>Tetrahedron</i>, 2011, 67, 8465–8469.</p>
	<p>(1) F. Zhou and T. G. Driver, <i>Org. Lett.</i> 2014, 16, 2916–2919. (2) Yan, L., Che, X., Bai, X. <i>et al. Mol. Divers.</i> 2012, 16, 489–501.</p>
	<p>(1) H.-Y. Li, J. Horn, A. Campbell, D. House, A. Nelson and S. P. Marsden, <i>Chem. Commun.</i> 2014, 50, 10222-10224. (2) Yan, L., Che, X., Bai, X. <i>et al. Mol. Divers.</i> 2012, 16, 489–501.</p>
 <p style="text-align: center;">3e</p>	<p>J.-R. Deng, W.-C. Chan, N. Chun-Him Lai, B. Yang, C.-S. Tsang, B. Chi-Bun Ko, S. Lai-Fung Chan, M.-K. Wong, <i>Chem. Sci.</i>, 2017, 8, 7537–7544.</p>

General Procedures

All reagents were commercially available and used without further purification. All peptides (>98% purity) were directly purchased from GL Biochem (Shanghai) Ltd. BSA, HSA and lysozyme were purchased from Sigma Aldrich and used without further purification. Milli-Q® water used as reaction solvent in peptide and protein modification, as well as LC-MS analysis, was deionised using a Milli-Q® Gradient A10 system (Millipore, Billerica, USA). Flash column chromatography was performed using silica gel 60 (230-400 mesh ASTM) with ethyl acetate/n-hexane or methanol/dichloromethane as eluent. All NMR spectra were recorded on a Bruker DPX-400 spectrometer. All chemical shifts are quoted on the scale in ppm using TMS or residual solvent as the internal standard. Coupling constants (J) are reported in Hertz (Hz) with the following splitting abbreviations: s = singlet, br s = broad singlet, d = doublet, dd = double doublet, t = triplet and m = multiplet. All mass spectra were obtained on an ESI source of Agilent 6540 Ultra High Definition (UHD) Accurate-Mass Q-TOF LC/MS systems in the positive and negative ion modes.

All the photochemical experiments were performed custom-made “lightbox” with 4 reaction vessels surrounded by 16 blue LED light bulbs. The temperature was maintained by a fan attached to “lightbox”. A voltage transformer was connected with the blue LEDs and employed to monitor the power of the light source ($P = U \times I = 14.3 \text{ V} \times 2.3 \text{ A} = 32.9 \text{ W}$). 4 reactions were performed in the “lightbox” every time for measurement of the reaction yields. The emission spectra of the blue LEDs revealed a maximum emission wavelength of the light source at $\lambda_{\text{max}} = 468 \text{ nm}$ (Figure S1).¹

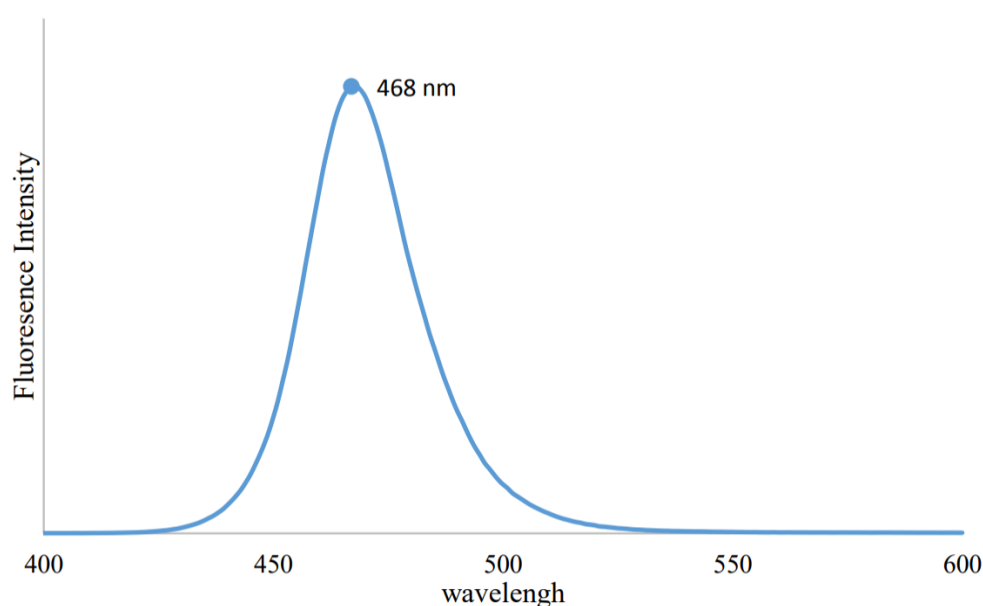


Figure S1. Emission spectrum of the Blue LEDs light source.

ESI-MS Analysis of Peptide Modification

LC-MS analyses for peptide identification were performed by using an Agilent 6540 UHD Accurate-Mass Q-TOF LC/MS system equipped with an ion spray source and an Agilent 1290 Infinity LC, using an Agilent ZORBAX RRHD SB300-C18 (1.8 μm , 2.1 x 100 mm) column. 3 μL of the sample was injected with a flow rate of the flow rate was 0.2 mL/min. Mobile phase A was made of Milli-Q[®] water containing 0.1% formic acid. Mobile phase B was made of HPLC grade acetonitrile containing 0.1% formic acid. The initial conditions for separation were 5% B for 3 min, followed by a linear gradient to 95% B by 22 min. The composition was maintained for 1 min, followed by a linear gradient to 5% B by 1 min. The composition was maintained for 4 min. Operating conditions optimized for the detection of the reaction mixture were the following: Gas temperature: 380 °C, Drying gas: 8 L/min, Nebulizer: 35 psig, Sheath gas temperature: 270 °C, Sheath gas flow: 11 L/min, VCap: 3500 V, Nozzle voltage: 1000 V.

ESI-MS Analysis of Protein Modification

LC-MS analyses for protein identification were performed by using an Agilent 6540 UHD Accurate-Mass Q-TOF LC/MS system equipped with an ion spray source and an Agilent 1290 Infinity LC, using an Agilent ZORBAX RRHD SB300-C3 (1.8 μm , 2.1 x 100 mm) column. 3 μL of the sample was injected with a flow rate of the flow rate was 0.3 mL/min. Mobile phase A was made of Milli-Q[®] water containing 0.1% formic acid. Mobile phase B was made of HPLC-grade acetonitrile containing 0.1% formic acid. The initial conditions for separation were 5% B for 2 min, followed by a linear gradient to 95% B by 12 min. The composition was maintained for 1 min, followed by a linear gradient to 5% B by 0.1 min. The composition was maintained for 1.9 min. Operating conditions optimized for the detection of the reaction mixture were the followings: Gas temperature: 320 °C, Drying gas: 8 L/min, Nebulizer: 45 psig, Sheath gas temperature: 380 °C, Sheath gas flow: 11 L/min, VCap: 3500 V, Nozzle voltage: 1000 V.

Calculation of Peptide Conversion

The crude reaction mixture of unmodified peptide (starting) and modified peptide (product) was subjected to LC-MS analysis with elution time of 31 min. After data processing by Agilent MassHunter software, peptide conversion at different time intervals was determined by measuring the peak areas of starting and product in the total ion chromatogram (TIC) and extracted ion chromatogram (XIC) as follows:

Equation 1

$$\text{Peptide Conversion (\%)} = \left(\frac{\text{Peak Area of Product}}{\text{Peak Areas of Starting and Product}} \right) \times 100\%$$

1a-modified STSSSCNLSK was used as an example of the calculation of the peptide conversion. After integrating the peak areas of STSSSCNLSK, **1a**-modified STSSSCNLSK and dimerized STSSSCNLSK, **1a**-modified STSSSCNLSK and dimerized STSSSCNLSK were afforded in 89% and 6% conversions, respectively (Figure S2). The above method for calculating the peptide conversion has been used in all the bioconjugation reactions of peptides.

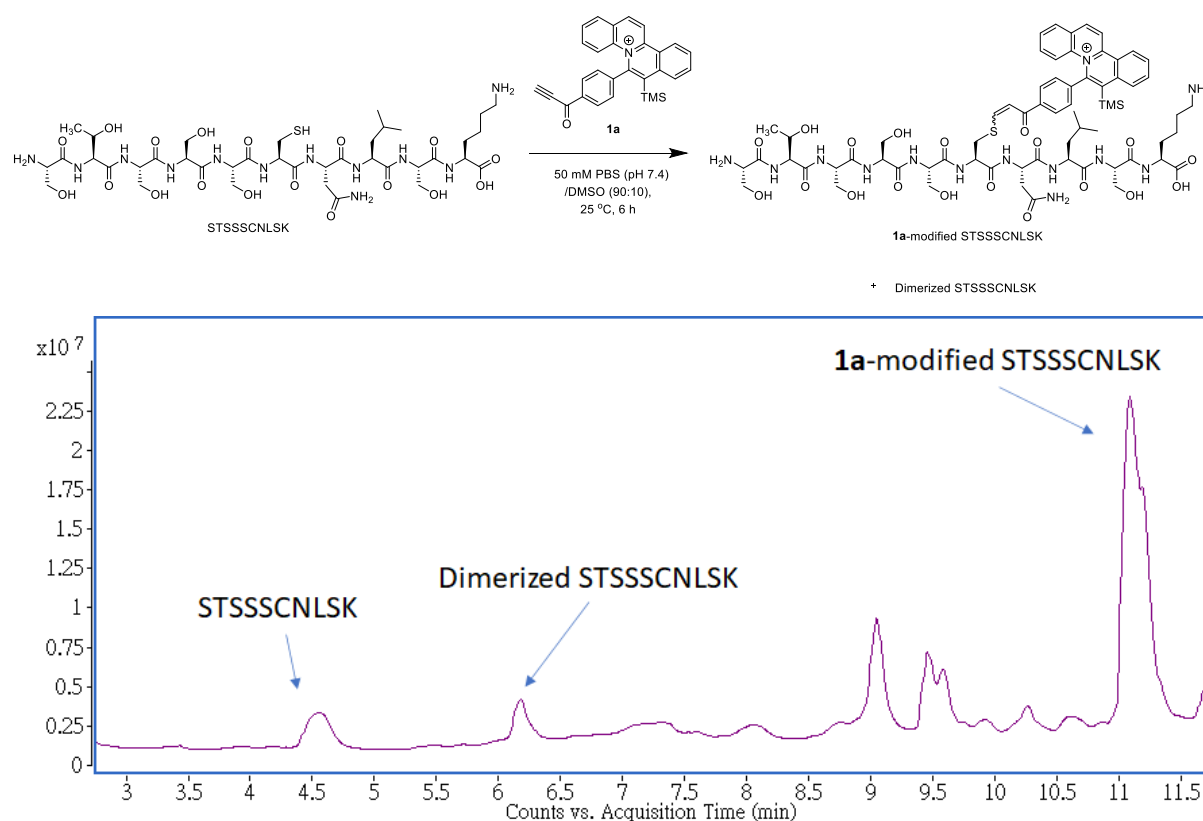


Figure S2. Modification of peptide STSSSCNLSK with quinolizinium **1a** in 50 mM pH 7.4 PBS buffer/DMSO (90:10) for 6 h (Top). Total ion chromatogram for crude reaction mixture of **1a**-modified STSSSCNLSK (Bottom).

Table S1. Expected and observed masses of the modified peptides.

Modified Peptide	Expected Mass [M]⁺	Observed Mass [M]⁺
1a -modified STSSCNLCK	1442.6117	1442.60
1b -modified STSSCNLCK	1518.6430	1518.66
1c -modified STSSCNLCK	1472.6223	1472.62
1d -modified STSSCNLCK	1457.6223	1457.62
1e -modified STSSCNLCK	1533.6539	1533.66
1f -modified STSSCNLCK	1487.6332	1487.64
1g -modified STSSCNLCK	1525.6100	1525.61
1h -modified STSSCNLCK	1457.6226	1457.62
1a -modified AYEMWCFHQR	1799.7318	1799.74
1b -modified AYEMWCFHQR	1875.7631	1875.77
1c -modified AYEMWCFHQR	1829.7423	1829.75
1d -modified AYEMWCFHQR	1814.7427	1814.74
1e -modified AYEMWCFHQR	1890.7740	1890.78
1f -modified AYEMWCFHQR	1844.7532	1844.75
1g -modified AYEMWCFHQR	1882.7300	1882.73
1h -modified AYEMWCFHQR	1814.7427	1814.74
1a -modified AYEMWCFHQK	1771.7256	1771.71
1d -modified AYEMWCFHQK	1786.7441	1786.71
1h -modified AYEMWCFHQK	1786.7441	1786.71
1a -modified CSKFR	1069.4784	1069.48
1d -modified CSKFR	1084.4893	1084.49
1h -modified CSKFR	1084.4893	1084.49
1a -modified KSTFC	1014.4250	1014.42
1d -modified KSTFC	1029.4359	1029.43
1h -modified KSTFC	1029.4359	1029.43
1a -modified ASCGTN	981.3631	981.35
1d -modified ASCGTN	996.3740	996.37
1h -modified ASCGTN	996.3740	996.37

Calculation of Protein Conversion²

The crude reaction mixture of unmodified protein (starting) and modified protein (product) was subjected to LC-MS analysis with an elution time of 15 min. After data processing by Agilent MassHunter software, protein conversion at different time intervals was determined by measuring the peak areas of starting and product in the total ion chromatograms and extracted ion chromatograms as follows:

Equation 2

$$\text{Protein Conversion (\%)} = \left(\frac{\text{Peak Area of Product}}{\text{Peak Areas of Starting and Product}} \right) \times 100\%$$

1a-modified BSA was used as an example of the calculation of the protein conversion. After integrating the peak areas of BSA and **1a**-modified BSA, the protein conversion was found to be 74% for **1a**-modified BSA (1 equiv. of **1a** used) in 50 mM PBS (pH 7.4/DMSO (95:5) (Figure S3). The above method for calculating the protein conversion has been used for all the bioconjugation reactions of proteins.

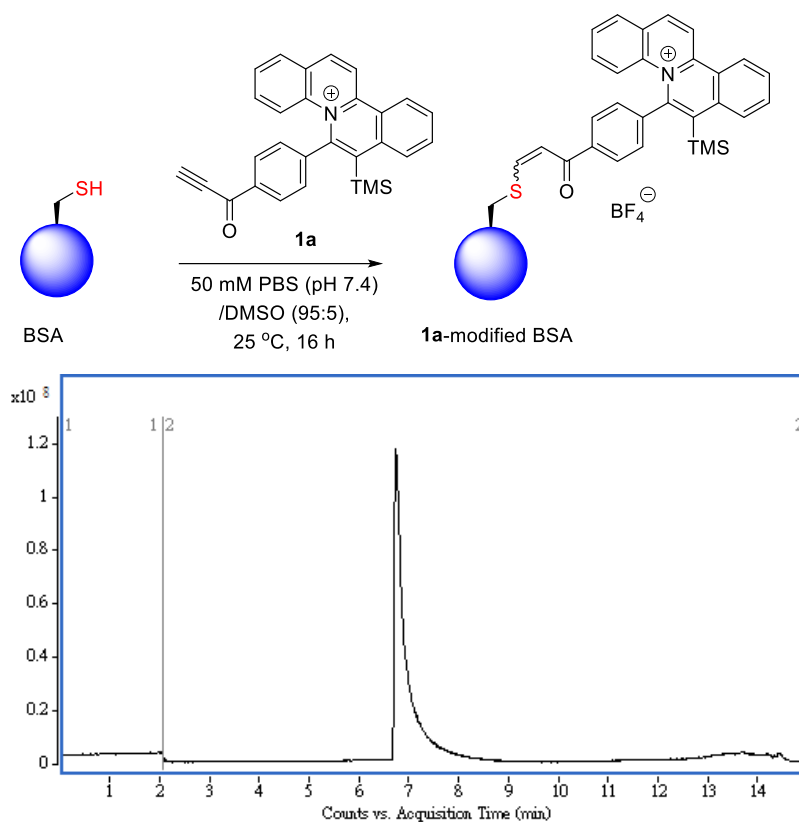


Figure S3. Modification of BSA with quinolizinium **1a** (1 equiv. of **1a** used) in 50 mM PBS buffer (pH 7.4) /DMSO (95:5) for 16 h (Top). Total ion chromatogram for crude reaction mixture of **1a**-modified BSA (Bottom).

The protein conversion measurement in the present bioconjugation by LC-MS analysis was investigated. Prior to LC-MS analysis, total protein concentrations of unmodified BSA and **1a**-modified BSA (1 equiv. of **1a** used) were found to be 6.124 mg/mL and 6.688 mg/mL BSA, respectively, by A280 assay using Thermo Scientific NanoDrop One. UV spectrum of **1a**-modified BSA was shown to be similar to that of BSA (Figure S4). Then, 0%, 25%, 50%, 75% and 100% of **1a**-modified BSA were prepared by pipetting different concentration ratios of BSA and **1a**-modified BSA and then subjected to LC-MS analysis. The protein conversions of 0%, 25%, 50%, 75% and 100% of **1a**-modified BSA were found to be 0%, 31%, 39%, 59% and 74% as determined by the extracted ion chromatograms (i.e. m/z 1385.00 for BSA; m/z 1393.94 for **1a**-modified BSA) using Equation 2. The corresponding deconvolution mass spectra were shown in Figure S5. A graph of conversion (%) by the extracted ion chromatogram (XIC) versus % of **1a**-modified BSA by A280 assay was plotted and showed good linearity with $R^2 = 0.975$ (Figure S6). Thus, Equation 2 is adopted for the determination of protein conversion.

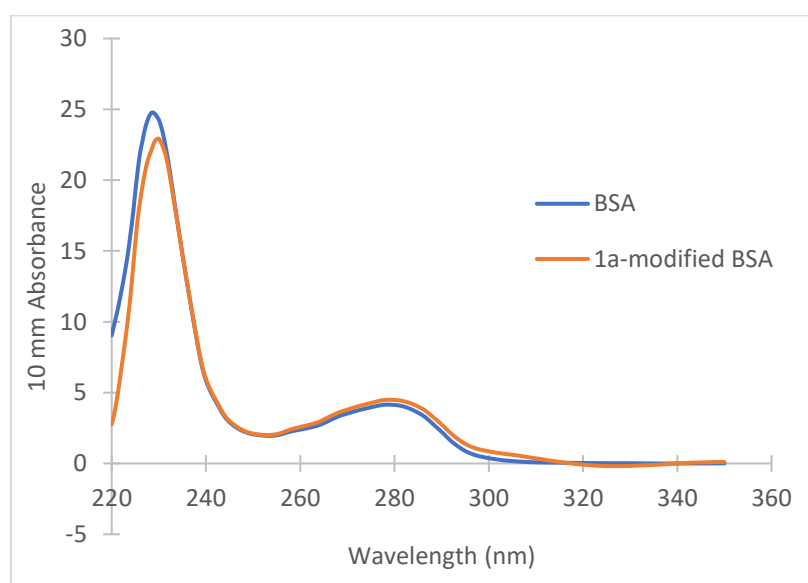


Figure S4. UV spectra of BSA and **1a**-modified BSA (1 equiv. of **1a** used) in Thermo Scientific NanoDrop One.

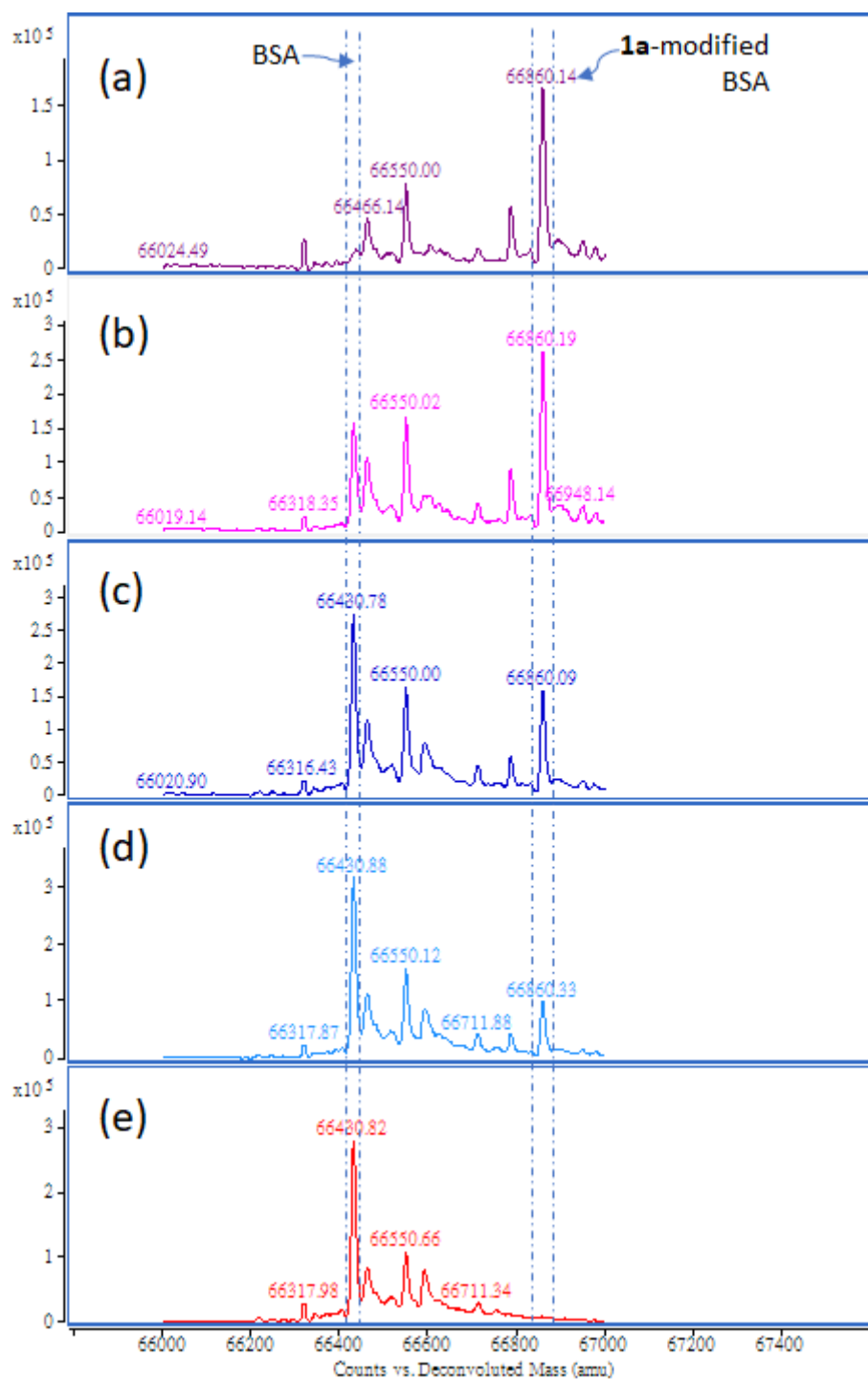


Figure S5. Deconvolution mass spectra of (a) 100%, (b) 75%, (c) 50%, (d) 25% and (e) 0% of 1a-modified BSA (1 equiv. of 1a used).

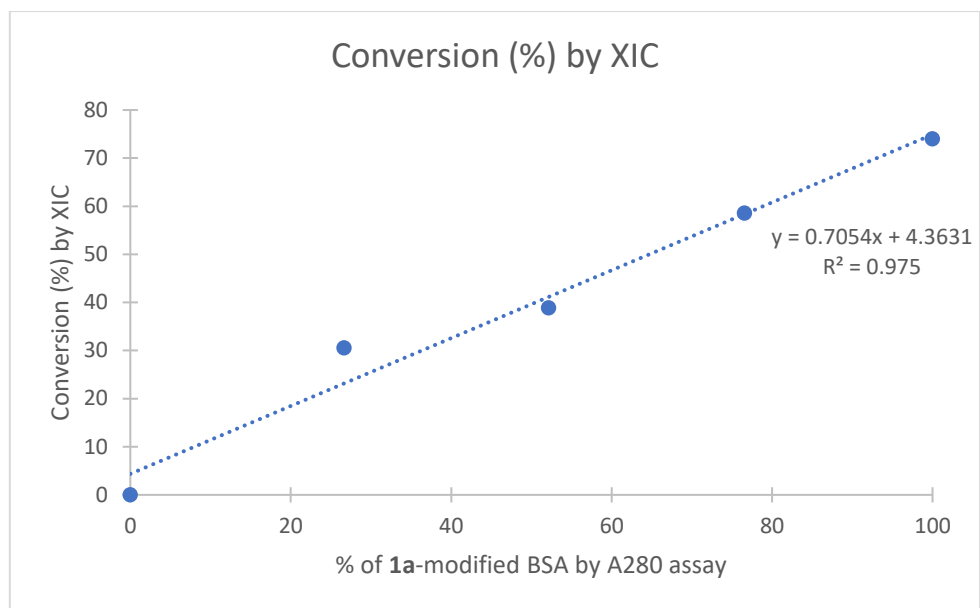
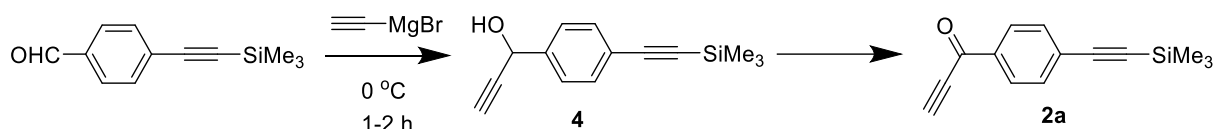


Figure S6. A graph of conversion (%) by XIC versus % of **1a**-modified BSA (1 equiv. of **1a** used) by A280 assay.

Table S2. Expected and observed masses of the modified proteins.

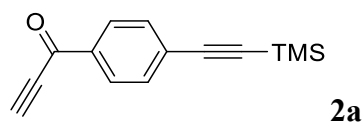
Modified Protein	Expected Mass [M]⁺	Observed Mass [M]⁺
1a -modified BSA	66861	66861
1b -modified BSA	66952	66952
1d -modified BSA	66876	66876
1e -modified BSA	66952	66952
1h -modified BSA	66876	66876
1a -modified HSA	66871	66870
1b -modified HSA	66947	66947
1d -modified HSA	66886	66883
1e -modified HSA	66962	66961
1h -modified HSA	66886	66884
1a -modified BCArg mutant	32878	32878
1b -modified BCArg mutant	32954	32954
1d -modified BCArg mutant	32893	32892
1e -modified BCArg mutant	32969	32969
1h -modified BCArg mutant	32893	32893

Synthesis of Compound 2a



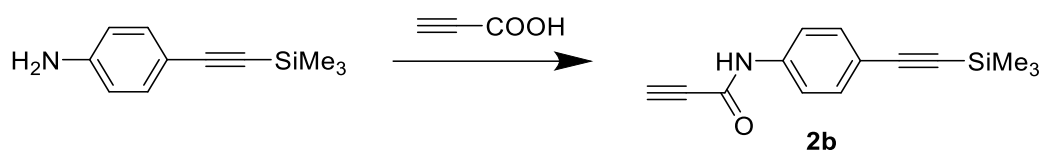
A solution of 4-[(trimethylsilyl)ethynyl]benzaldehyde (500 mg, 3 mmol) and ethynylmagnesium bromide solution (21 mL, 10.5 mmol) in 20 mL of anhydrous THF was stirred at $0\text{ }^\circ\text{C}$ for 1 h. 5 mL of H_2O was carefully added to the reaction mixture to quench the reaction. After evaporation of THF, the resulting solution was acidified with 10% H_2SO_4 . The reaction mixture was extracted with EtOAc ($3 \times 20\text{ mL}$). The combined organic layer was dried over anhydrous MgSO_4 , filtered, and concentrated under reduced pressure. The residue was purified by flash column chromatography (EtOAc/n-hexane) to give product 4.

A solution of 4 (98 mg, 0.46 mmol), chromium (VI) oxide (92 mg, 0.92 mmol) and CH_3COOH (276 mg, 4.6 mmol) in 5 mL of acetone was stirred at $0\text{ }^\circ\text{C}$ for 3 h. After the reaction, the residue was filtered by Celite, evaporated and then purified by flash column chromatography in ethyl acetate/n-hexane to give product 2a.

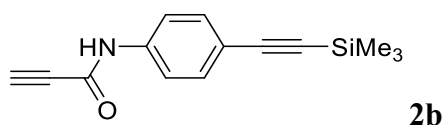


White solid, 43% yield. $^1\text{H NMR}$ (400 MHz, CDCl_3) δ 8.07 (d, $J = 8.3\text{ Hz}$, 2H), 7.55 (d, $J = 8.3\text{ Hz}$, 2H), 3.47 (s, 1H), 0.26 (s, 9H). $^{13}\text{C NMR}$ (100 MHz, CDCl_3) δ 176.65, 135.64, 132.33, 129.65, 104.04, 99.67, 81.44, 80.34, 77.47, 77.26, 77.05, 0.19, 0.00, -0.19. **HRMS** (ESI) m/z calcd. for $\text{C}_{14}\text{H}_{15}\text{OSi}^+ [\text{M} + \text{H}]^+$ 227.0887, found 227.0885.

Synthesis of Compound 2b

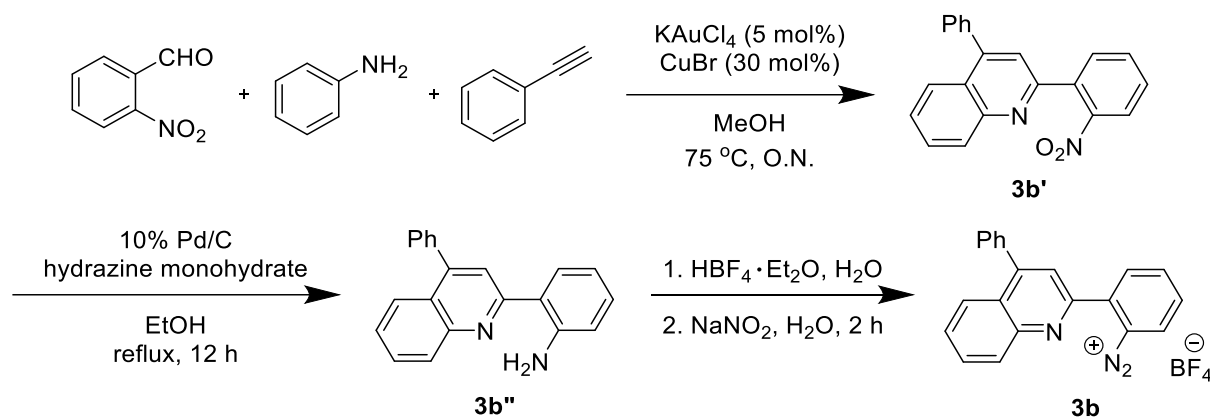


Under nitrogen atmosphere, 4-(2-trimethylsilylethynyl)aniline (100 mg, 0.34 mmol) was dissolved in anhydrous dichloromethane (20 mL) and then cooled down to 0 °C by placing the reaction flask into an ice-water bath. Propiolic acid (48 mg, 0.68 mmol), N,N'-dicyclohexylcarbodiimide (DCC) (140 mg, 0.68 mmol) and 4-di(methylamino)pyridine (DMAP) (1 mg, a catalytic amount) were added to the reaction mixture. The reaction mixture was stirred for 16 h. After evaporation of the solvent, and removing the white particulate by filtration, the residue was purified by flash column chromatography in ethyl acetate/n-hexane to afford product **2b**.



White solid, 70% yield. $^1\text{H NMR}$ (400 MHz, CDCl_3) δ 7.82 (s, 1H), 7.48 (d, $J = 8.7$ Hz, 2H), 7.42 (d, $J = 8.7$ Hz, 2H), 2.94 (s, 1H), 0.24 (s, 9H). $^{13}\text{C NMR}$ (100 MHz, CDCl_3) δ 149.71, 137.21, 132.98, 119.90, 119.62, 104.60, 94.54, 77.56, 74.65, 0.08. **HRMS** (ESI) m/z calcd. for $\text{C}_{14}\text{H}_{16}\text{NOSi}^+$ $[\text{M} + \text{H}]^+$ 242.0996, found 242.0993.

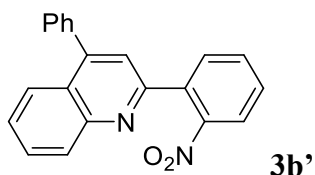
Synthesis of Aryl Diazonium **3b**.



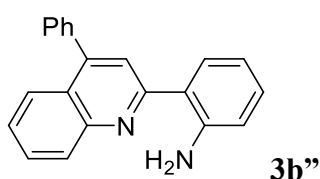
A mixture of 2-nitrobenzaldehyde (10 mmol, 1 equiv.), aniline (12 mmol, 1.2 equiv.), phenylacetylene (12 mmol, 1.2 equiv.), KAuCl_4 (5 mol%) and CuBr (30 mol%) in 20 mL of methanol were heated in a 50 mL round bottom flask at $40\text{ }^\circ\text{C}$ under nitrogen overnight. The solvent was removed by evaporation under reduced pressure, and the residue was purified by flash column chromatography using ethyl acetate/n-hexane as eluent to give compound **3b'**.

An ethanol suspension (20 mL) of compound **3b'** (1 mmol, 326 mg) was heated to $50\text{ }^\circ\text{C}$ in the presence of 10 mg of 10% Pd/C , and 0.3 mL of hydrazine monohydrate was added over 30 min to this suspension. The reaction mixture became clear as the reaction proceeded. It was kept at reflux for another 12 h. Upon completion of the reaction, the mixture was filtered over Celite to remove the Pd/C catalyst. The ethanol was removed under reduced pressure. The crude product was purified by flash column chromatography using ethyl acetate/n-hexane as eluent to afford compound **3b''**.

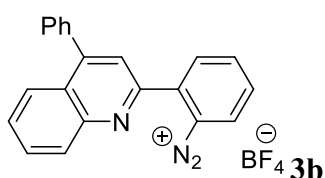
Under an ice-water bath, a solution of anilines **3b''** (5 mmol, 1 equiv.) in 5 mL of H_2O in a 25 mL round bottom flask was treated with tetrafluoroboric acid $\text{HBF}_4 \cdot \text{Et}_2\text{O}$ (0.82 mL, 1.2 equiv.) by dropwise addition. After that, NaNO_2 (0.52 g, 1.5 equiv.) was dissolved in 3.5 mL of H_2O and dropwise added into the reaction mixture. The resulting mixture was stirred at room temperature for 3 h. Then, the mixture was filtered, and the solid was stepwise washed by ethanol and followed by diethyl ether and further collected as products **3b**.



Brownish yellow oil, 75% yield. **¹H NMR** (400 MHz, CDCl₃) δ 8.15 (d, *J* = 8.4 Hz, 1H), 7.92 (s, 2H), 7.72 (s, 2H), 7.64 (t, *J* = 7.5 Hz, 1H), 7.55 – 7.42 (m, 9H). **¹³C NMR** (100 MHz, CDCl₃) δ 155.14, 149.31, 149.22, 148.47, 137.71, 135.71, 132.71, 131.66, 130.05, 129.86, 129.61, 129.45, 129.24, 128.65, 127.13, 125.76, 125.74, 124.53, 120.76, 118.41, 115.06. **HRMS** (ESI) *m/z* calcd. for C₂₁H₁₄N₂O₂ [M + Na]⁺ 349.0947, found 349.1001.



Brown oil, 99% yield. **¹H NMR** (400 MHz, CDCl₃) δ 8.17 (d, *J* = 8.4 Hz, 1H), 7.92 (d, *J* = 8.4 Hz, 1H), 7.81 (s, 1H), 7.74 (t, *J* = 7.4 Hz, 2H), 7.61 – 7.47 (m, 6H), 7.24 (t, *J* = 7.8 Hz, 1H), 6.90 – 6.80 (m, 2H). **¹³C NMR** (100 MHz, CDCl₃) 158.84, 149.11, 147.56, 147.45, 138.43, 130.39, 129.93, 129.62, 129.54, 129.27, 128.66, 128.46, 126.23, 125.67, 125.03, 121.63, 120.87, 117.51, 117.40. **HRMS** (ESI) *m/z* calcd. for C₂₁H₁₆N₂ [M + H]⁺ 297.1386, found 298.1380.



Yellow powder, 45% yield. **¹H NMR** (400 MHz, DMSO-*d*₆) δ 8.98 (d, *J* = 8.1 Hz, 1H), 8.93 (d, *J* = 8.0 Hz, 1H), 8.45 (s, 1H), 8.43 – 8.34 (m, 2H), 8.15 (t, *J* = 7.8 Hz, 1H), 8.01 (t, *J* = 7.7 Hz, 2H), 7.81 (t, *J* = 7.6 Hz, 1H), 7.73 – 7.60 (m, 5H). **¹³C NMR** (101 MHz, DMSO-*d*₆) δ 151.35, 148.20, 146.01, 140.67, 140.51, 137.07, 136.51, 132.59, 131.79, 129.82, 129.53, 129.09, 128.13, 127.97, 126.30, 126.09, 119.14, 118.94, 115.86, 40.15, 39.94, 39.73, 39.52, 39.31, 39.10, 38.89. **HRMS** (ESI) *m/z* calcd. for C₂₁H₁₄N⁺ [M - N₂ - BF₄]⁺ 280.1121, found 280.1047.

Photophysical Properties of Compounds

The absorption and emission spectra were measured by Cary 8454 UV-Vis Diode Array System and Cary Eclipse Fluorescence Spectrophotometer, respectively, and each quinolizinium compound in CH₂Cl₂ was diluted in CH₂Cl₂ prior to measurement. The excitation slit and emission slit for emission measurement were set at 5 nm with scan rate at 120 nm/min and medium PMT voltage. Fluorescent quantum yield of each compound was determined by a comparative method employing fluorescein ($\Phi = 0.95$ in 0.1 N NaOH solution) as standard and calculated with the following equation.³

Equation 3

$$\Phi_{sample} = \Phi_{standard} \times \left(\frac{Grad_{sample}}{Grad_{standard}} \right) \times \left(\frac{n_{sample}}{n_{standard}} \right)^2$$

Where Φ is the fluorescence quantum yield, Grad the gradient from the plot of integrated fluorescence intensity vs absorbance, and n is the refractive index of the solvent.

Table S3. Photophysical properties of compounds **1a-1h**.^a

Compound	λ_{ex} (nm)	λ_{em} (nm)	Stokes Shift (cm ⁻¹)	Quantum Yield (Φ_F) ^b	Molar Absorptivity (ϵ) (M ⁻¹ cm ⁻¹)
1a	422	482	2950	0.22	10200
1b	435	512	3457	0.20	9900
1c	412	478	3351	0.11	15700
1d	430	555	5238	0.10	6900
1e	445	550	4290	0.22	7400
1f	425	517	4187	0.12	10200
1g	440	550	4545	0.05	5300
1h	405	498	4611	0.21	9200

^a Absorption and emission properties were measured in CH₂Cl₂ at concentration of μ M level. ^b Quantum yields were measured using coumarin 153 ($\Phi_F = 0.54$ in EtOH) as a standard.

Procedure of Peptide Modification

A mixture of 10 μ L of cysteine-containing peptides (1 mM in H₂O), 10 μ L of quinolininiums **1a–h** (1 mM in DMSO) and 80 μ L of 50 mM pH 7.4 PBS buffer was treated in a 1.5 -mL Eppendorf tube at 25 °C for 6 h. The modified product was characterized by LC-MS and LC-MS/MS analysis.

Procedure of Protein Modification

A mixture of 10 μ L of proteins (1 mM in 50 mM pH 7.4 PBS buffer), 5 μ L of compound **1a, 1b, 1d, 1e** or **1h** (4 mM in DMSO) and 85 μ L of 50 mM pH 7.4 PBS buffer was treated in a 1.5 -mL Eppendorf tube at 25 °C for 16 h. The modified proteins were purified by Bio-Rad Bio-Spin® 6 column prior to SDS-PAGE, LC-MS (and LC-MS/MS) analysis and trypsin digestion. For the BCArg mutant, 20 mM Tris-HCl buffer pH 7.4 was used instead of 50 mM pH 7.4 PBS buffer.

As shown in Figures S62 and S73, the spectra depict several peaks that are assigned to the commercially available BSA (66433 Da) and HSA (66441 Da), and to the corresponding post-translational modification (PTMs) products, which are attributed to the cysteinylolation of Cys34 (66553 Da and 66560 Da, respectively) and non-enzymatic glycation (66723 Da) of HSA.⁴

Procedure for SDS-PAGE Analysis

Protein conjugates (10 μ L) were mixed with 2X loading buffer (10 μ L) in a 0.5 mL Eppendorf tube and then boiled at 100 °C water bath for 5 min. Samples were analyzed by SDS-PAGE by loading a sample of the boiled solution (10 μ L) in each lane of a 15% SDS-PAGE gel and running in a Mini-PROTEAN Tetra Cell (Bio-Rad, USA) at 150 V at room temperature until the front of the dye reached the bottom of the gel. After SDS-PAGE separation, the protein conjugates were visualized at UV 472 nm with Azure C600 Gel Imaging System and finally stained with Coomassie blue.

Procedure for Trypsin Digestion

A ratio of 1:50 (w/w) and 1:100 of trypsin (V5280, Promega) to BSA (or HSA) was used for the trypsin digestion of protein conjugates. The reaction mixture was incubated at 37 °C for 24 h and the trypsin-digested mixture was quenched by adding TFA or formic acid to a final concentration of 1% for LC-MS/MS analysis.

In some cases, BCArg mutant did not generate useful peptide sequences after trypsin digestion. Thus, chymotrypsin was required to promote protein cleavage. A ratio of 1:10:25 (w/w/w) and 1:10:50 of trypsin (V5280, Promega), chymotrypsin (V1062, Promega) and BCArg mutant was used for the trypsin digestion of protein conjugates. The reaction mixture was incubated at 37 °C for 24 h and the trypsin-digested mixture was quenched by adding formic acid to a final concentration of 1% for LC-MS/MS analysis.

Procedure for Site-Directed Mutagenesis of BCArg

A Cys161 was mutated on Ser161 of BCArg mutant following the procedures as shown below.

Cloning

The BCArg mutant plasmid was constructed following the procedures depicted in the patent.⁵

Protein Expression and Purification

DNA plasmid pET3a/BCArg mutant was transformed into competent *E.coli* BL21 (DE3) and the cells were incubated in a Lysogeny broth (LB) plate containing 100 µg/ml ampicillin at 37 °C overnight. Glycerol stocks were prepared with 18% glycerol and stored at -80 °C. BCArg mutant proteins were expressed in pET3a plasmid containing strong T7 promoter by 0.06% lactose induction at 30 °C for 18 h. Cells were collected by centrifugation and the cell pellet was lysed by an ultrasonic homogenizer (QSonica sonicators) in resuspension buffer (1 mM MnCl₂, 20 mM Tris buffer, pH 7.4). The crude cell lysates were centrifuged at 16,000 rpm for 2 hours at 4 °C. The clarified supernatant was incubated with 10 mM MnCl₂ at 74 °C for 15 min and any white precipitates formed were removed by centrifugation. Proteins were buffer exchanged into binding buffer (20 mM Tris buffer, pH 7.0) and then applied to HiTrap Q HP (GE Healthcare) column. The target proteins bound on the column were eluted by 30% step elution buffer (1 M NaCl/20 mM Tris buffer, pH 7.0). Proteins were buffer exchanged to 20 mM Tris buffer, pH 7.0 and stored in 4 °C.

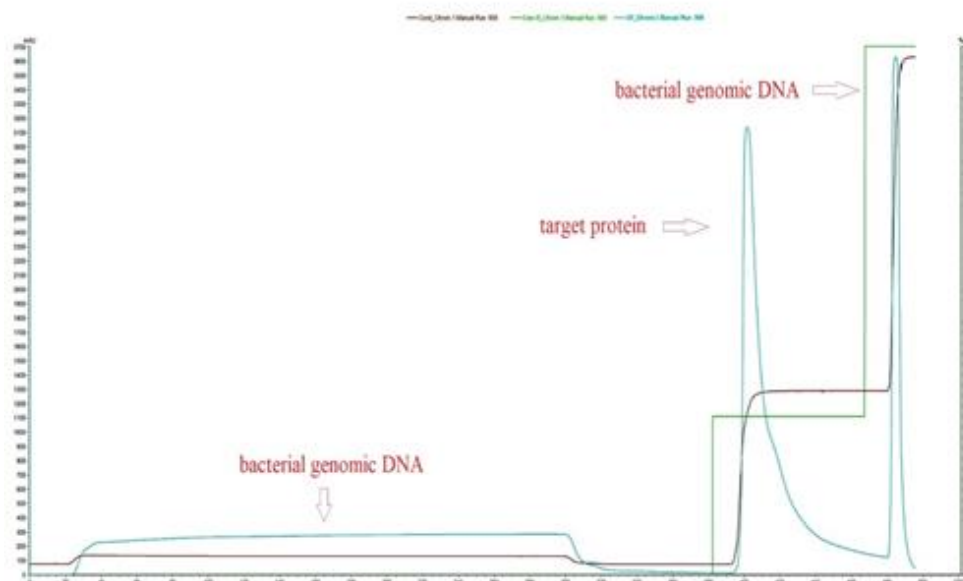


Figure S7. Chromatogram of BCArg mutant purification by Q column. The target protein was collected by 30% elution buffer and bacterial genomic DNA was removed in the flow-through and 100% elution.

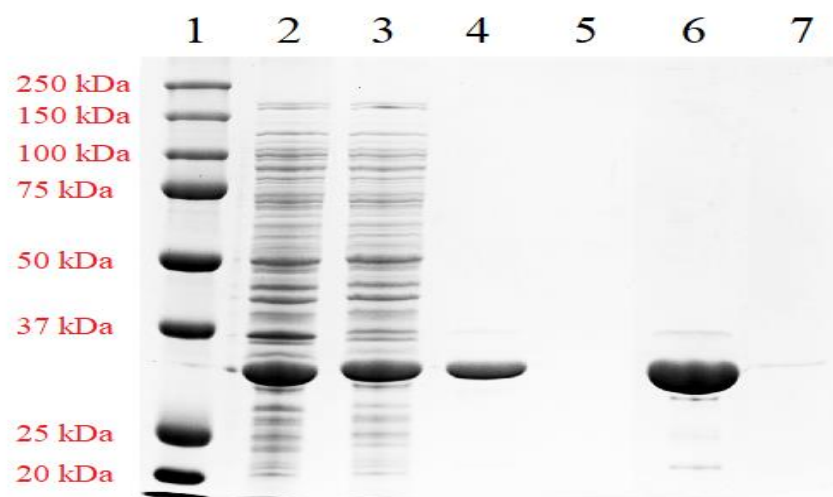


Figure S8. SDS-PAGE analysis of BCArg mutant. Lane 1, protein marker; Lane 2, BCArg mutant crude total protein; Lane 3, BCArg mutant -supernatant total protein; Lane 4, 74 °C heat treatment; Lane 5, flow-through from Q column; Lane 6, 30% elution from Q column; Lane 7, 100% from Q column.”

Mutated BCArg Peptide Sequence

MKPISIIGVP MDLGQTRRGP DMGPSAMRYA GVIERLERLH YDIEDLGDIP
IGKAERLHEQ GDSRLRNLKA VAEANEKLAA AVDQVVQRGR FPLVLGGDHS
IAIGTLAGVA KHYERLGVIW YDAHGDVNTA ETSPSGNIHG MPLAASLGFG
HPALTQIGGY CPKIKPEHVV LIGVRSLEDEG EKKFIREKGI KIYTMHEVDR
LGMTRVMEET IAYLKERTDG VHLSLDLDGL DPSDAPGVGT PVIGGLTYRE
SHLAMEMPLAE AQIITSAEFV EVNPILDERN KTASVAVALM GSLFGEKLM

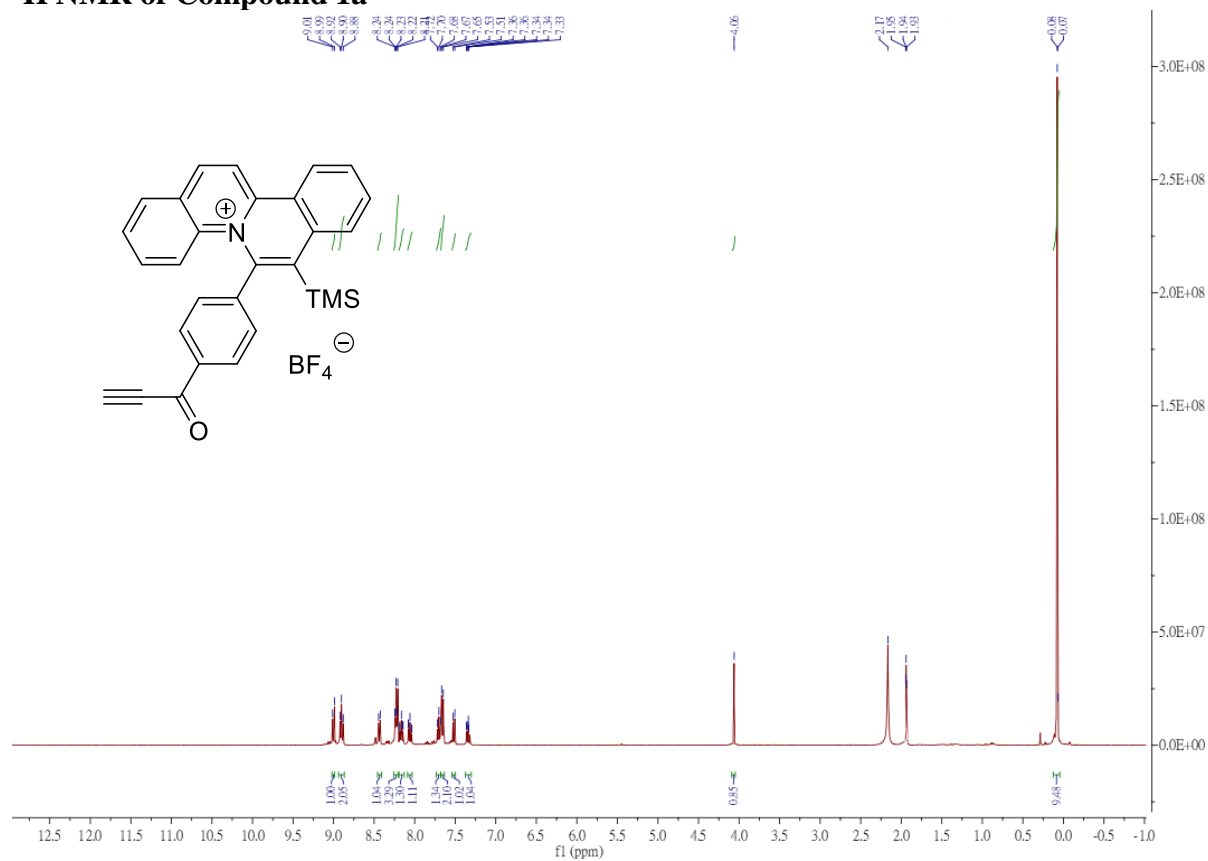
Enzyme Activity

This assay was used to study the amount of urea produced by BCArg mutant. 200 μ L of 20 mM L-Arg solutions were incubated at 37 °C. Reactions were started by adding 5 μ L of 20 mM BCArg mutant for 30 seconds and stopped by 15 μ L 80% trichloroacetic acid. A colouring reagent was prepared by 1 volume of a mixture of 80 mM diacetyl monoxime and 2.0 mM thiosemicarbazide and 3 volumes of a mixture of 3 M H₃PO₄, 6 M H₂SO₄, 2 mM FeCl₃. 800 μ L of the colouring reagent were added to each solution and incubated at 100 °C for 10 min. Absorbance at 530 nm (A₅₃₀ nm) was evaluated by UV-Vis spectroscopy. The specific activity of BCArg mutant is defined as the micromoles of urea produced per minute under given conditions per mg proteins at 37 °C, pH 7.4 in the phosphate-buffered saline buffer.⁵

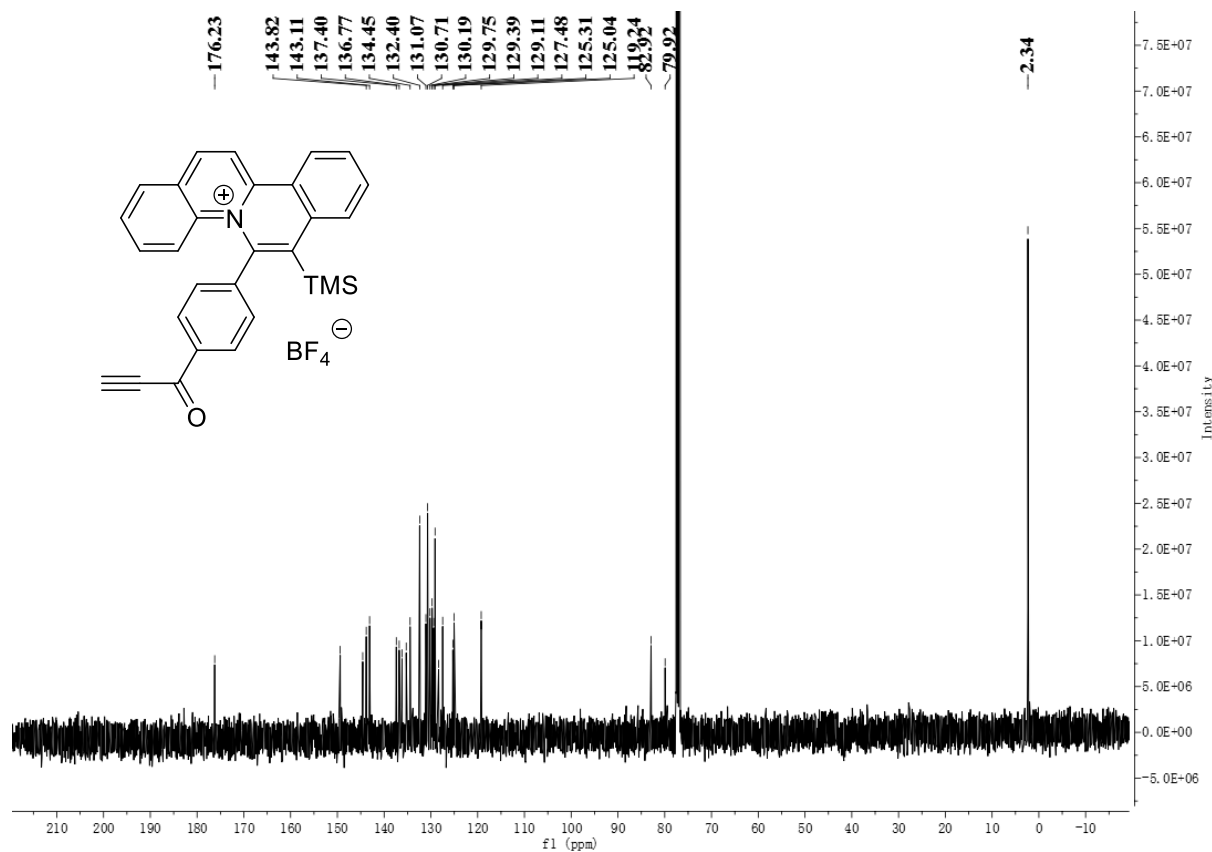
Inhibition of *in vitro* Cancer Cell Proliferation

LoVo cancer cell line (CCL-229™, American Type Culture Collection) was grown in Roswell Park Memorial Institute 1640 Medium (Thermo Fisher Scientific) at 37°C. Cancer Cells were seeded about 3000 cells per well in 96-well plates. The started concentration of BCArg mutant was diluted in 2-fold serial dilution and the plates were incubated for 3 days. Quantitative cell proliferation assays were determined by the 3-(4,5-dimethylthiazol-2-yl)-2,5-diphenyltetrazolium bromide reagent according to the manufacturer's instructions. Three independent experiments were performed in triplicate.

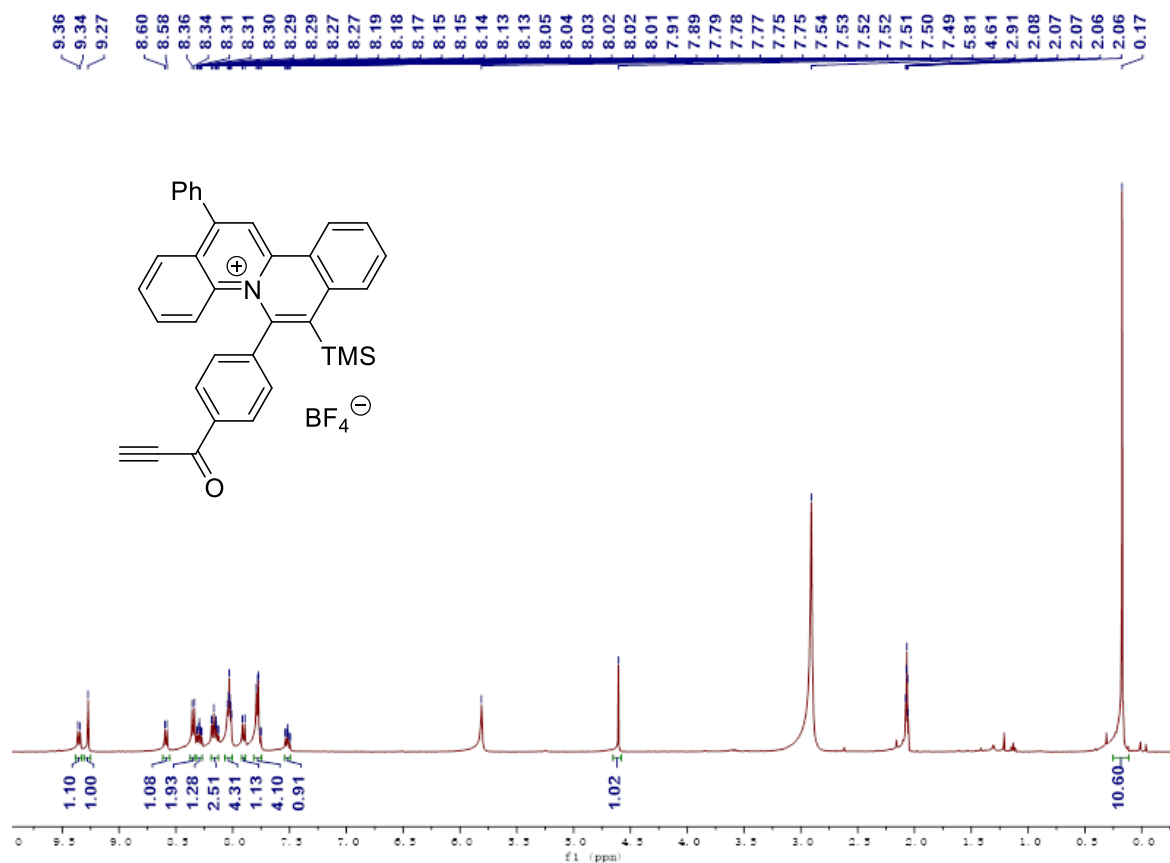
¹H NMR of Compound 1a



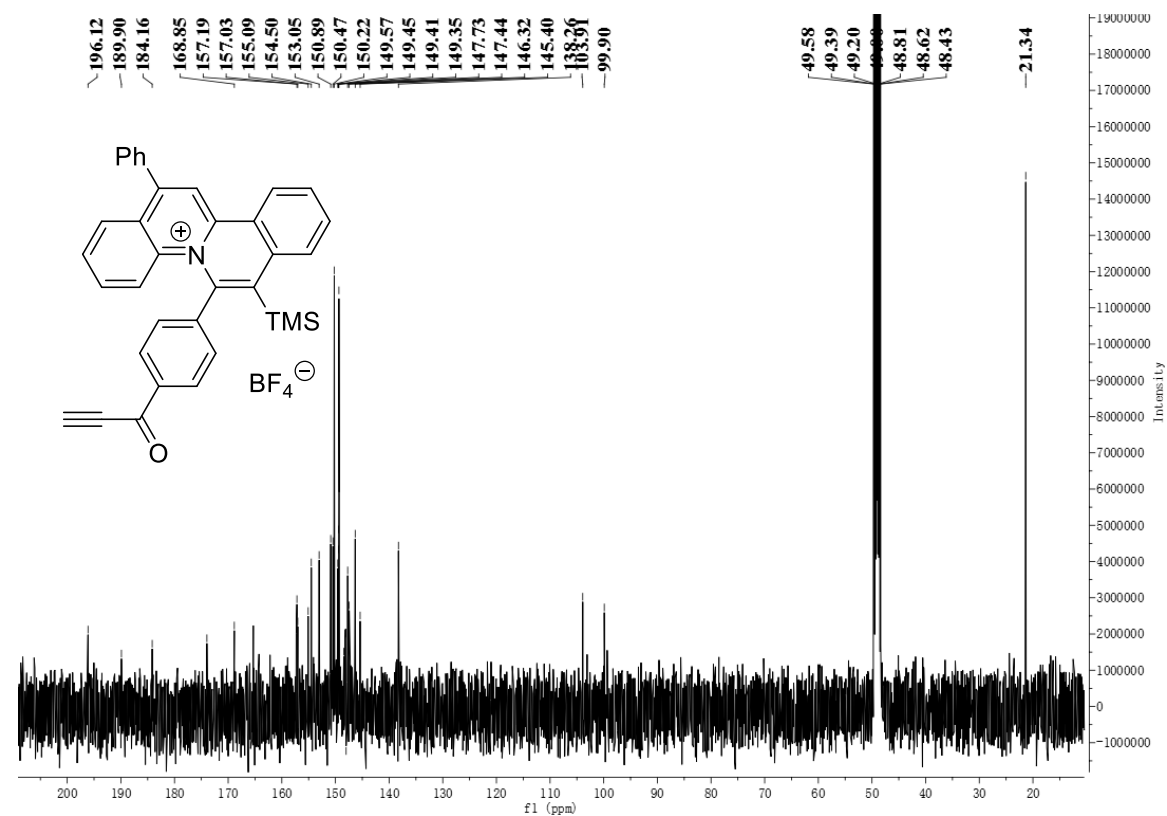
¹³C NMR of Compound 1a



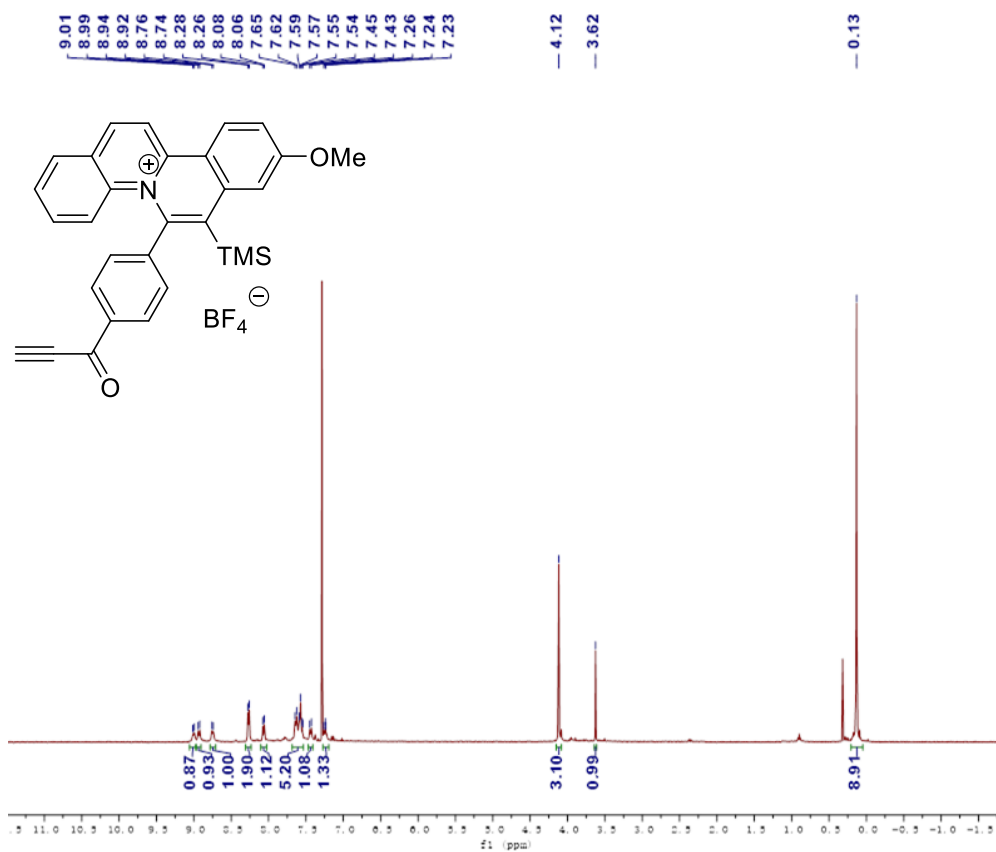
¹H NMR of Compound 1b



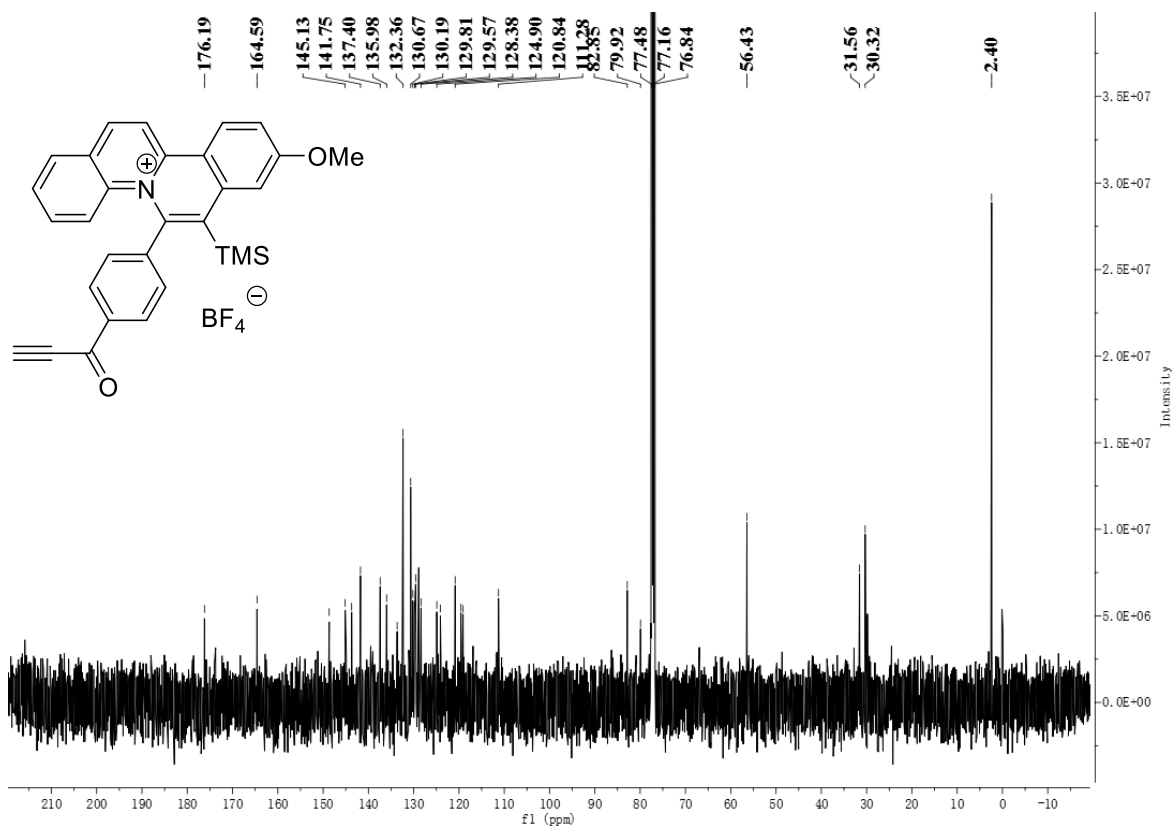
¹³C NMR of Compound 1b



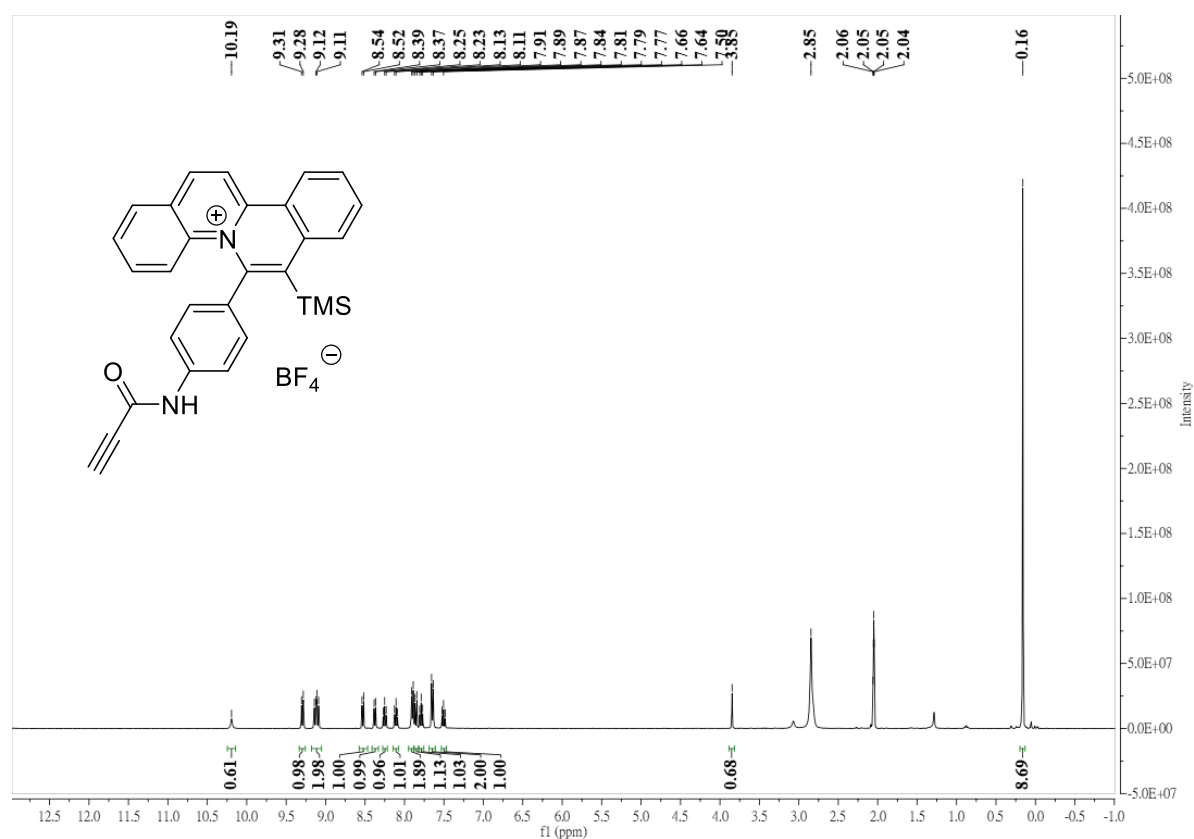
¹H NMR of Compound 1c



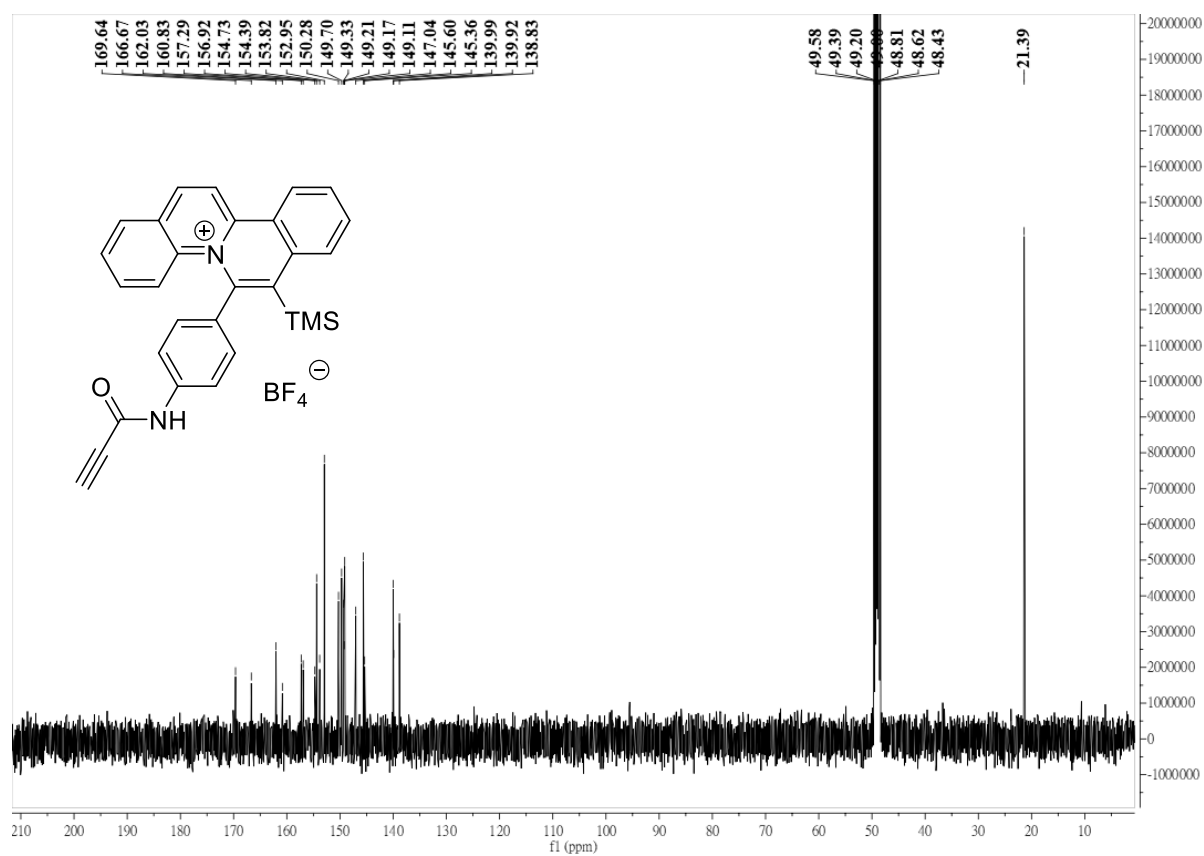
¹³C NMR of Compound 1c



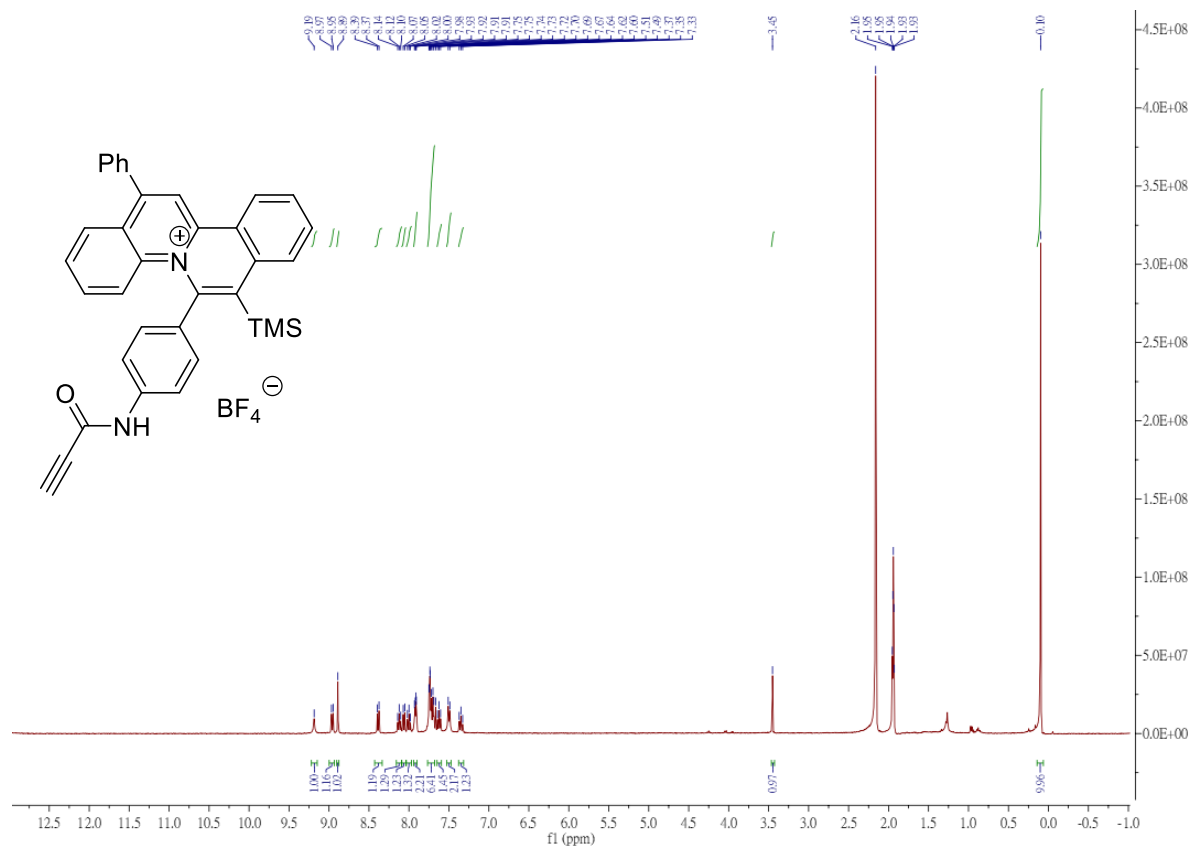
¹H NMR of Compound 1d



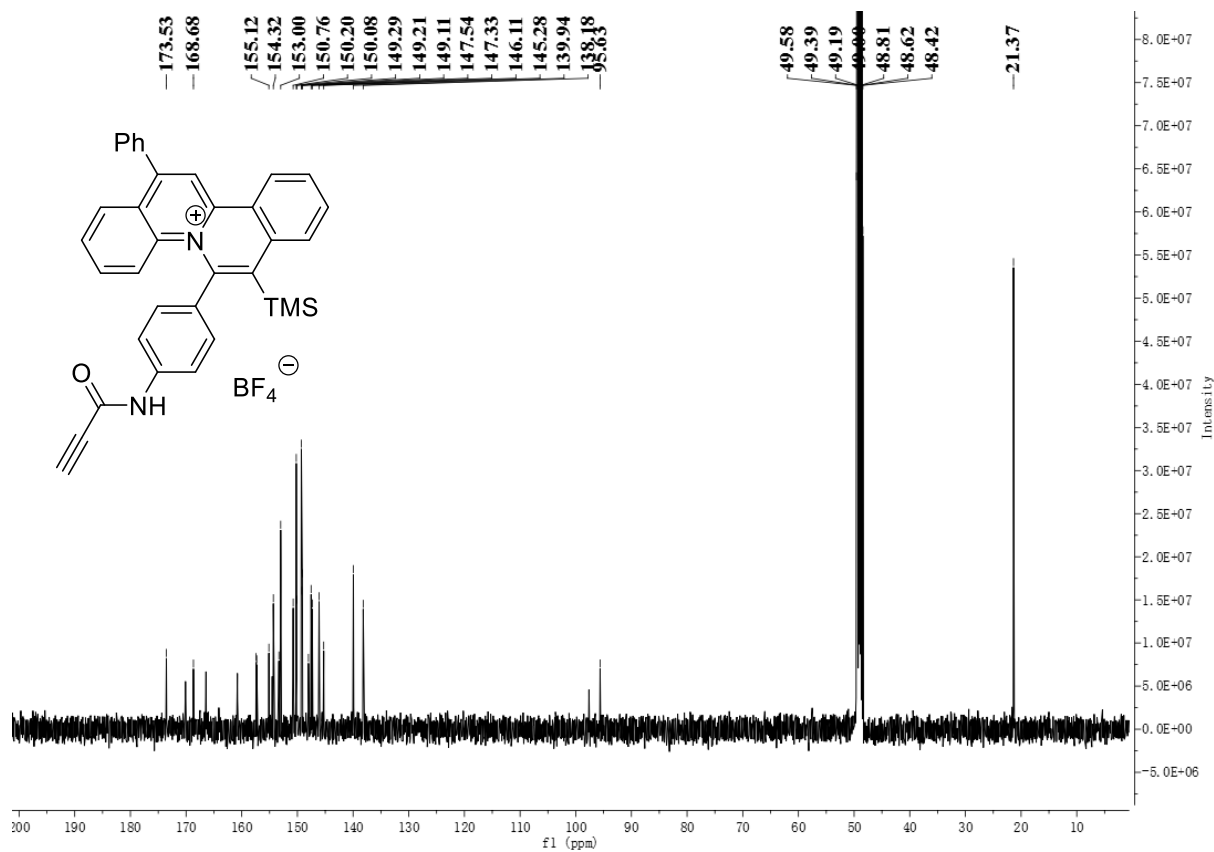
¹³C NMR of Compound 1d



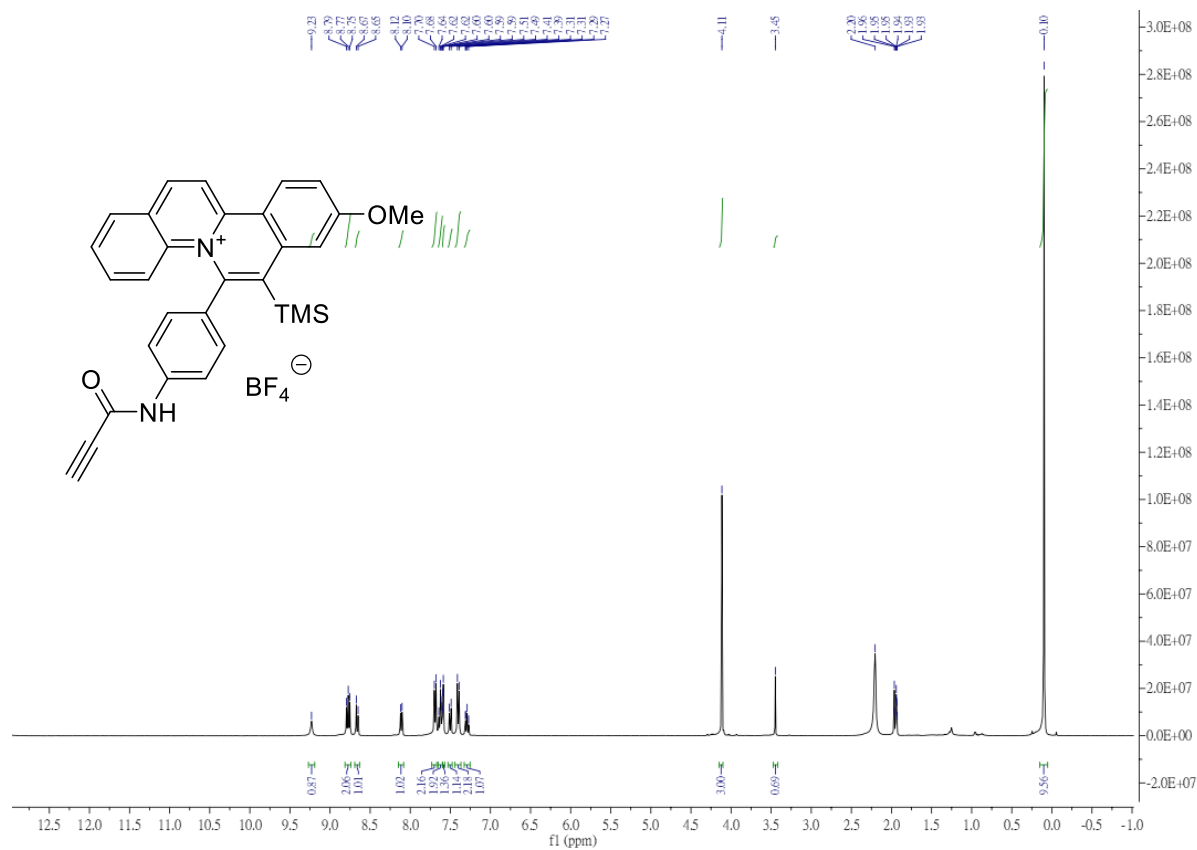
¹H NMR of Compound 1e



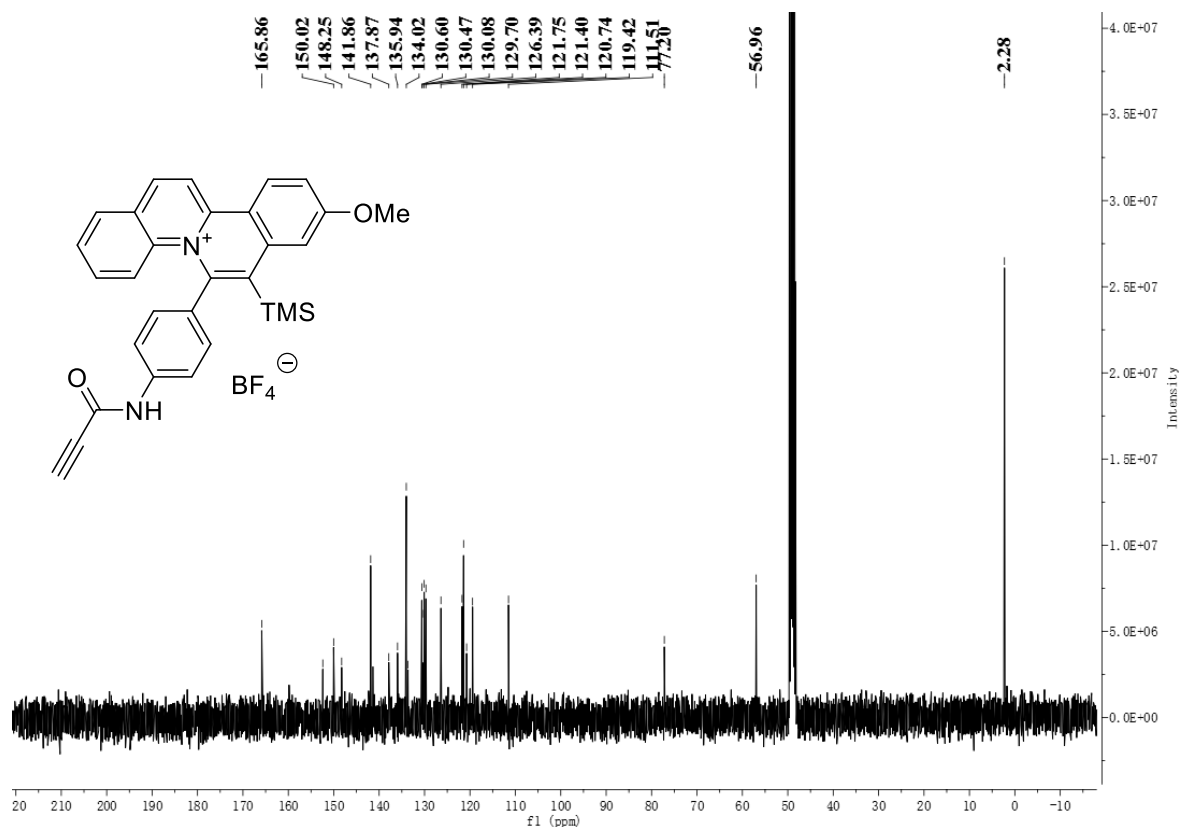
¹³C NMR of Compound 1e



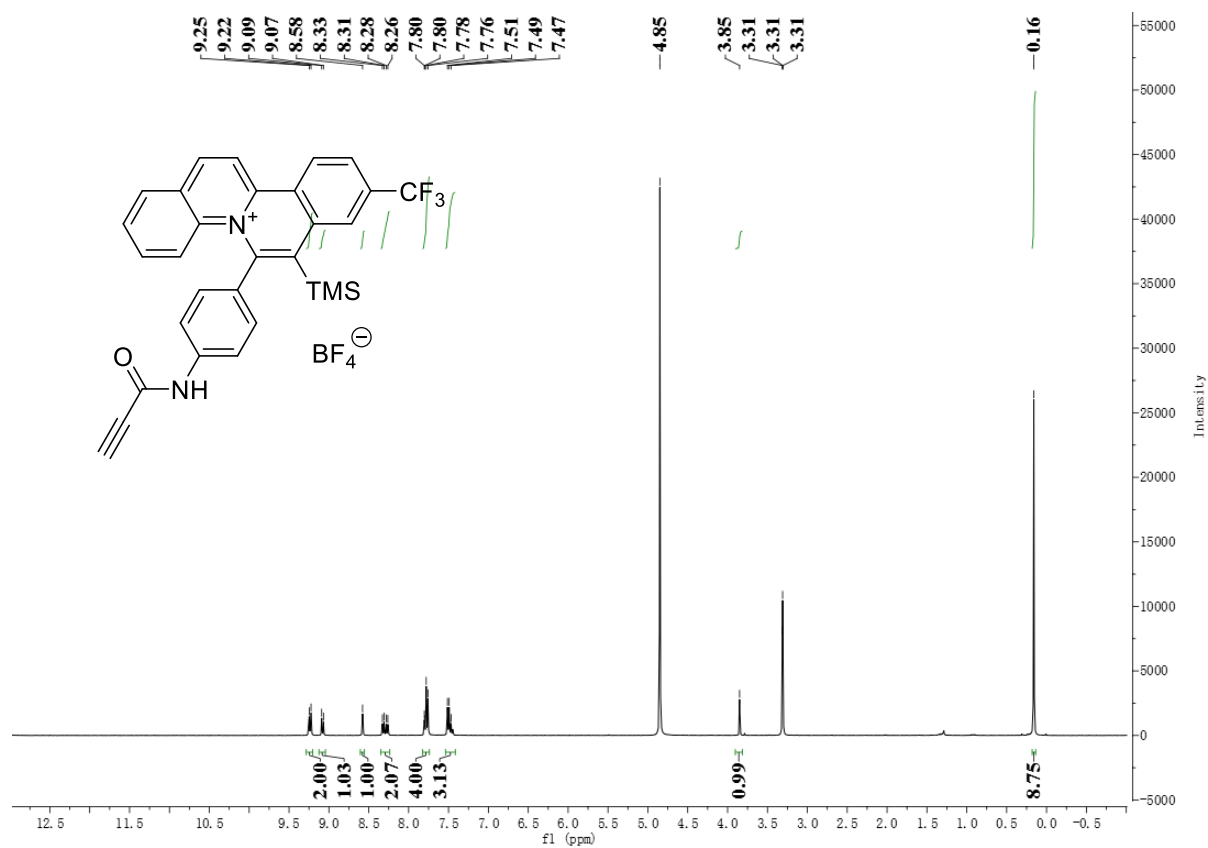
¹H NMR of Compound 1f



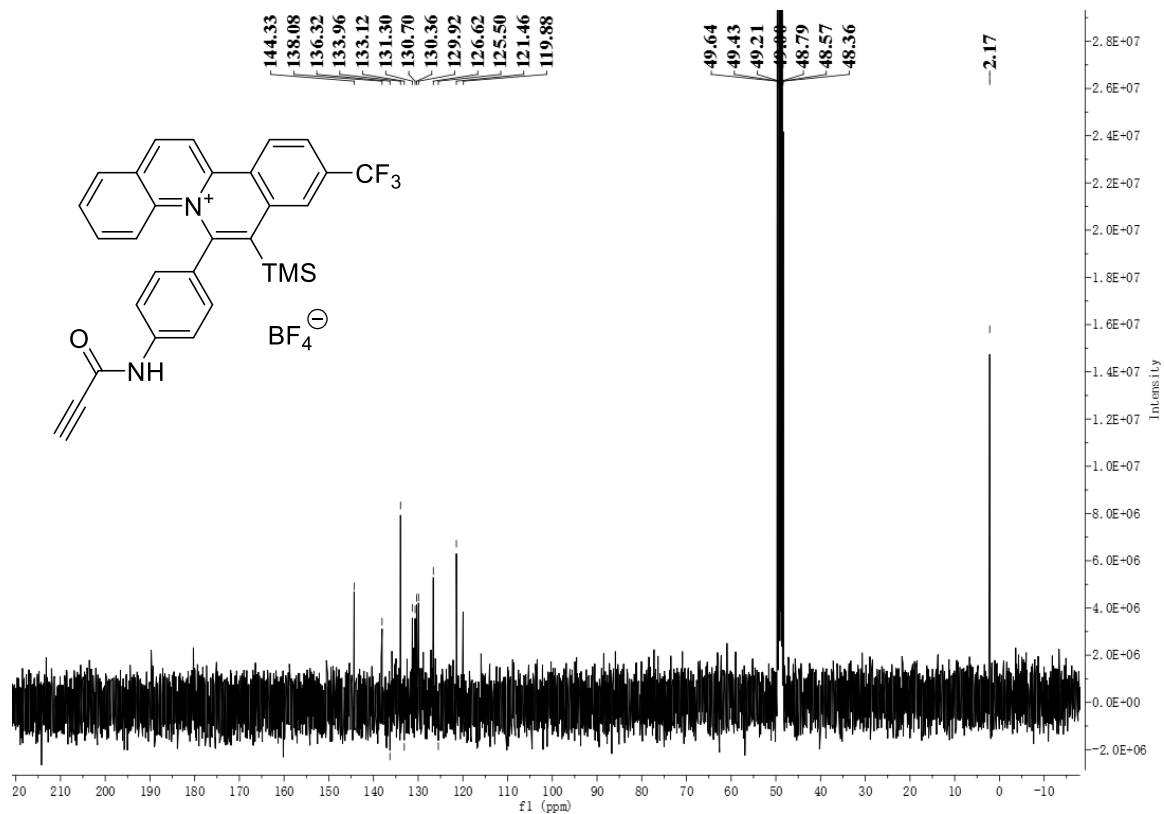
¹³C NMR of Compound 1f



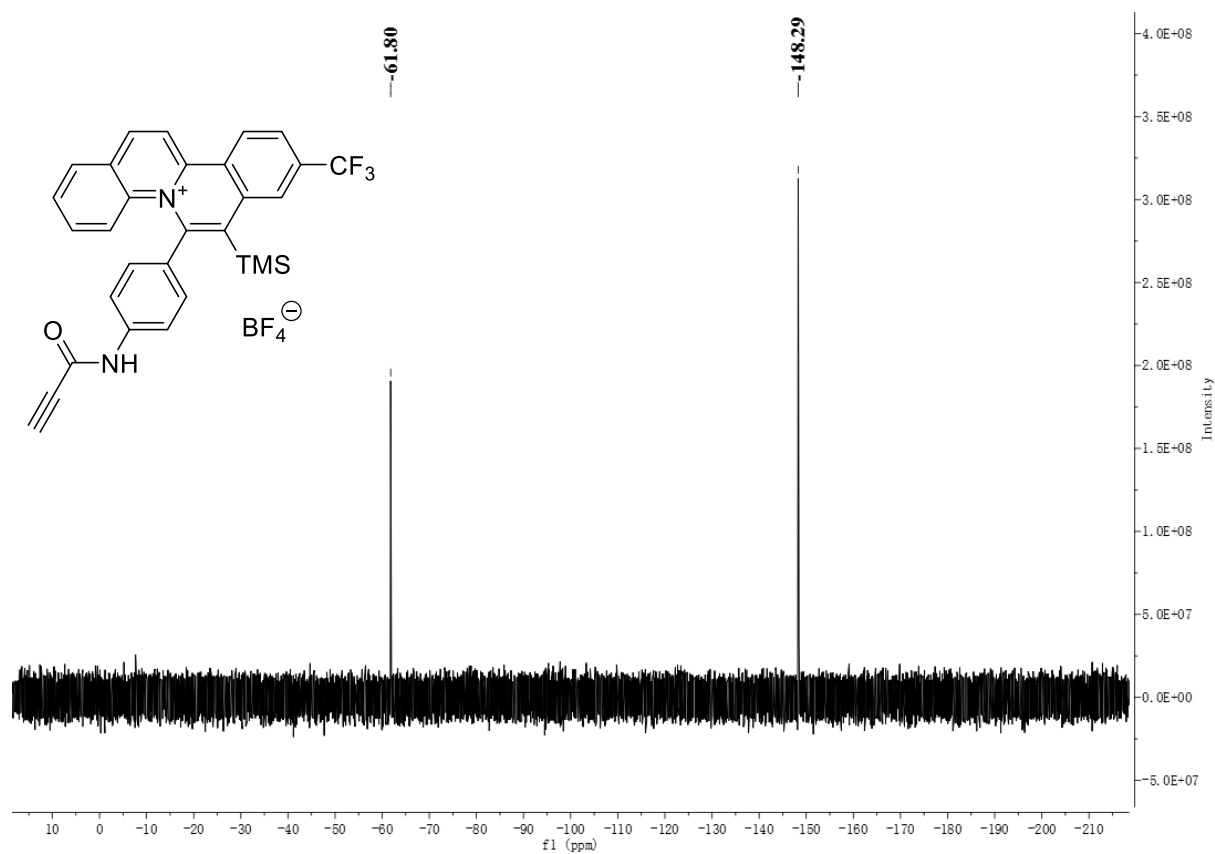
¹H NMR of Compound 1g



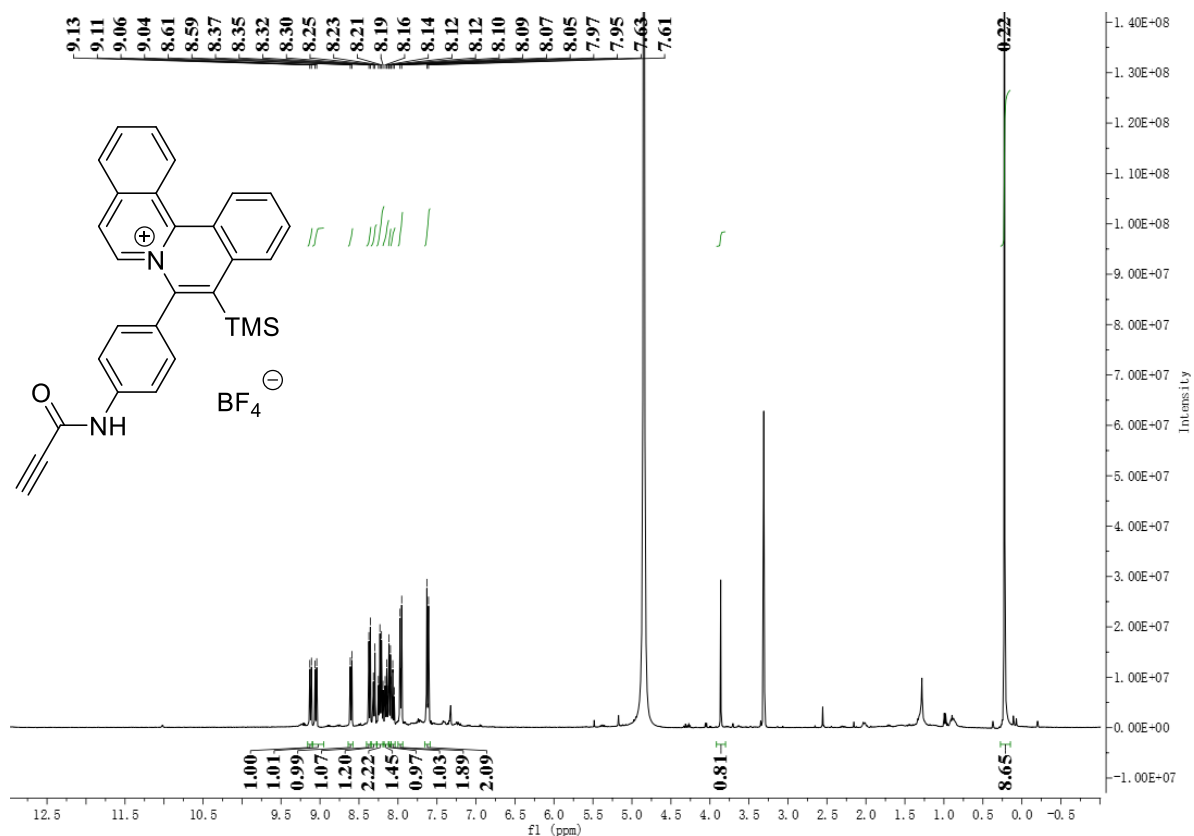
¹³C NMR of Compound 1g



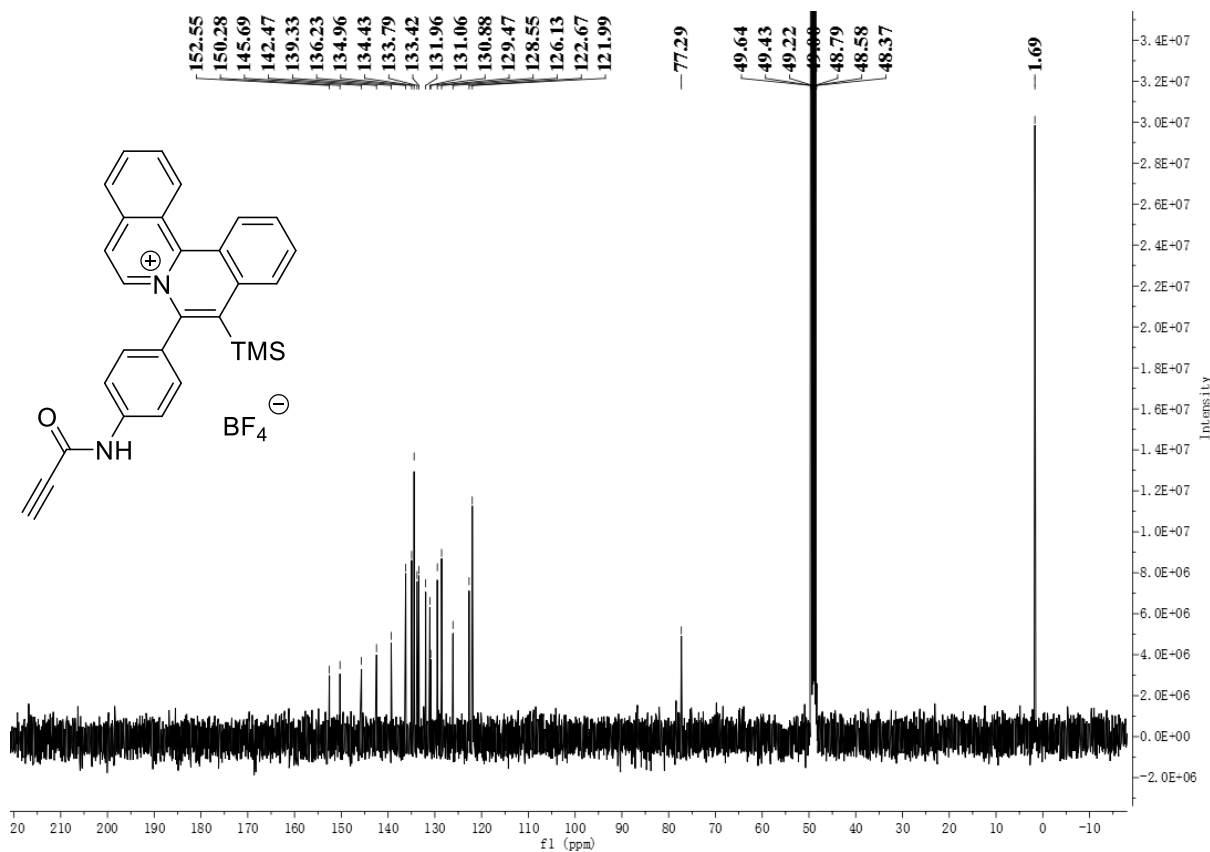
¹⁹F NMR of Compound 1g



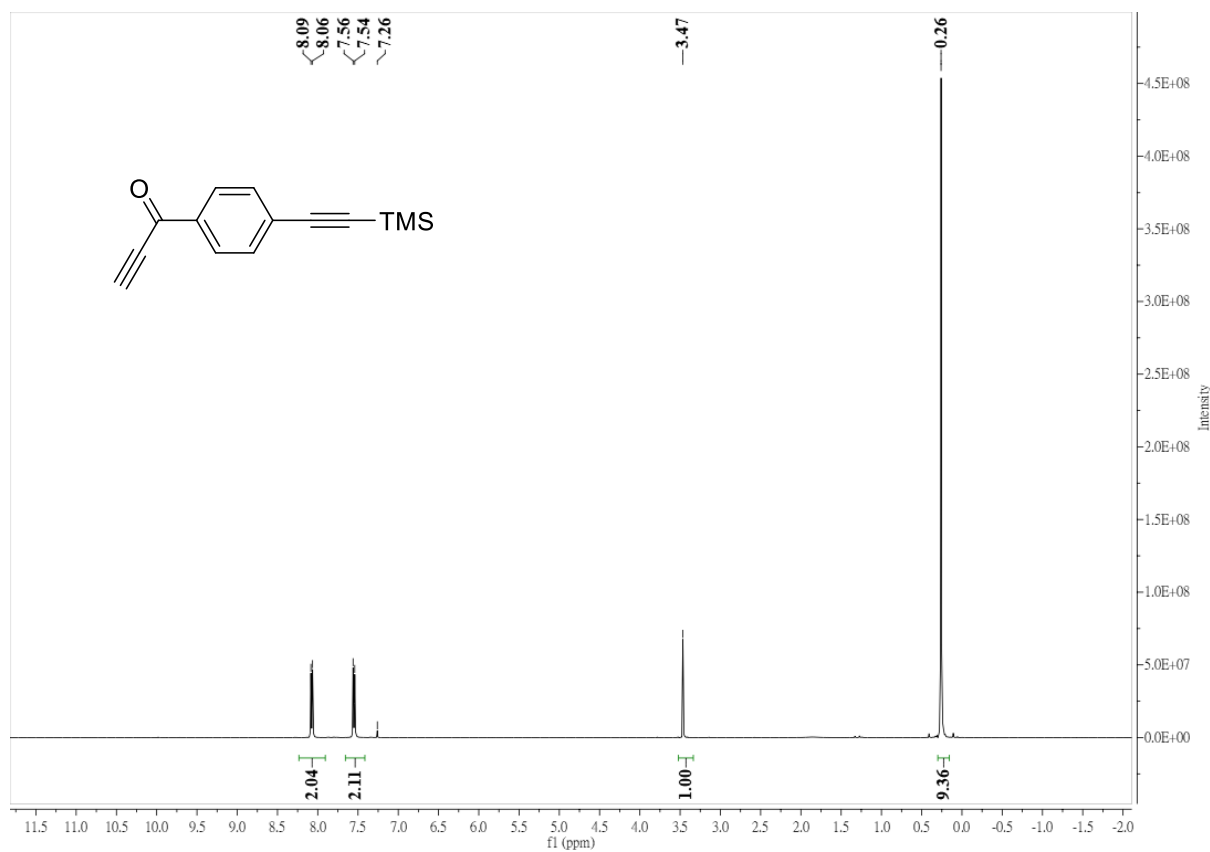
¹H NMR of Compound 1h



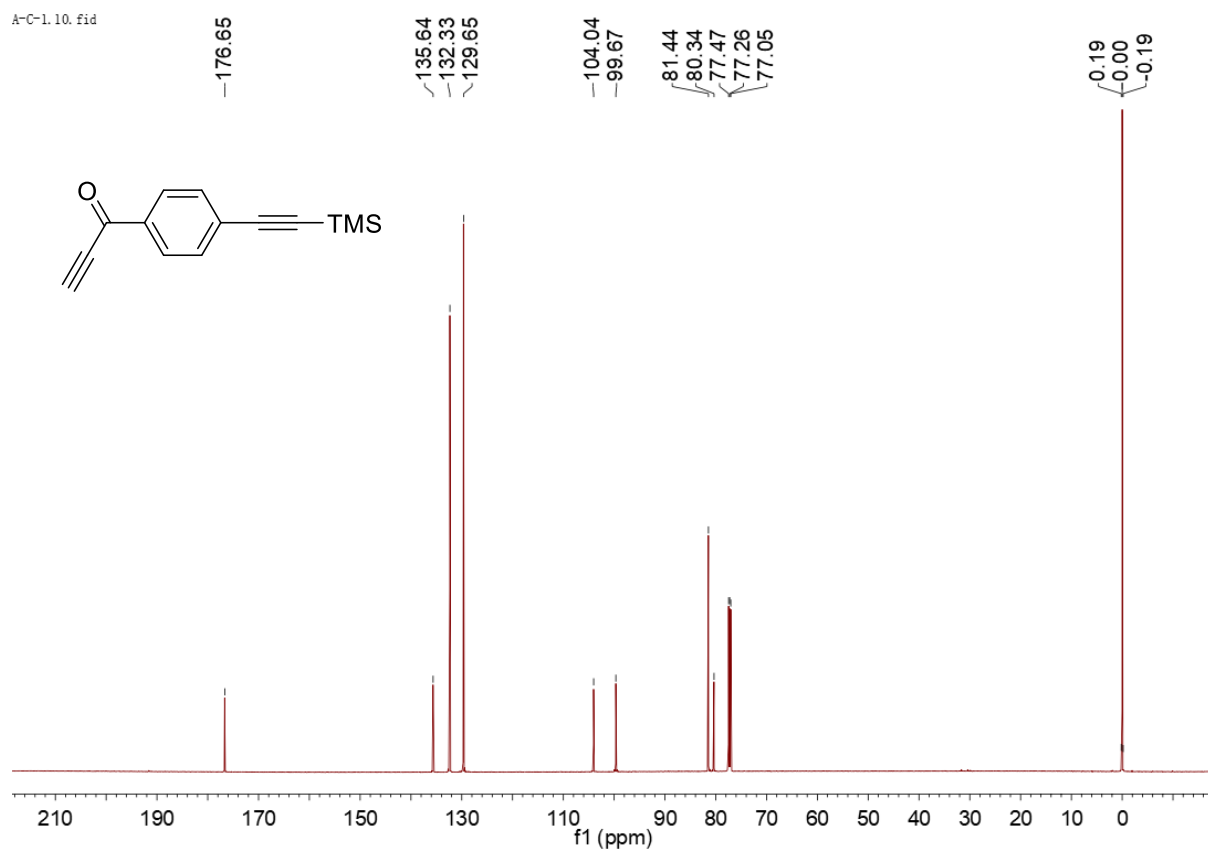
¹³C NMR of Compound 1h



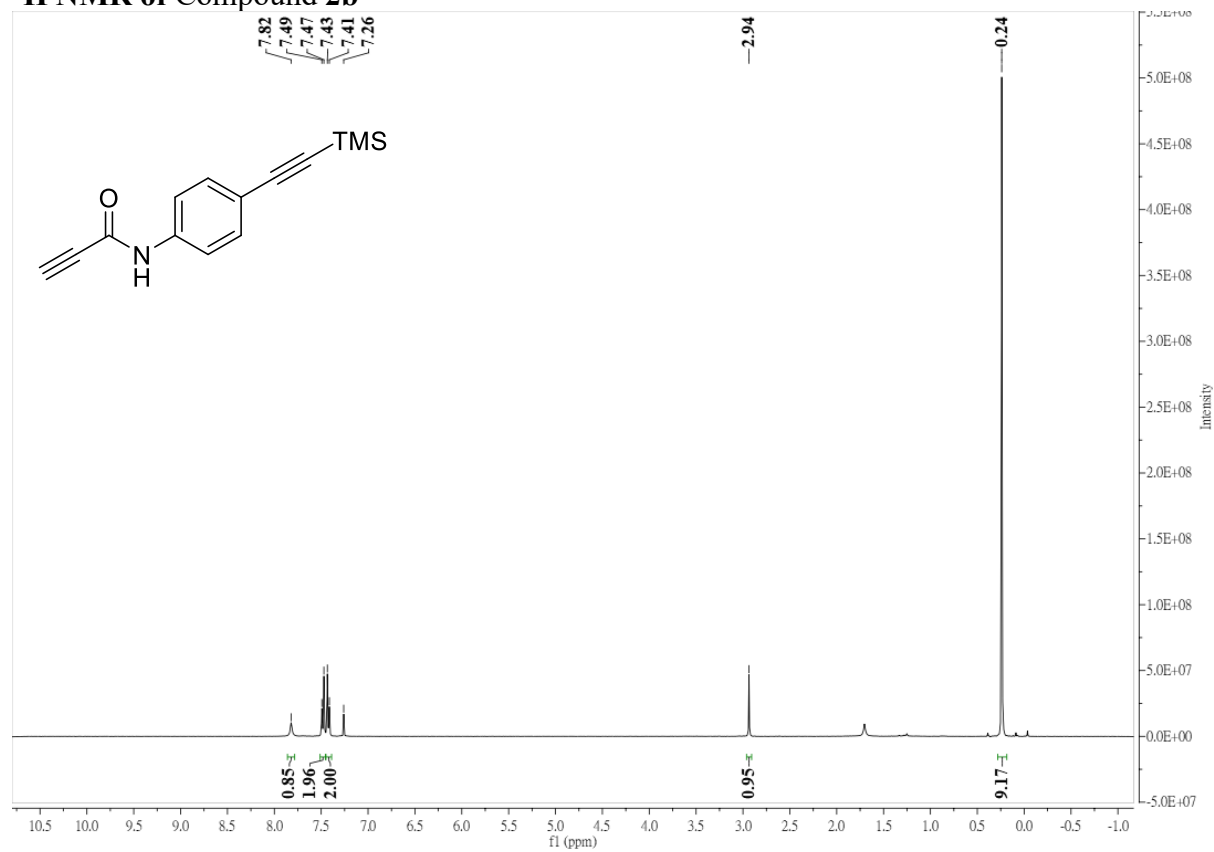
¹H NMR of Compound 2a



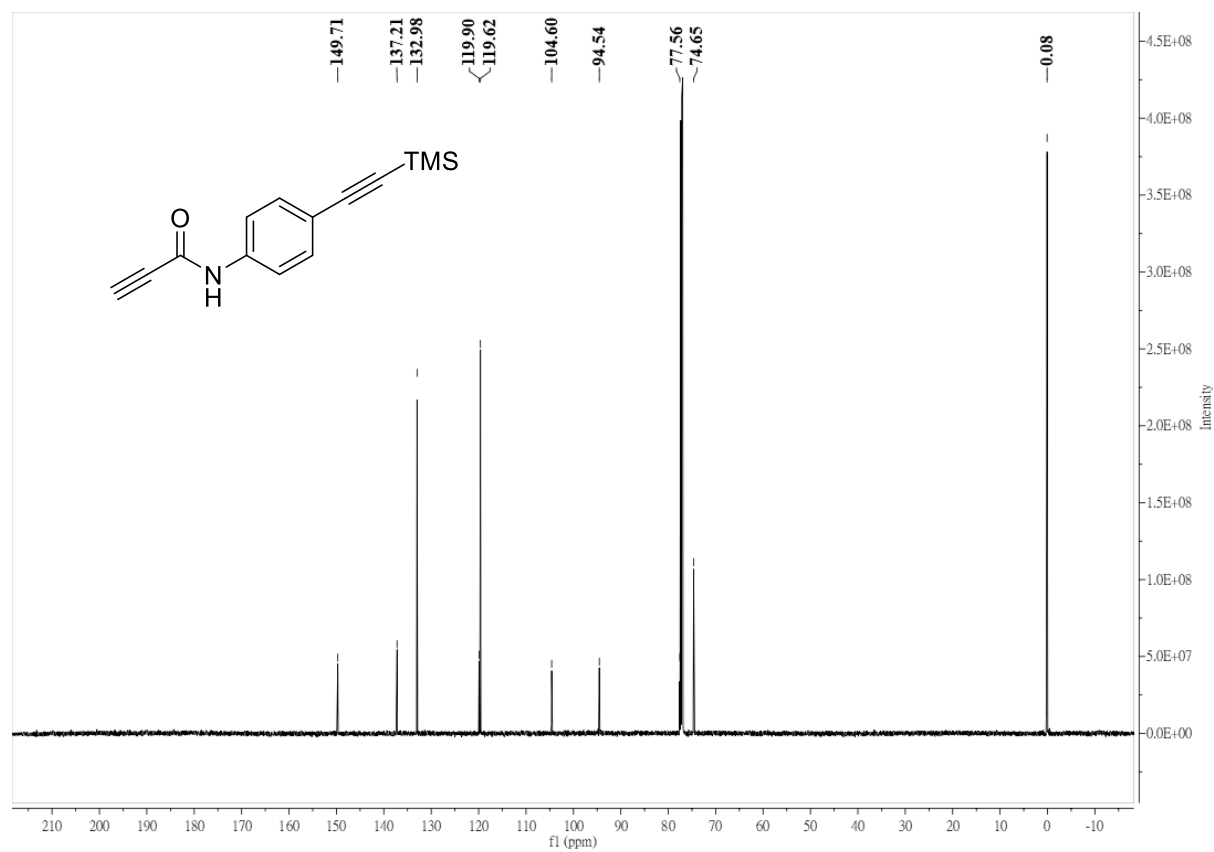
¹³C NMR of Compound 2a



¹H NMR of Compound 2b

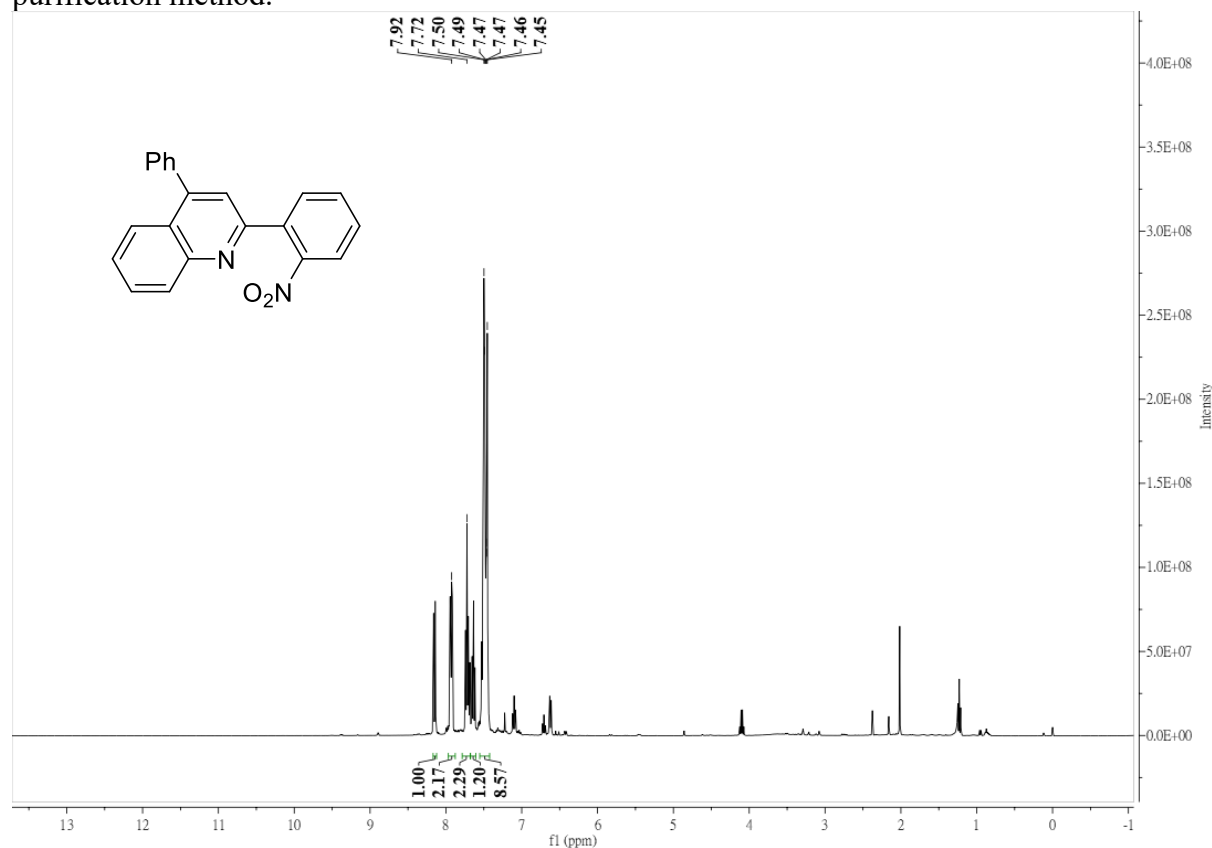


¹³C NMR of Compound 2b

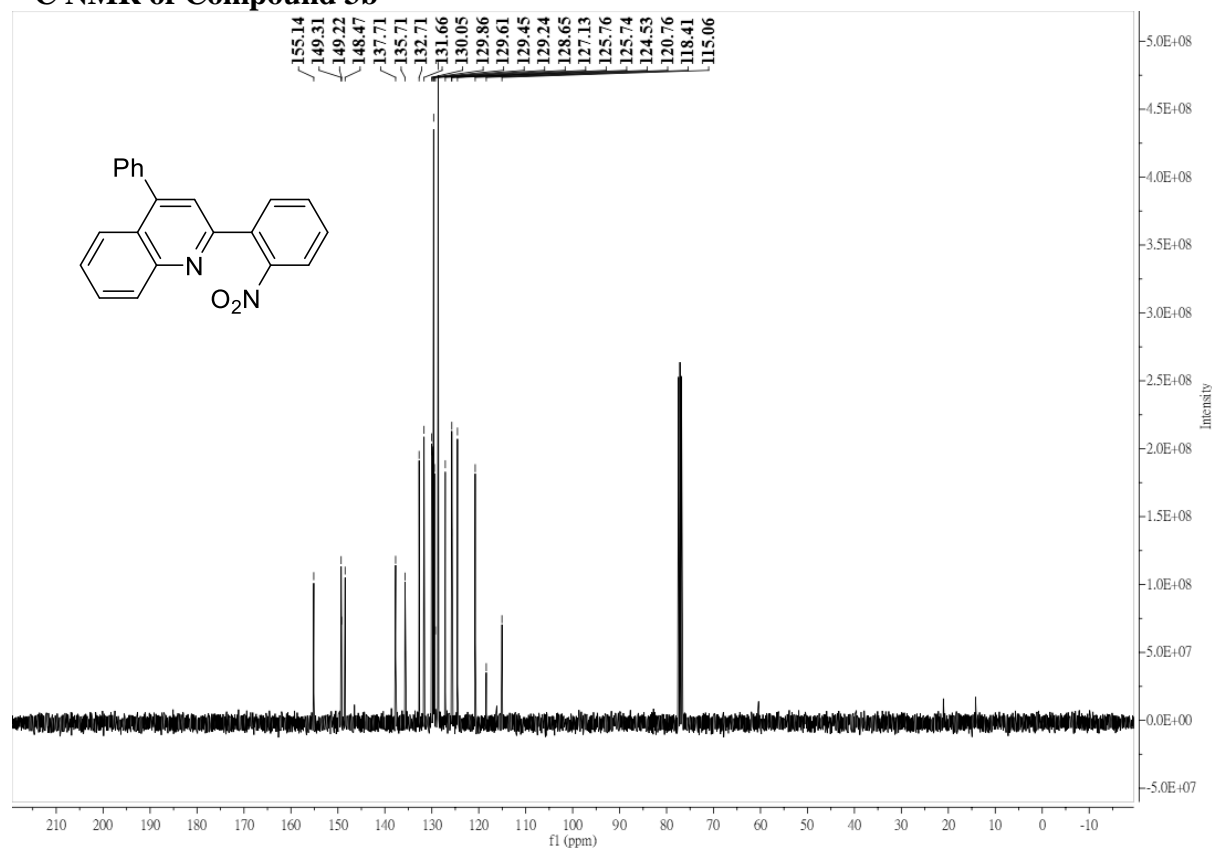


¹H NMR of Compound 3b'

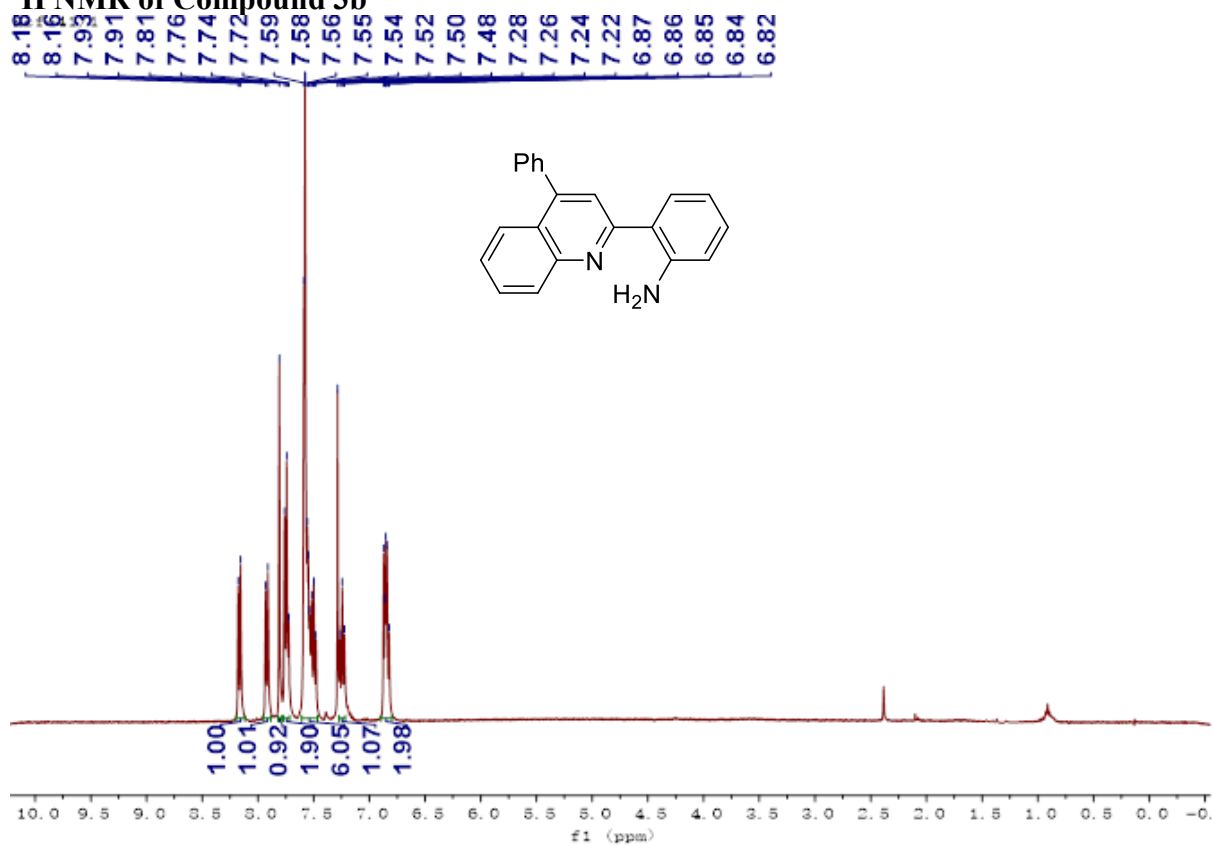
Additional peaks arise due to trace impurities with silicone-grease from the reaction and purification method.



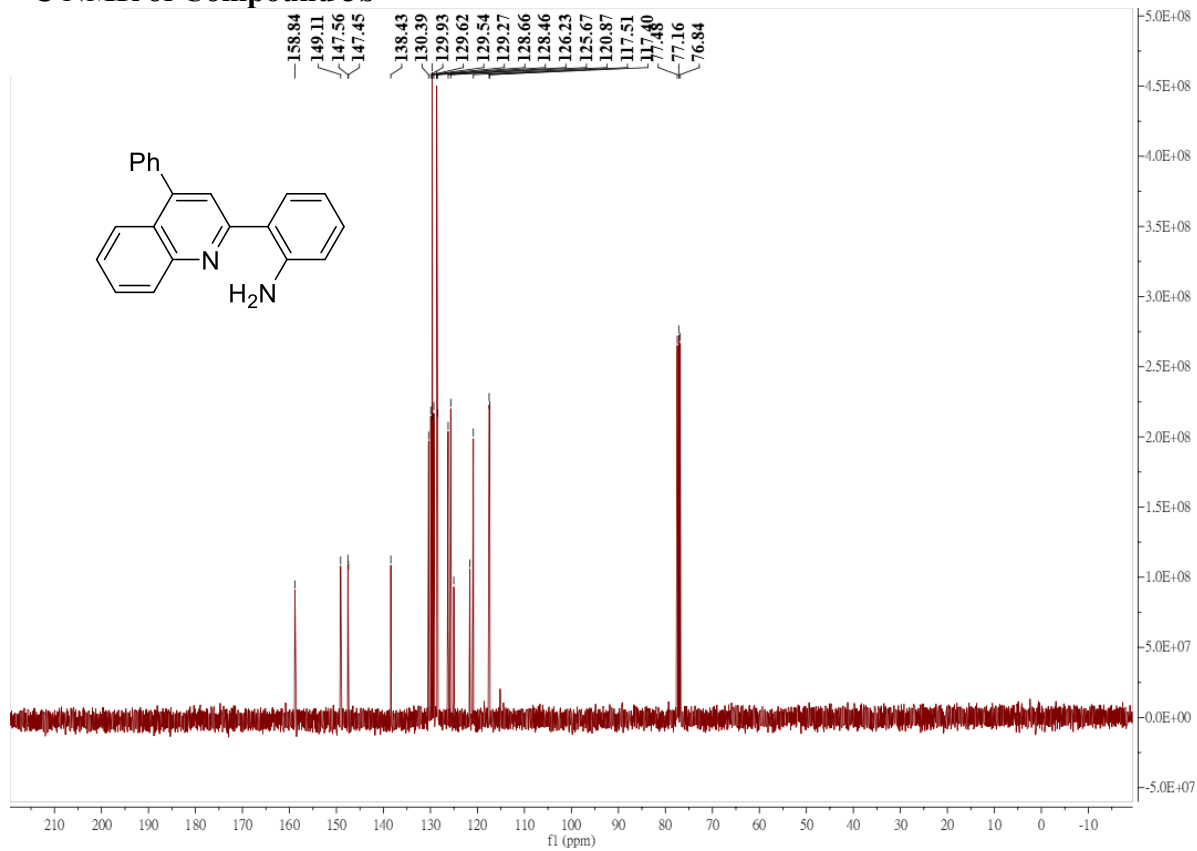
¹³C NMR of Compound 3b'



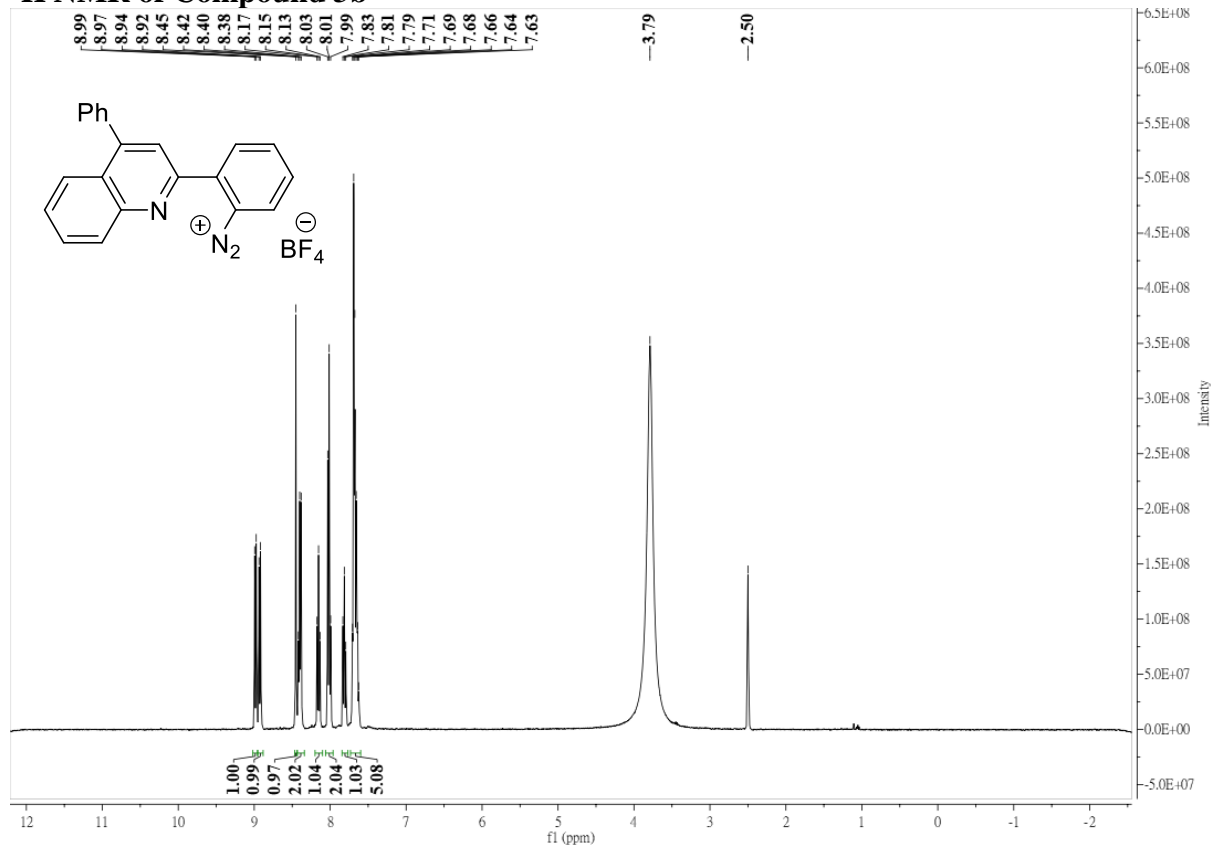
¹H NMR of Compound 3b''



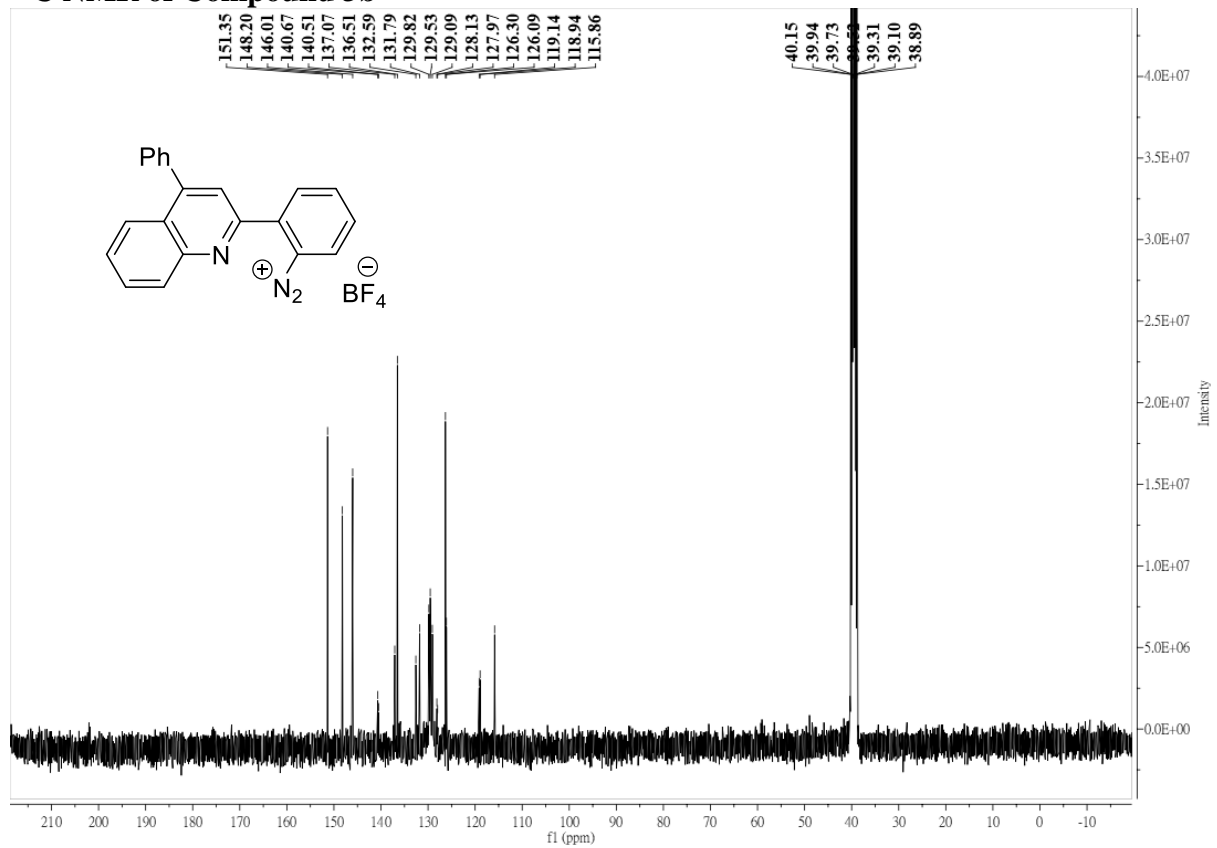
¹³C NMR of Compound 3b''



¹H NMR of Compound 3b



¹³C NMR of Compound 3b



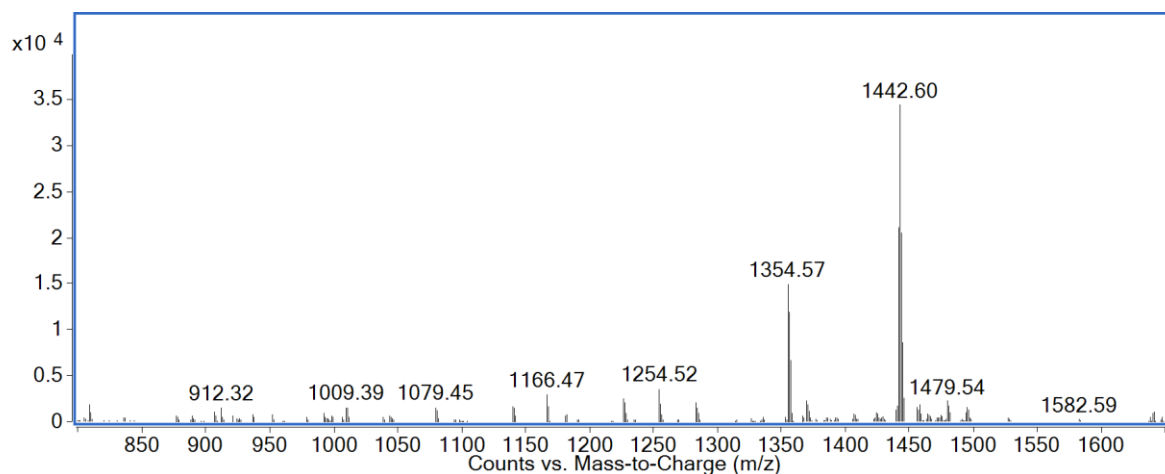
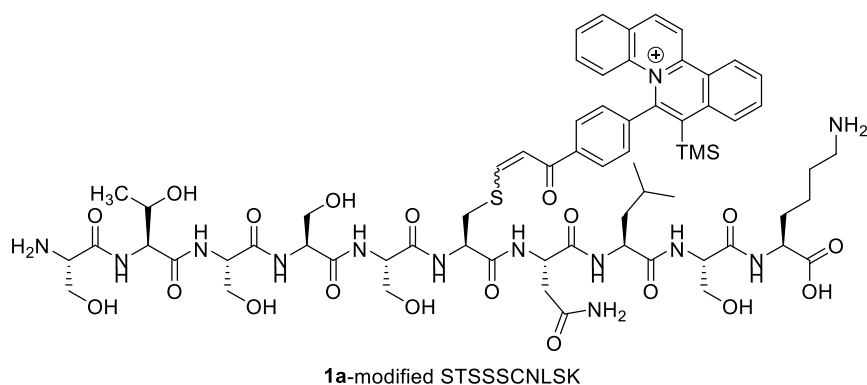


Figure S9. Deconvoluted mass spectrum of **1a**-modified STSSSCNLSK (m/z 1442.60).

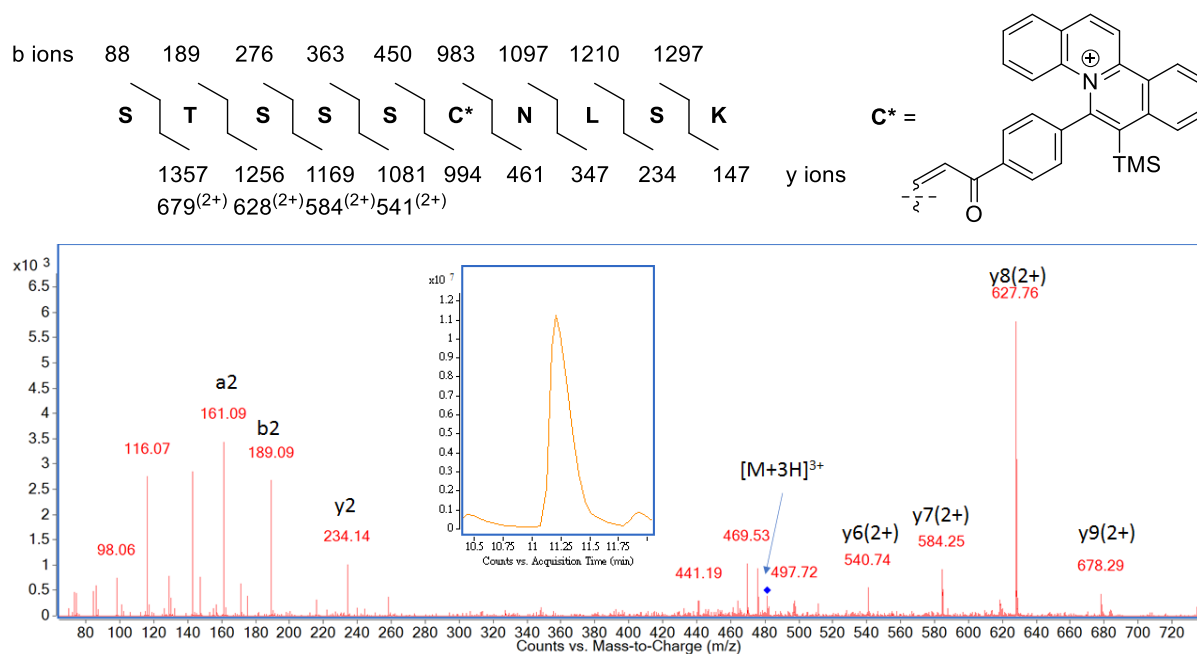


Figure S10. MS/MS spectrum and extracted ion chromatogram (Inset) of **1a**-modified STSSSCNLSK (ESI source, triply charged ion of m/z 481.88).

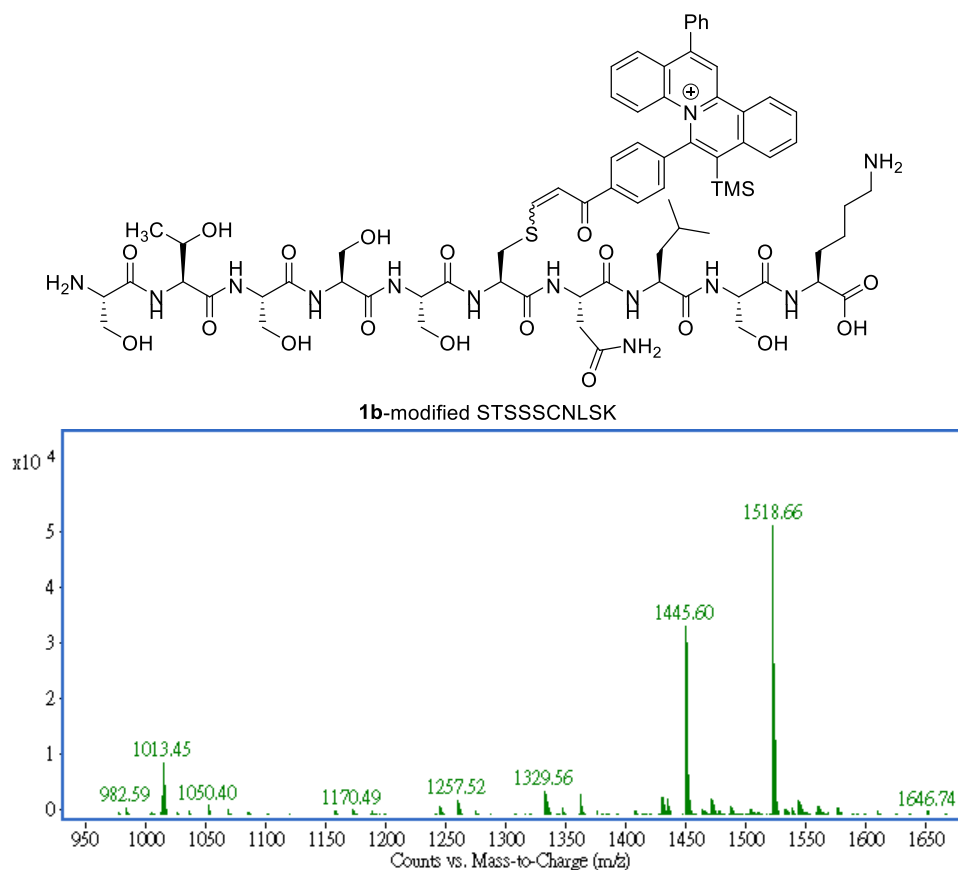


Figure S11. Deconvoluted mass spectrum of **1b**-modified STSSSCNLSK (m/z 1518.66).

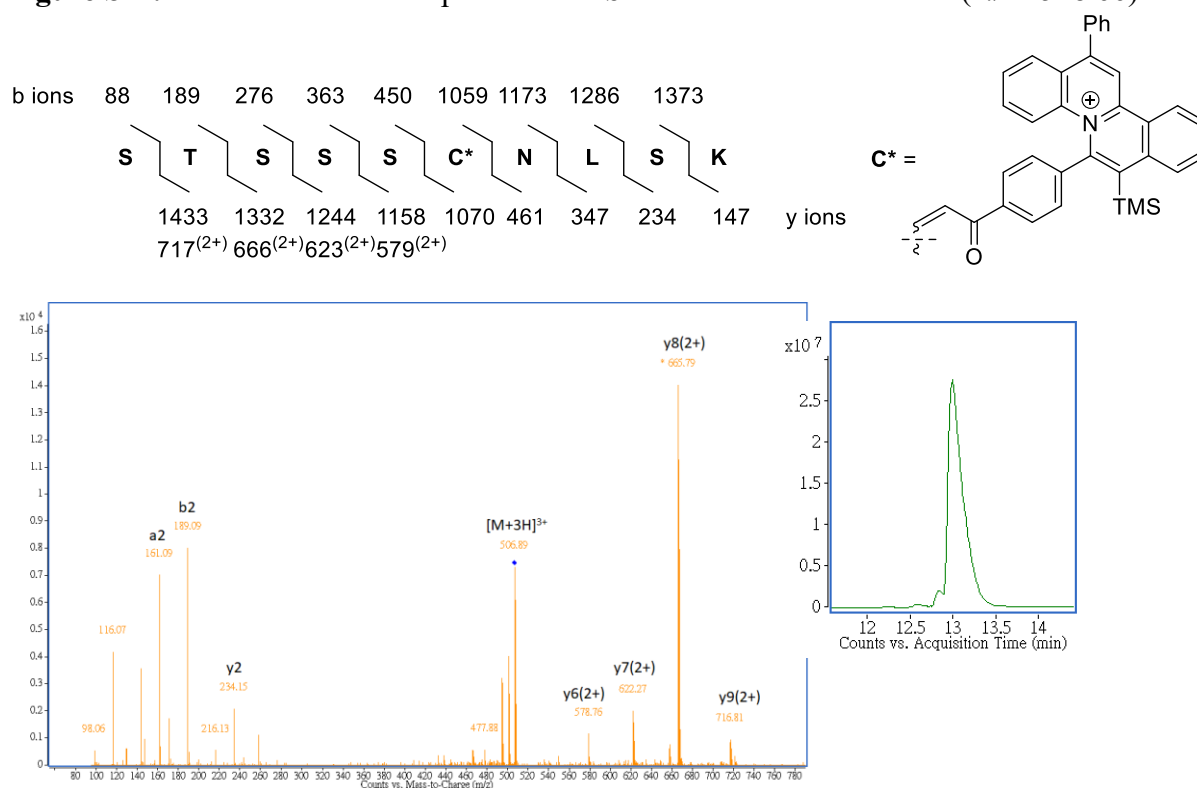


Figure S12. MS/MS spectrum and extracted ion chromatogram (Inset) of **1b**-modified STSSSCNLSK (ESI source, triply charged ion of m/z 506.90).

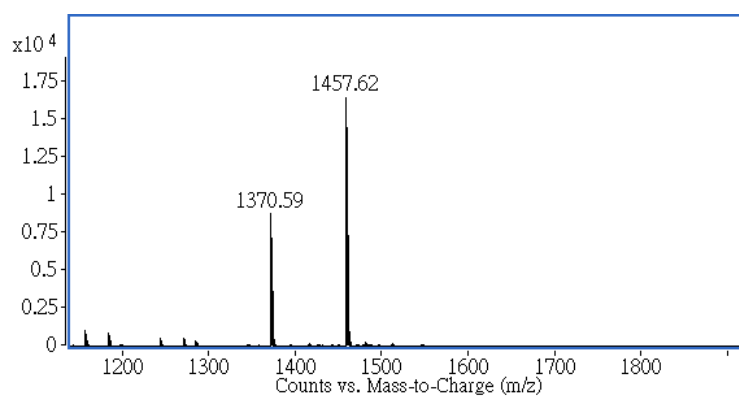
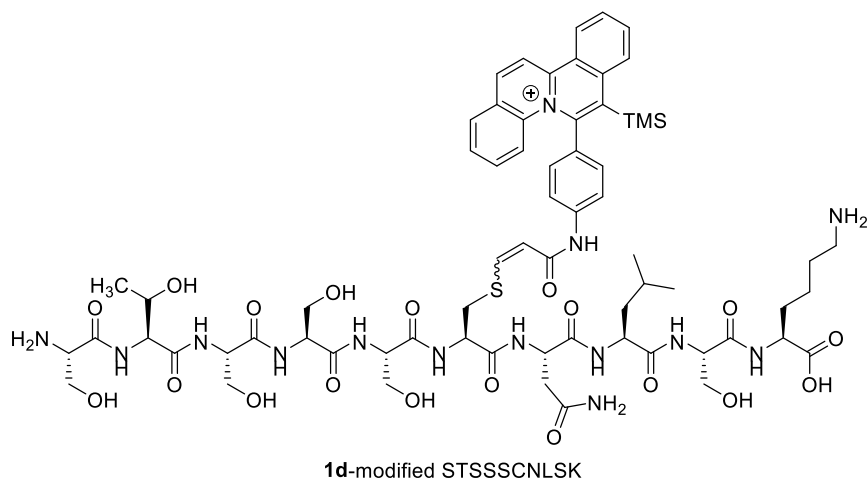


Figure S15. Deconvoluted mass spectrum of **1d**-modified STSSCNLSK (m/z 1457.62).

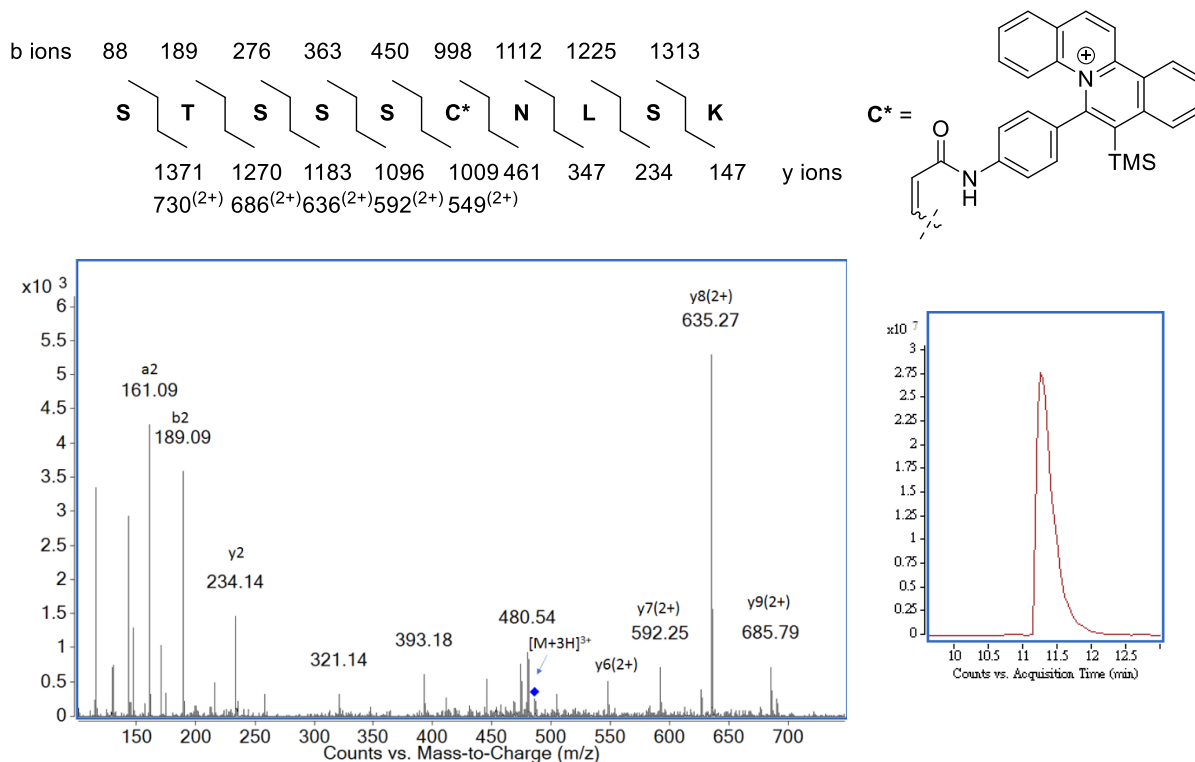


Figure S16. MS/MS spectrum and extracted ion chromatogram (Inset) of **1d**-modified STSSCNLSK (ESI source, triply charged ion of m/z 486.88).

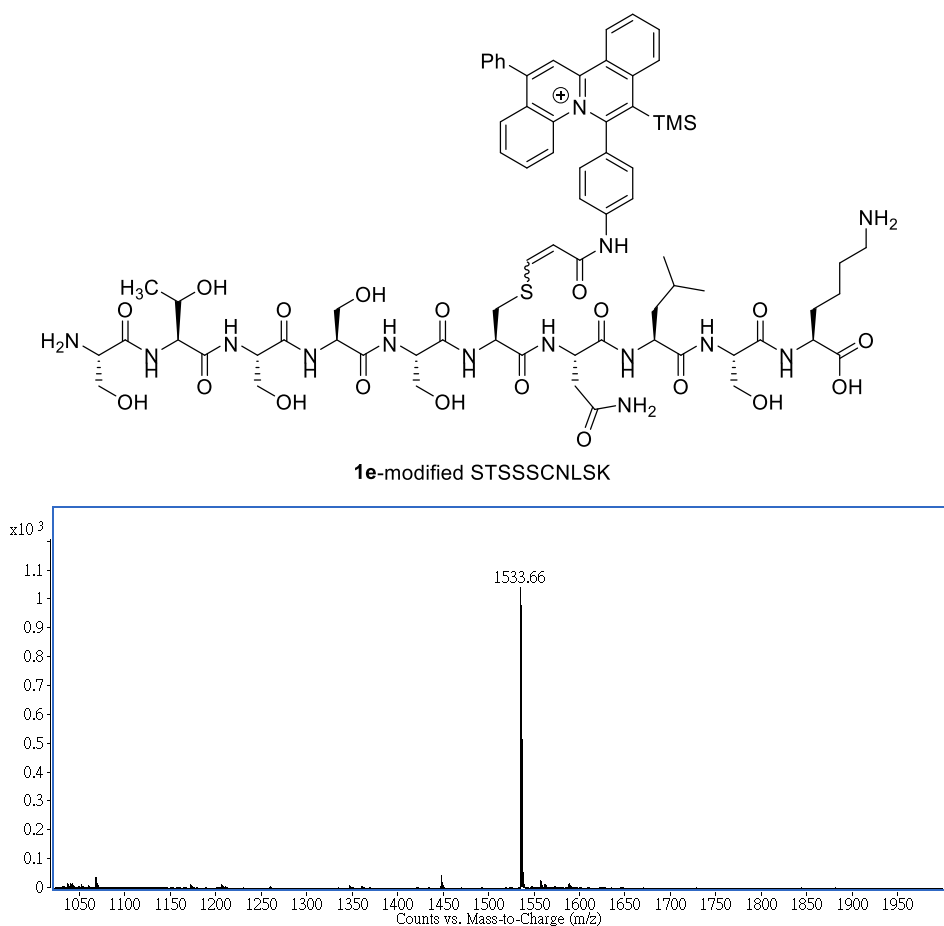


Figure S17. Deconvoluted mass spectrum of **1e**-modified STSSCNLSK (m/z 1533.66).

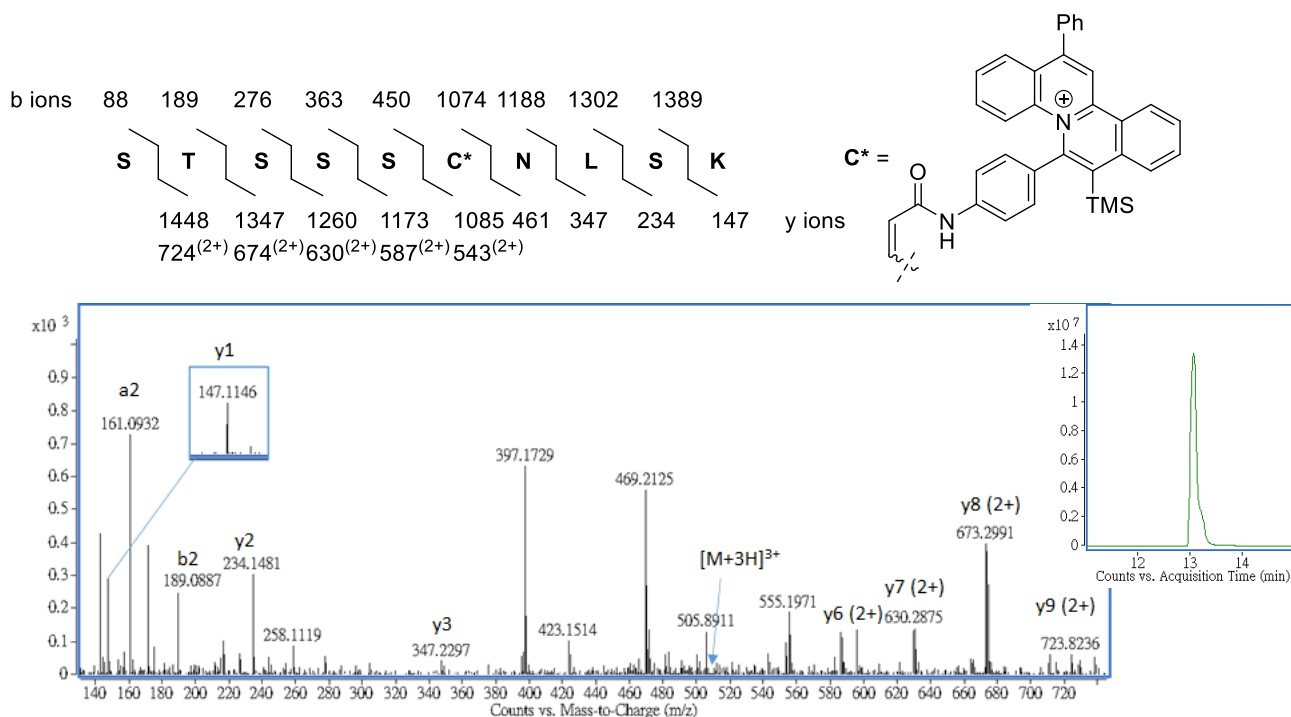


Figure S18. MS/MS spectrum and extracted ion chromatogram (Inset) of **1e**-modified STSSCNLSK (ESI source, triply charged ion of m/z 512.22).

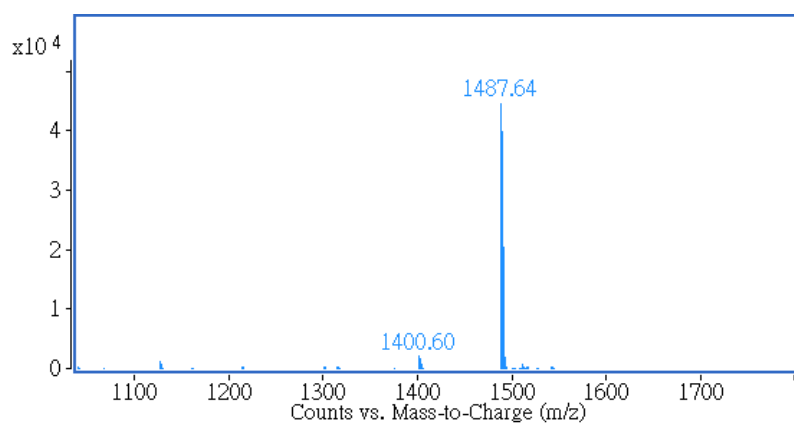
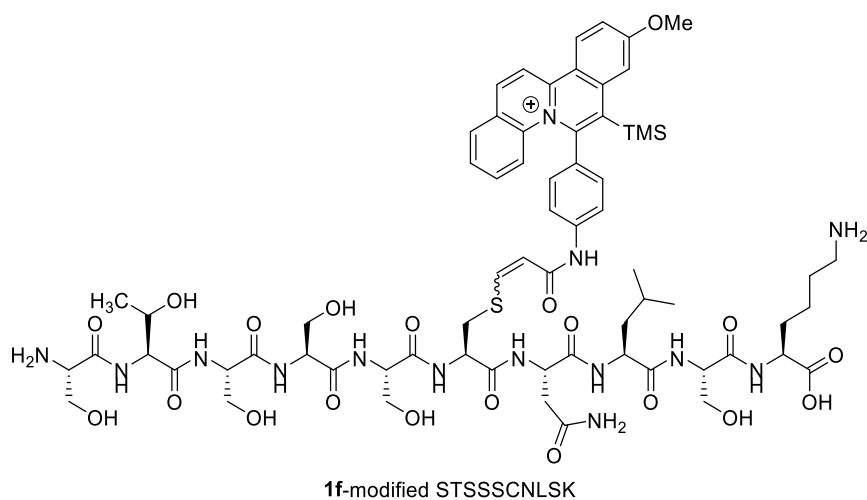


Figure S19. Deconvoluted mass spectrum of **1f**-modified STSSSCNLSK (m/z 1487.64).

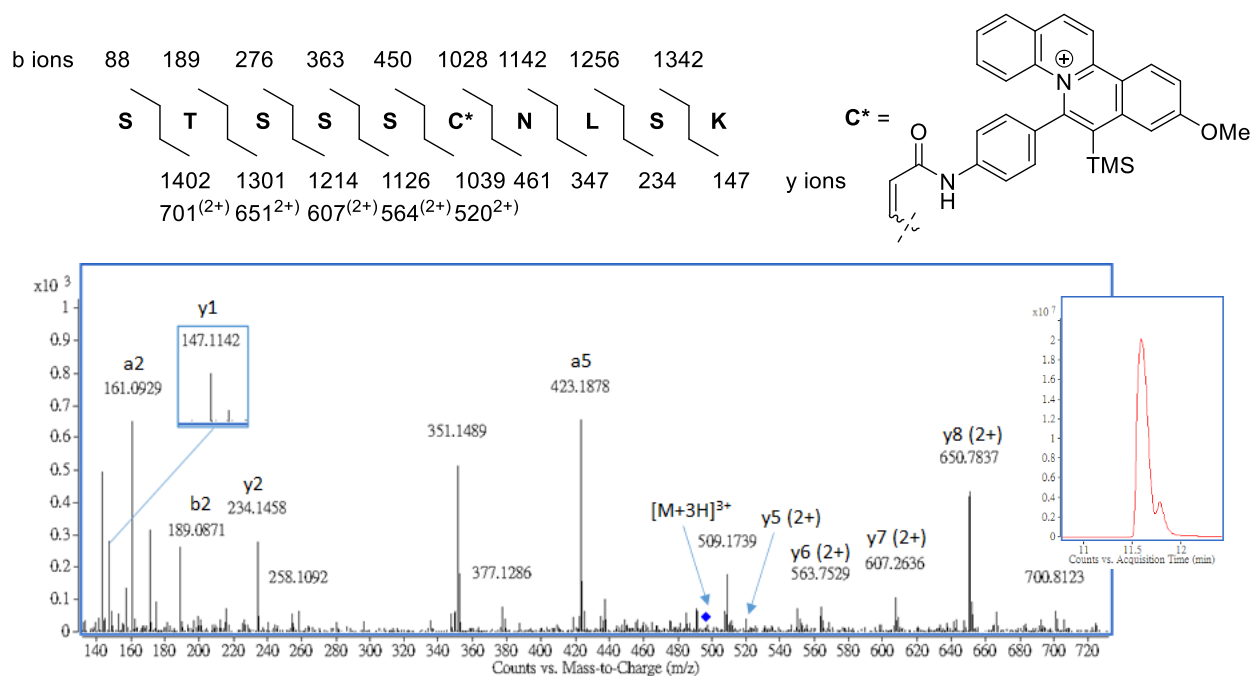


Figure S20. MS/MS spectrum and extracted ion chromatogram (Inset) of **1f**-modified STSSSCNLSK (ESI source, triply charged ion of m/z 496.88).

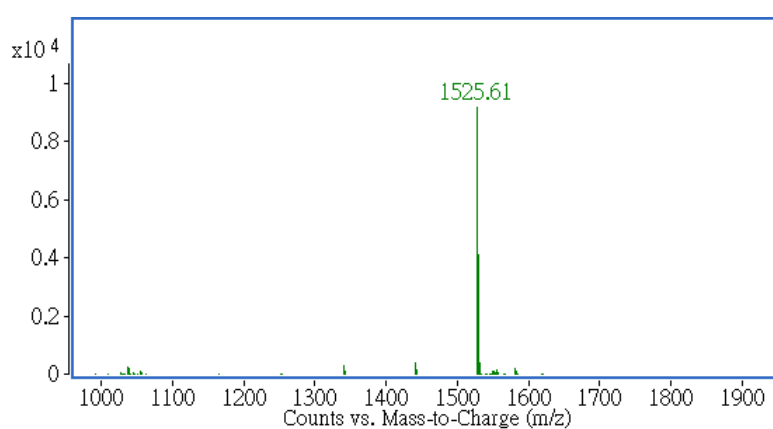
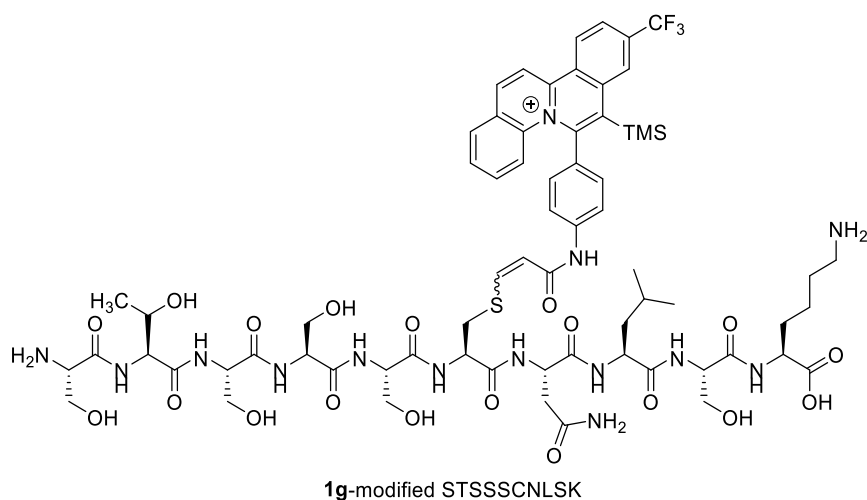


Figure S21. Deconvoluted mass spectrum of **1g**-modified STSSCNLSK (m/z 1525.61).

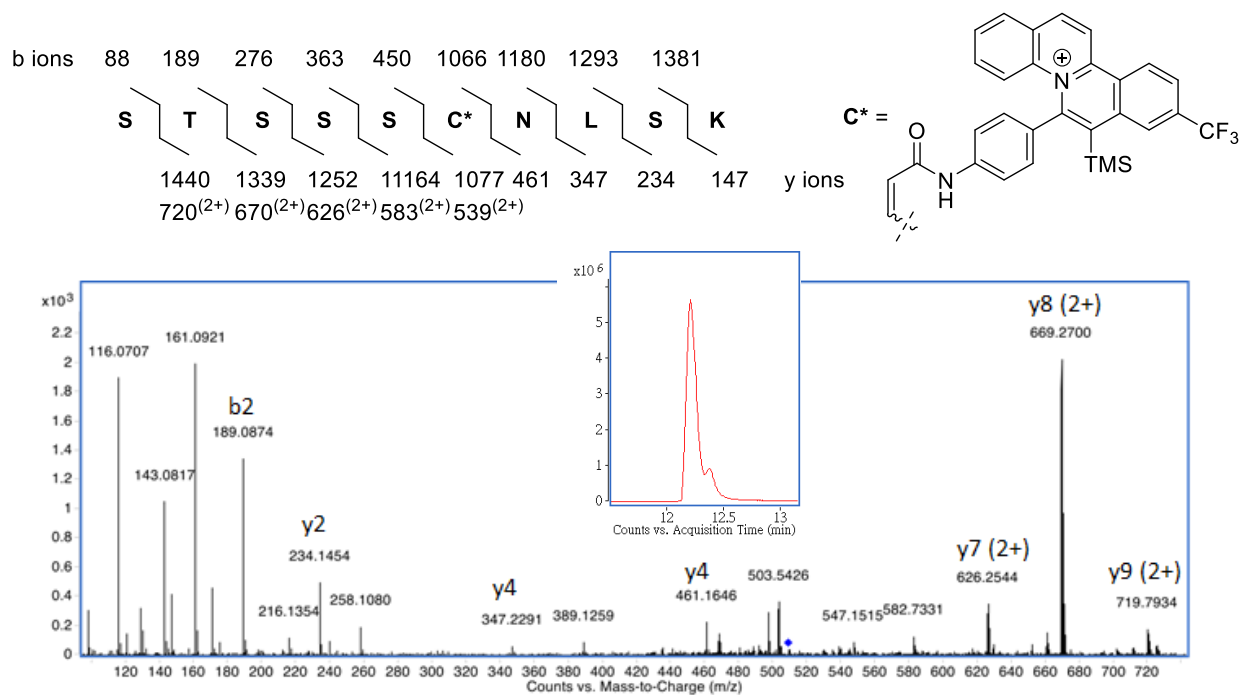


Figure S22. MS/MS spectrum and extracted ion chromatogram (Inset) of **1g**-modified STSSCNLSK (ESI source, triply charged ion of m/z 509.54).

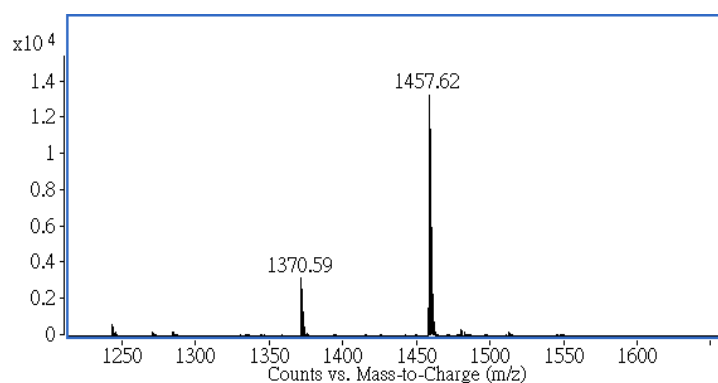
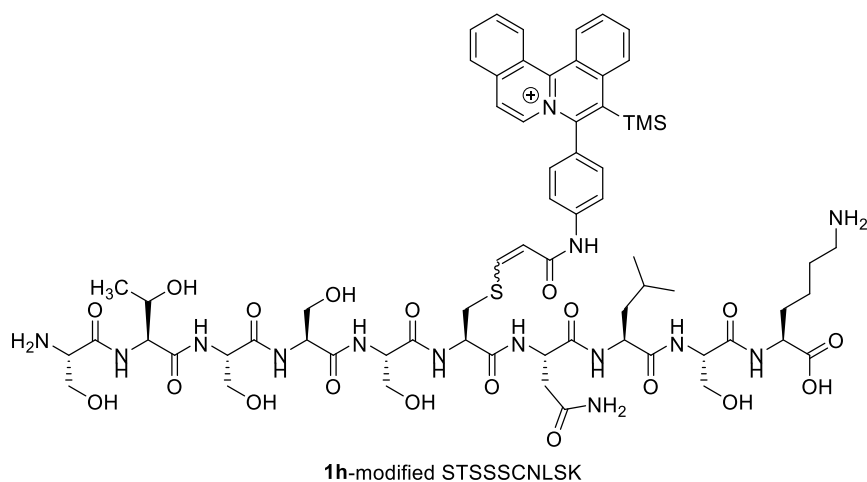


Figure S23. Deconvoluted mass spectrum of **1h**-modified STSSCNLSK (m/z 1457.62).

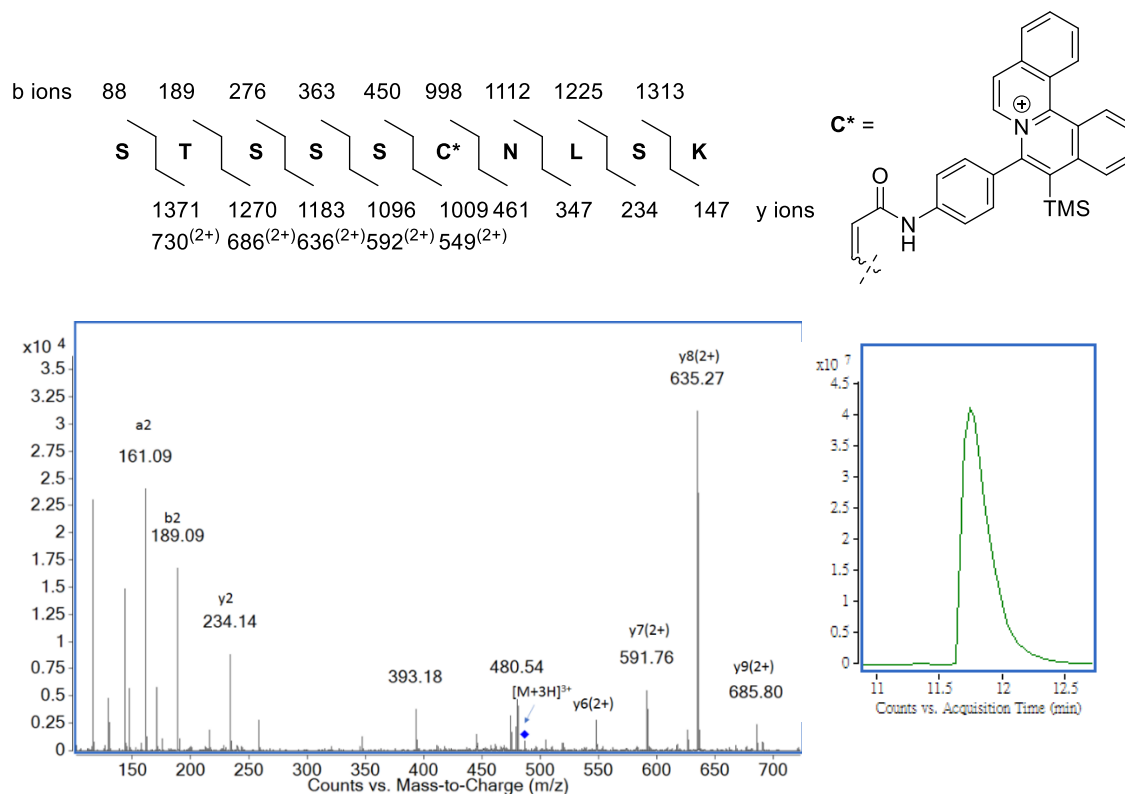
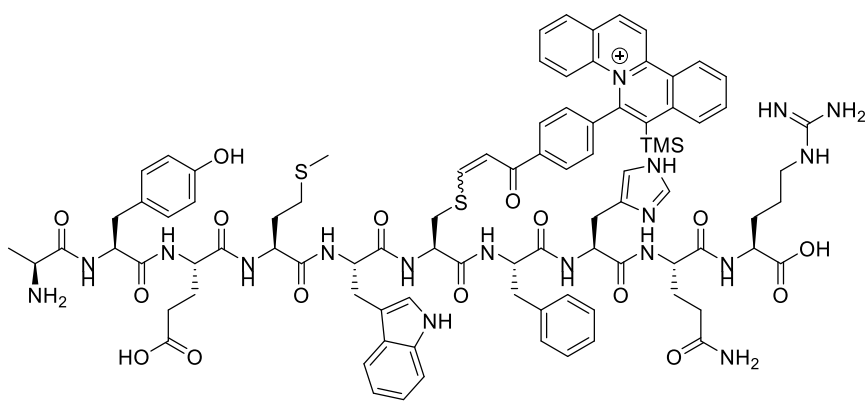


Figure S24. MS/MS spectrum and extracted ion chromatogram (Inset) of **1h**-modified STSSCNLSK (ESI source, triply charged ion of m/z 486.88).



1a-modified AYEMWCFHQR

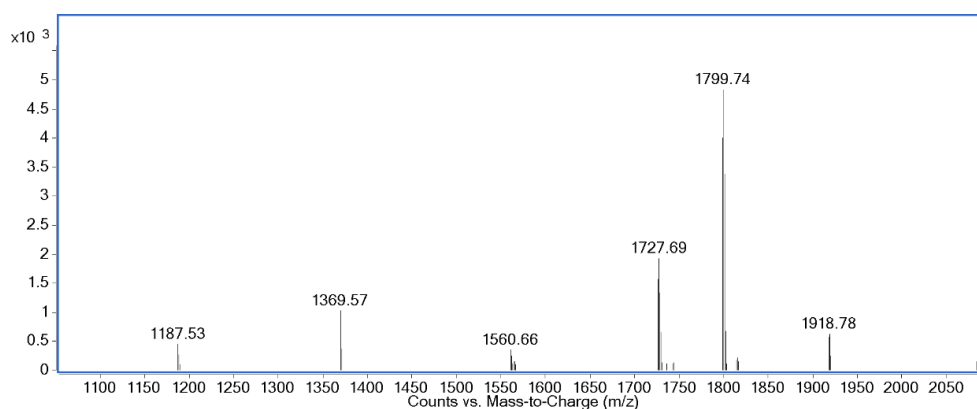


Figure S25. Deconvoluted mass spectrum of **1a**-modified AYEMWCFHQR (m/z 1799.74).

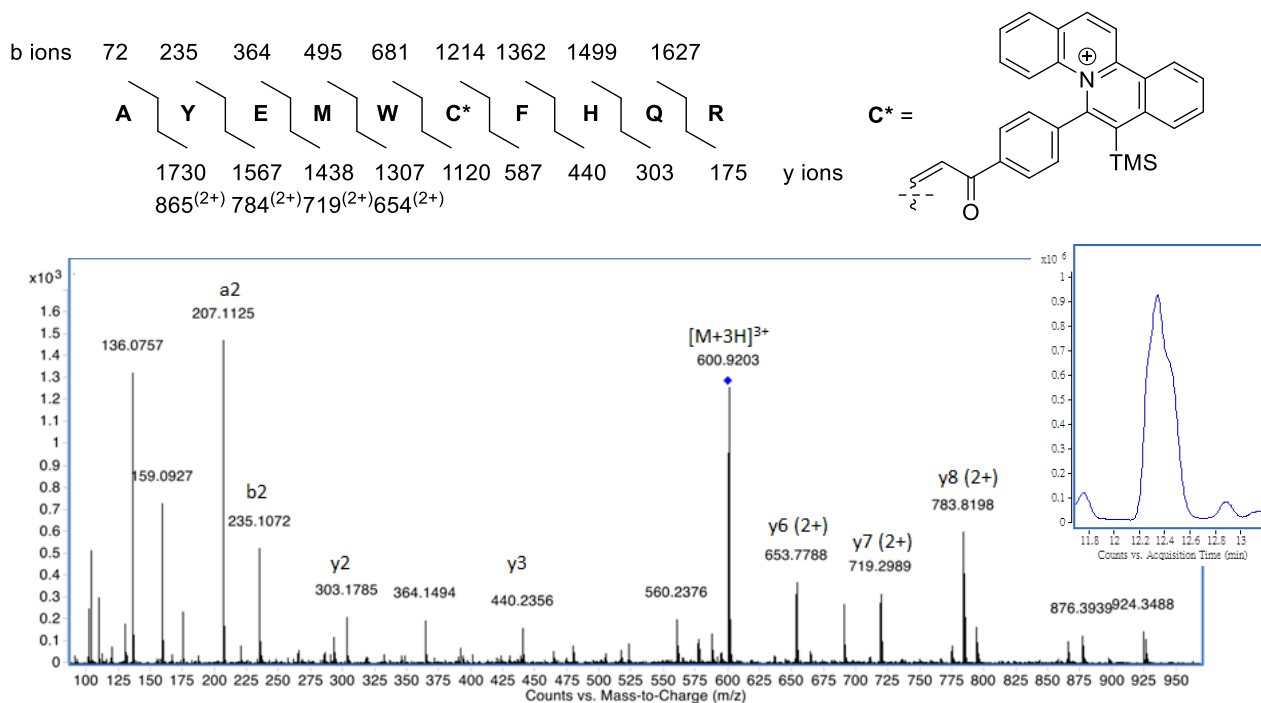
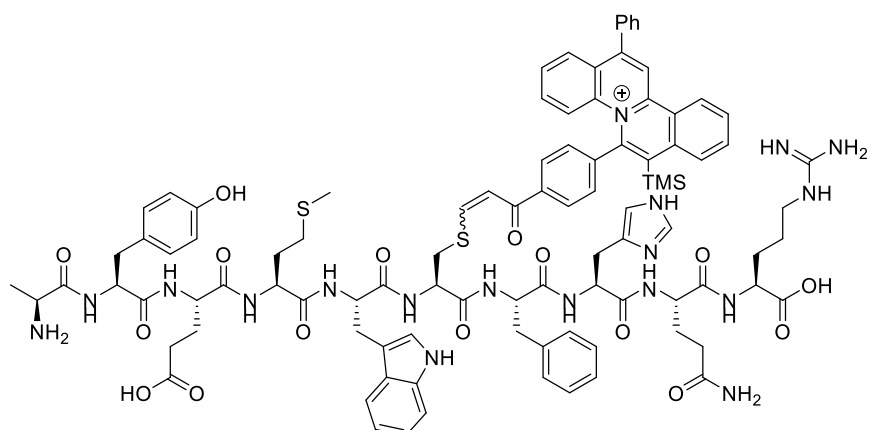


Figure S26. MS/MS spectrum and extracted ion chromatogram (Inset) of **1a**-modified AYEMWCFHQR (ESI source, triply charged ion of m/z 600.92).



1b-modified AYEMWCFHQR

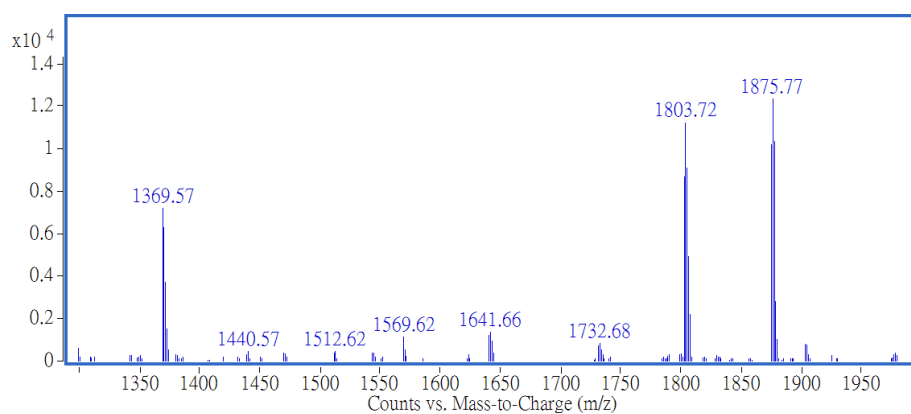


Figure S27. Deconvoluted mass spectrum of **1b**-modified AYEMWCFHQR (m/z 1875.77).

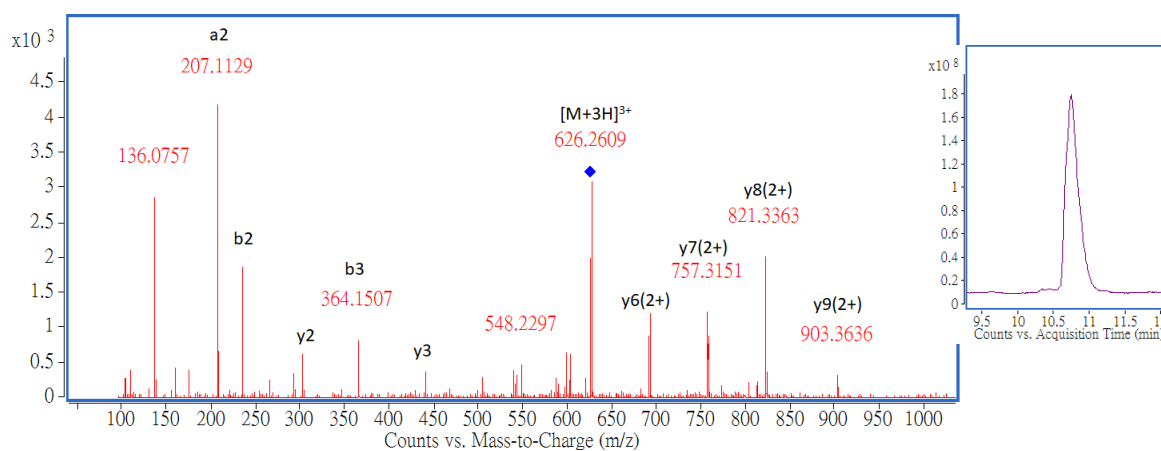
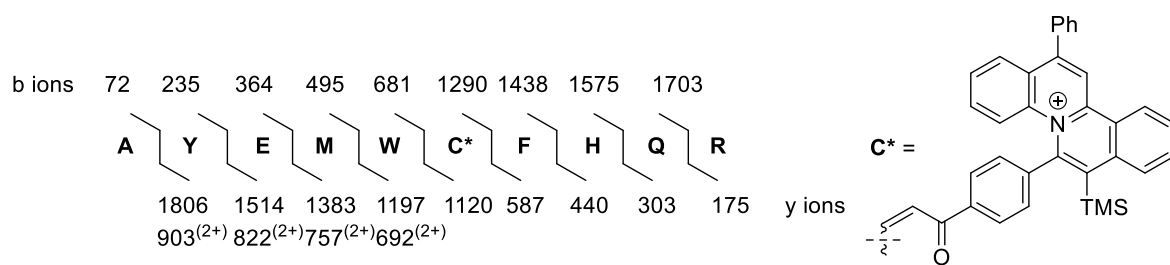


Figure S28. MS/MS spectrum and extracted ion chromatogram (Inset) of **1b**-modified AYEMWCFHQR (ESI source, triply charged ion of m/z 626.26).

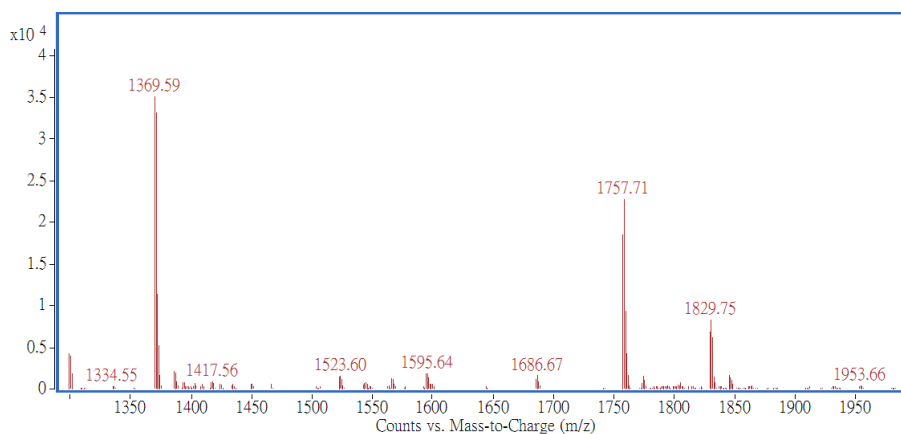
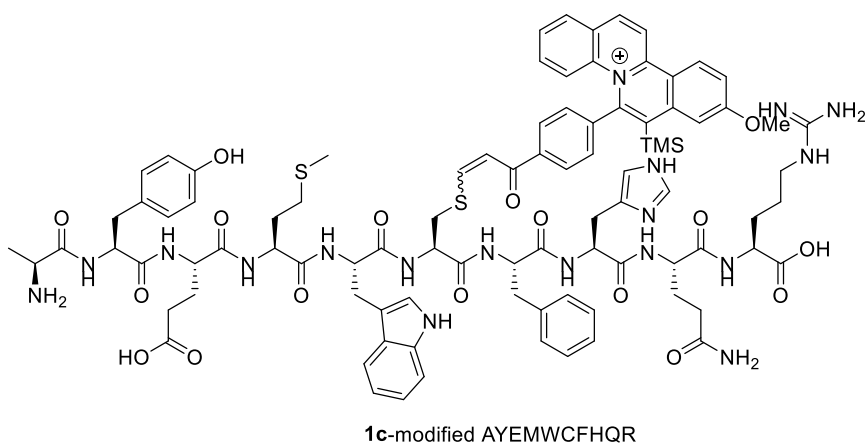


Figure S29. Deconvoluted mass spectrum of **1c**-modified AYEMWCFHQR (m/z 1829.75).

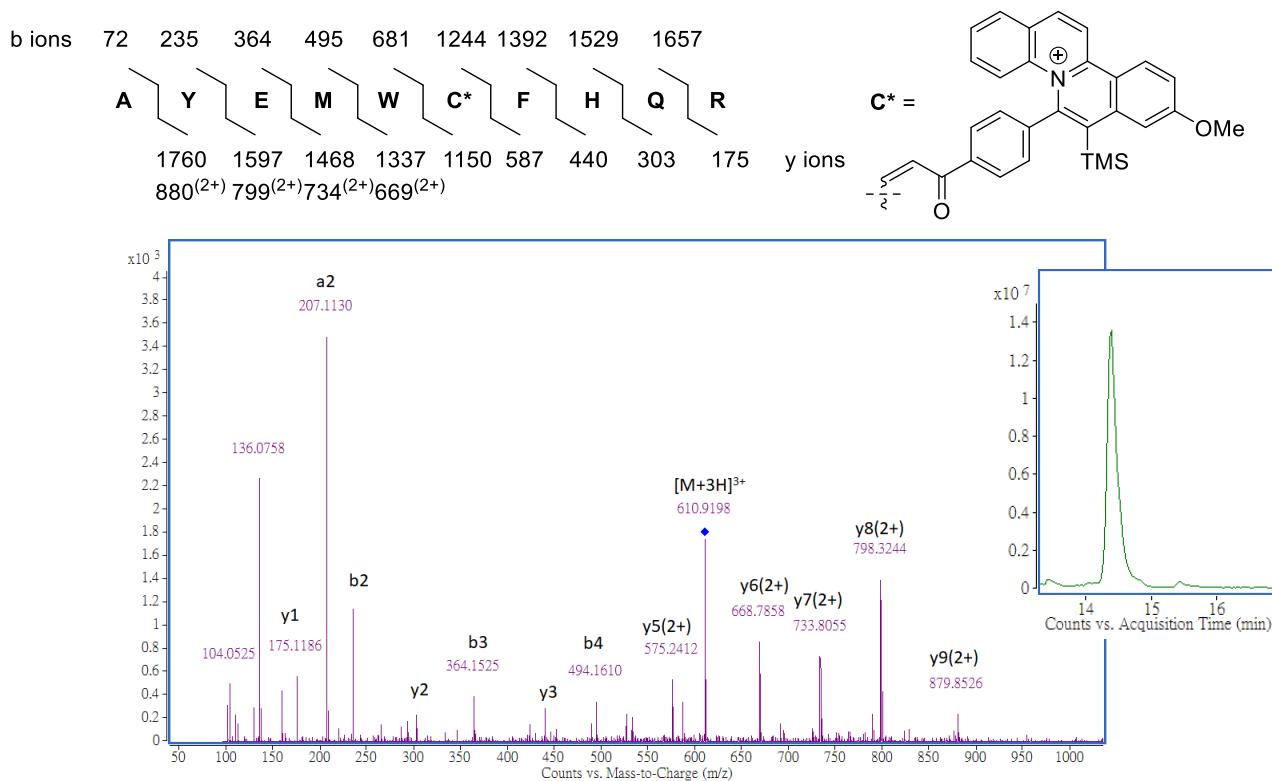


Figure S30. MS/MS spectrum and extracted ion chromatogram (Inset) of **1c**-modified AYEMWCFHQR (ESI source, triply charged ion of m/z 610.92).

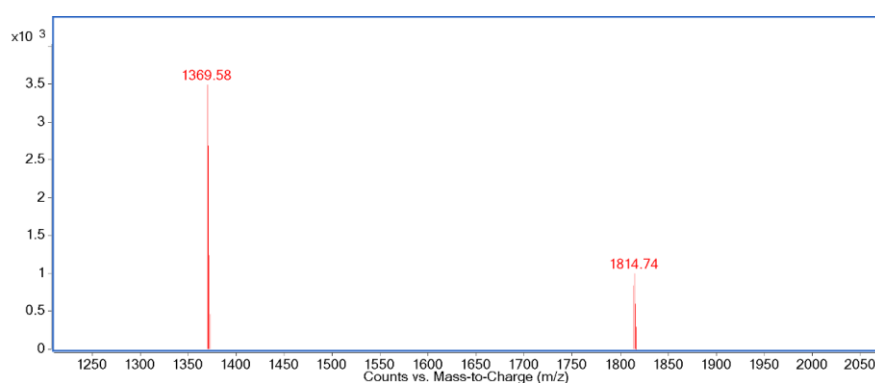
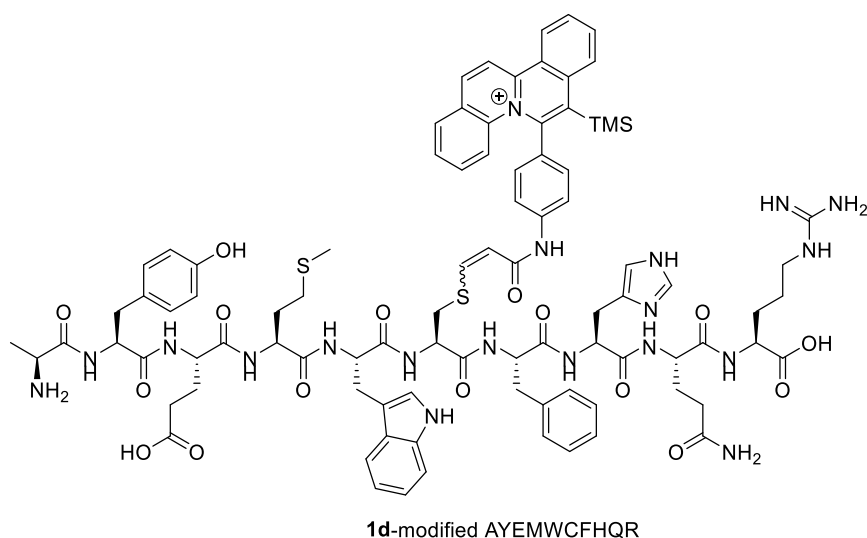


Figure S31. Deconvoluted mass spectrum of **1d**-modified AYEMWCFHQR (m/z 1814.74).

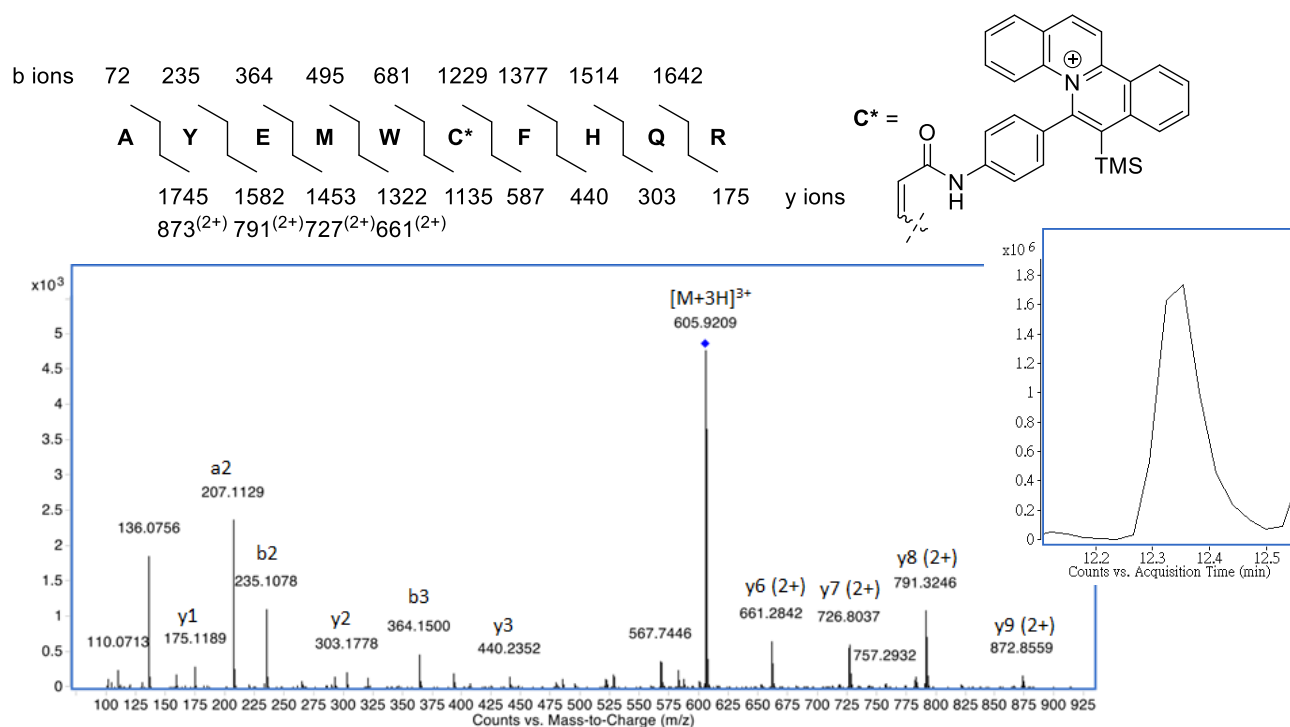


Figure S32. MS/MS spectrum and extracted ion chromatogram (Inset) of **1d**-modified AYEMWCFHQR (ESI source, triply charged ion of m/z 605.92).

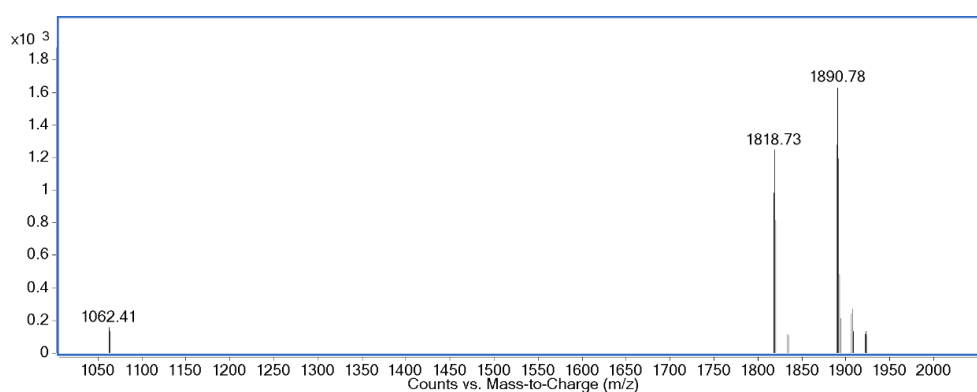
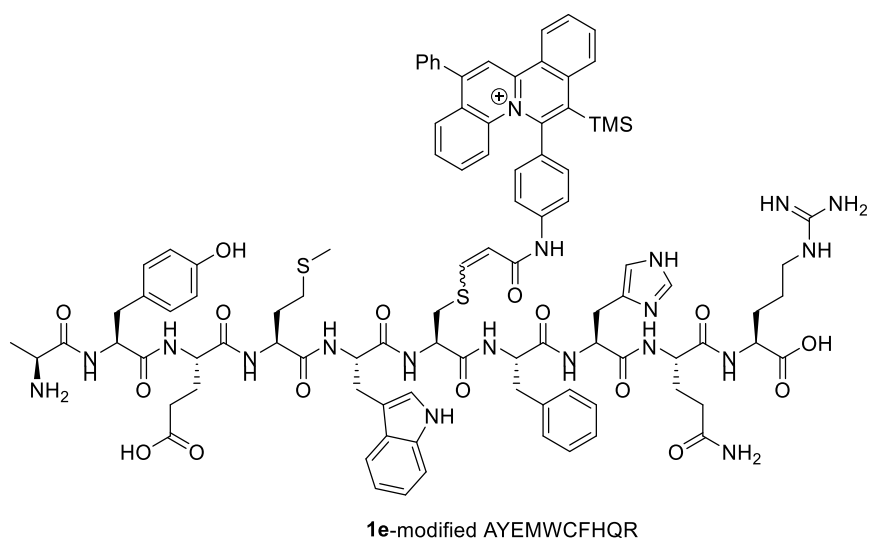


Figure S33. Deconvoluted mass spectrum of **1e**-modified AYEMWCFHQR (m/z 1890.78).

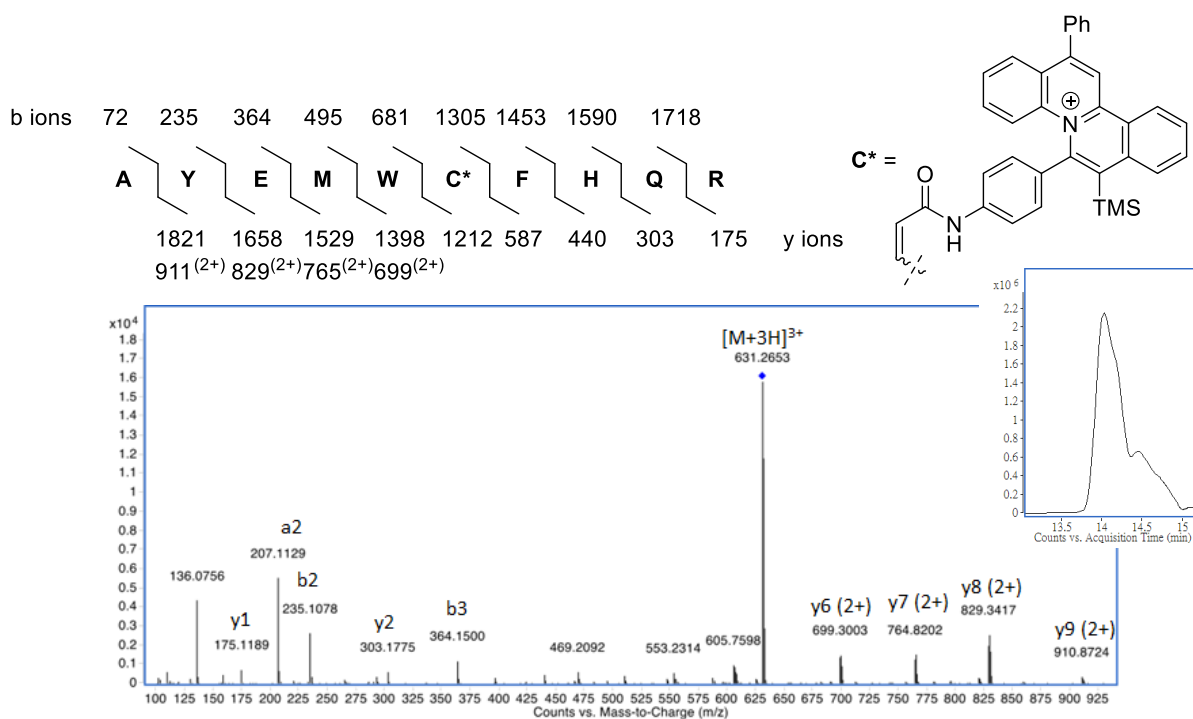


Figure S34. MS/MS spectrum and extracted ion chromatogram (Inset) of **1e**-modified AYEMWCFHQR (ESI source, triply charged ion of m/z 631.26).

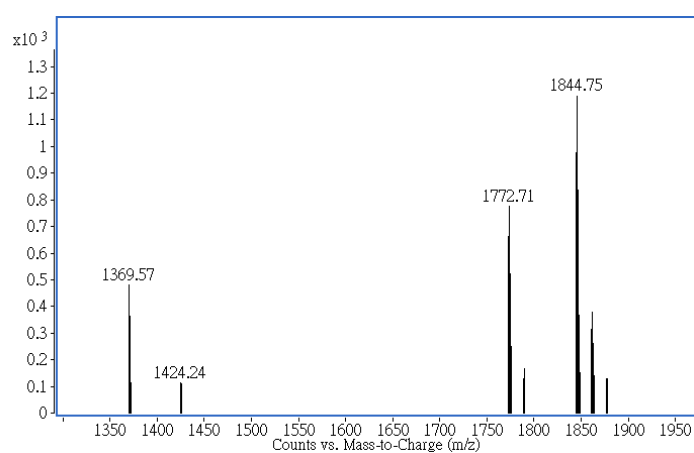
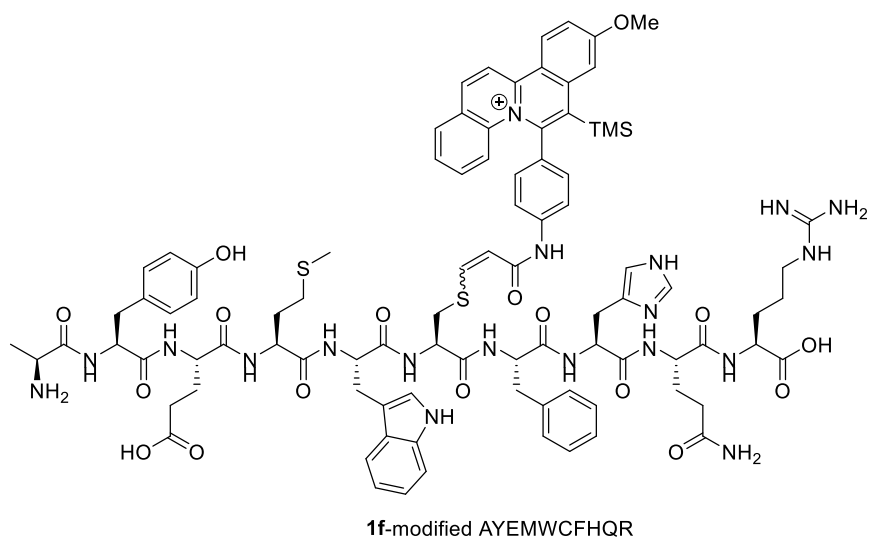


Figure S35. Deconvoluted mass spectrum of **1f**-modified AYEMWCFHQR (m/z 1844.75).

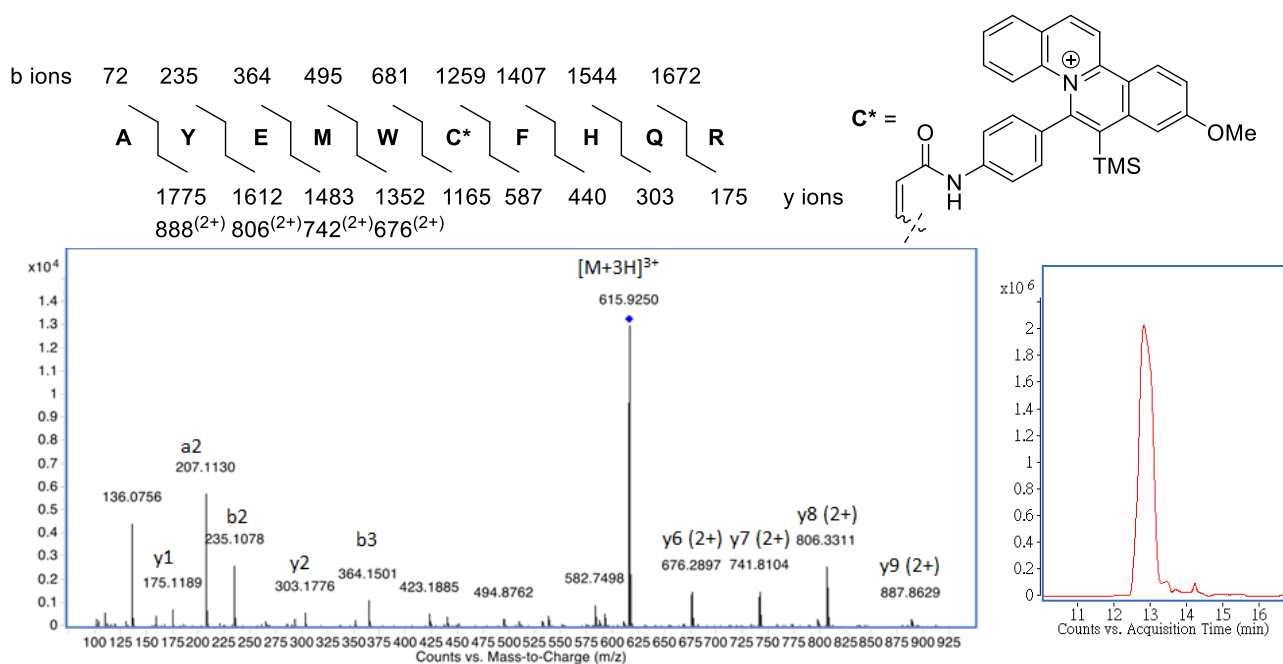


Figure S36. MS/MS spectrum and extracted ion chromatogram (Inset) of **1f**-modified AYEMWCFHQR (ESI source, triply charged ion of m/z 615.92).

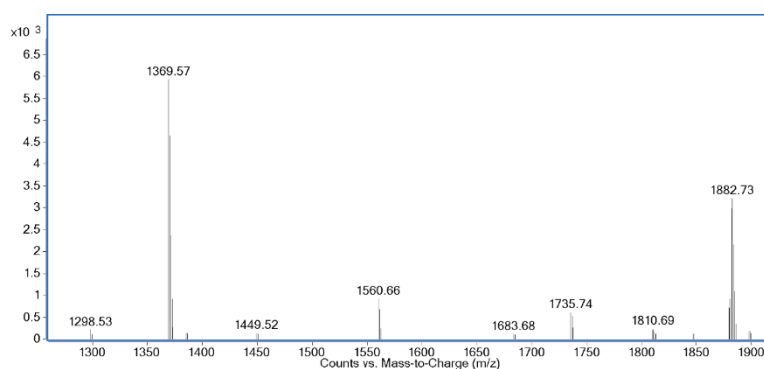
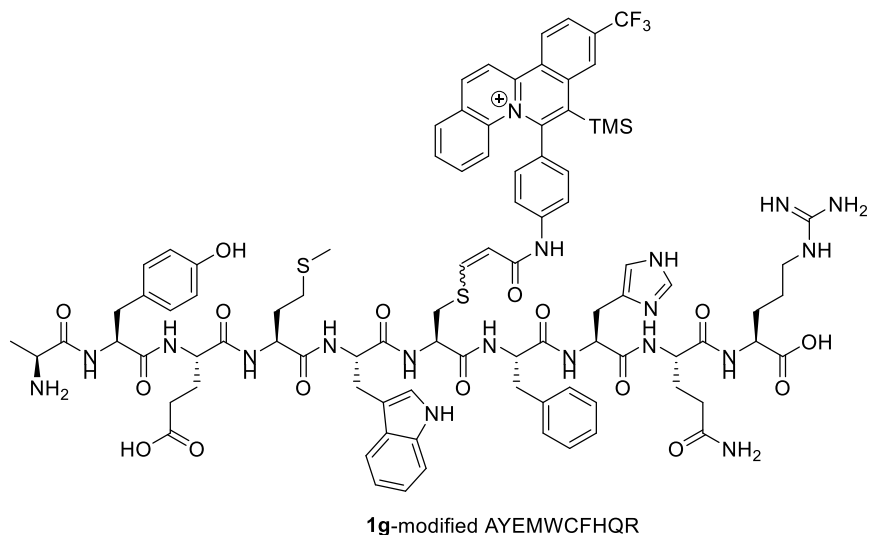


Figure S37. Deconvoluted mass spectrum of **1g**-modified AYEMWCFHQR (m/z 1844.75).

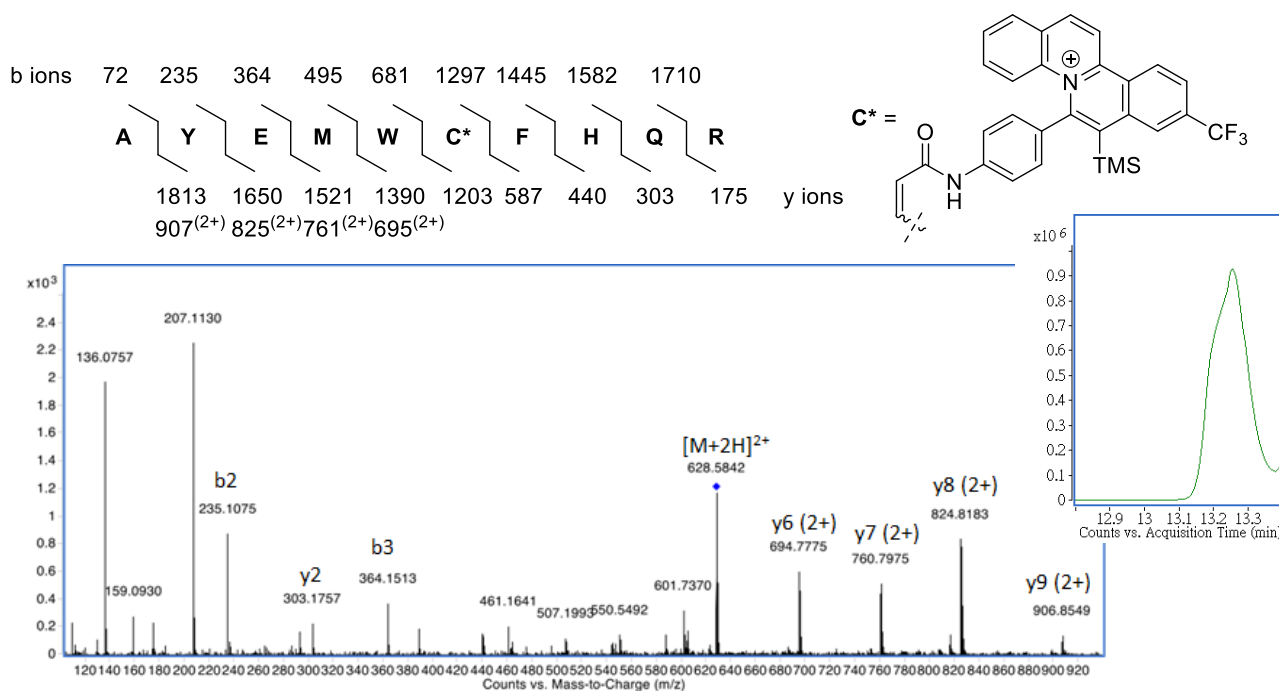


Figure S38. MS/MS spectrum and extracted ion chromatogram (Inset) of **1g**-modified AYEMWCFHQR (ESI source, triply charged ion of m/z 628.58).

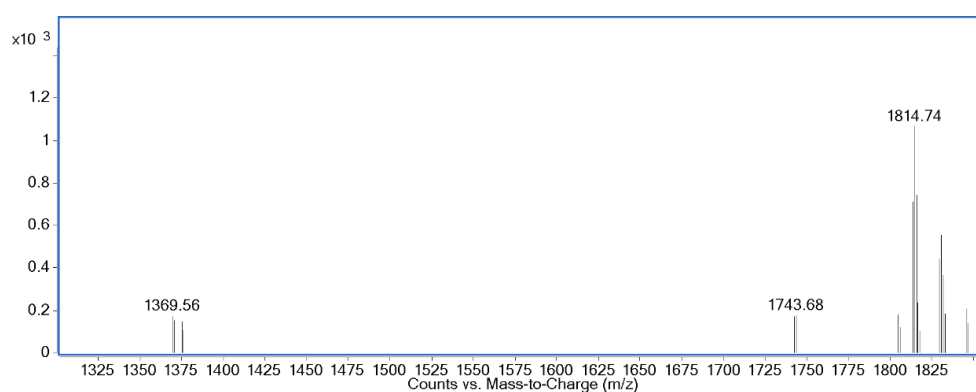
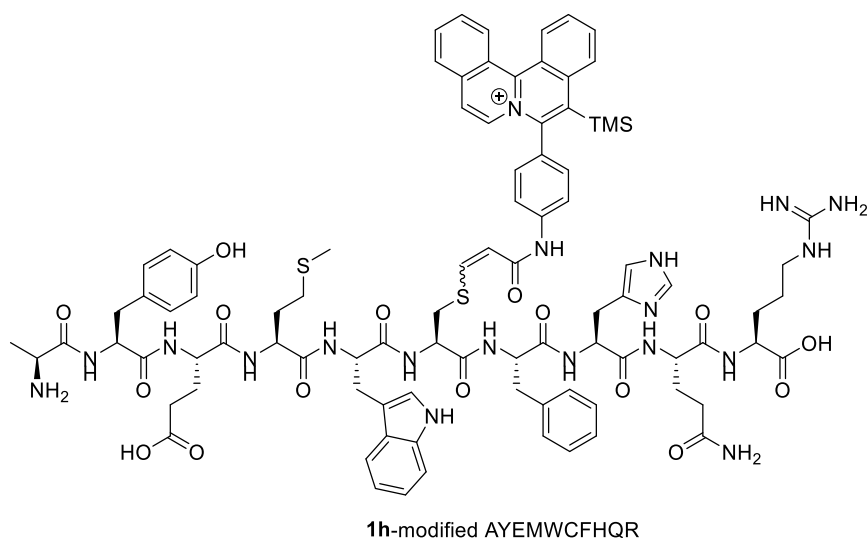


Figure S39. Deconvoluted mass spectrum of **1h**-modified AYEMWCFHQR (m/z 1814.74).

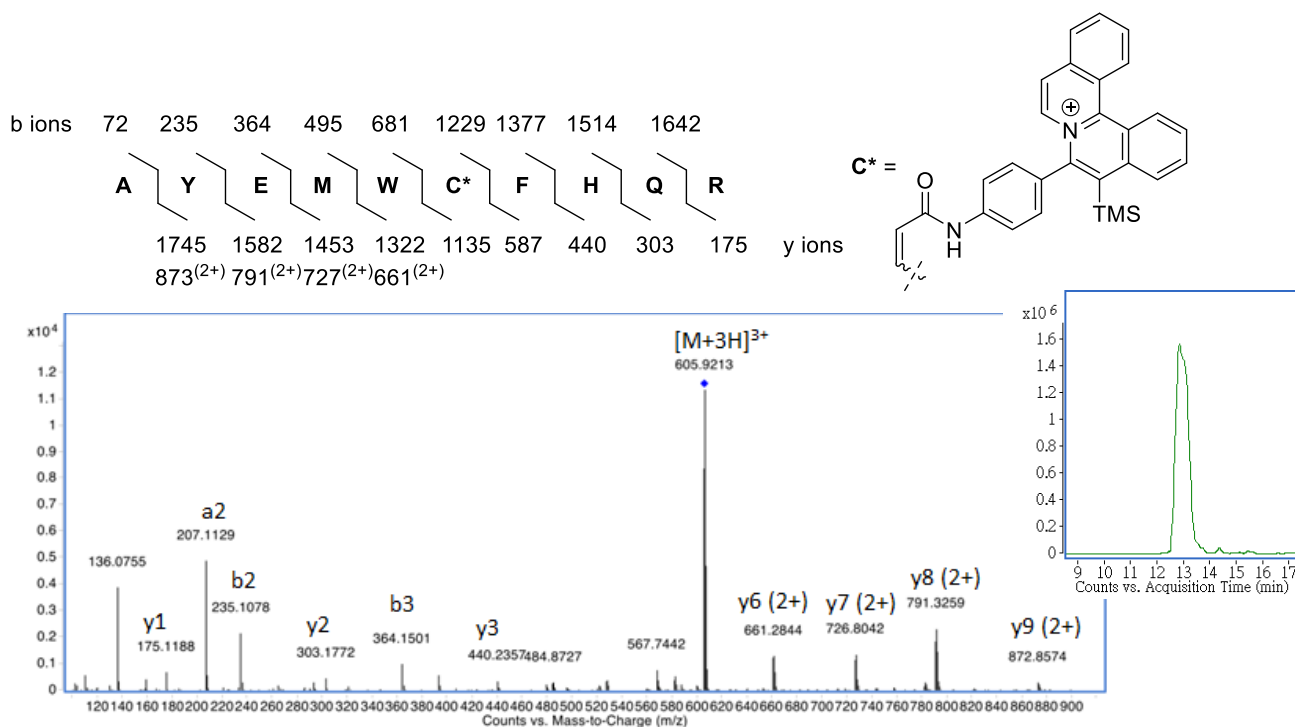


Figure S40. MS/MS spectrum and extracted ion chromatogram (Inset) of **1h**-modified AYEMWCFHQR (ESI source, triply charged ion of m/z 605.92).

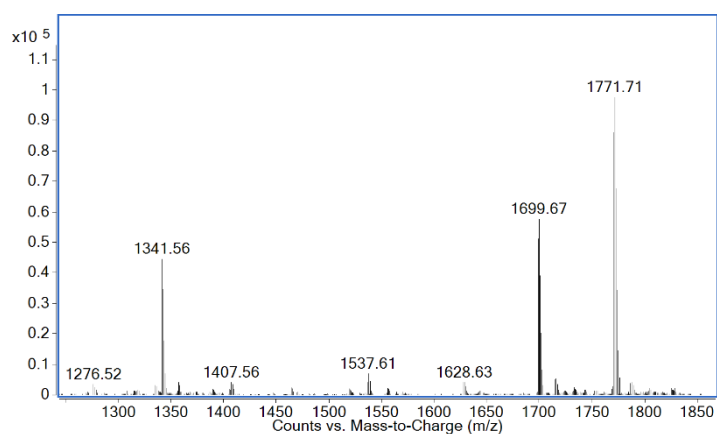
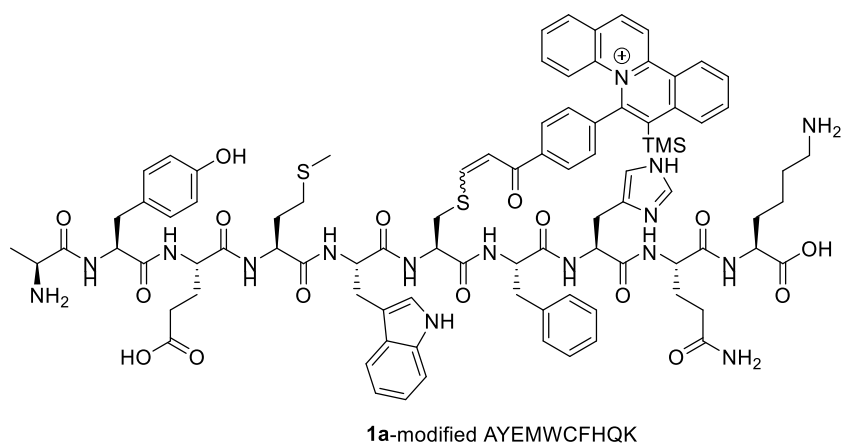


Figure S41. Deconvoluted mass spectrum of **1a**-modified AYEMWCFHQK (m/z 1771.71).

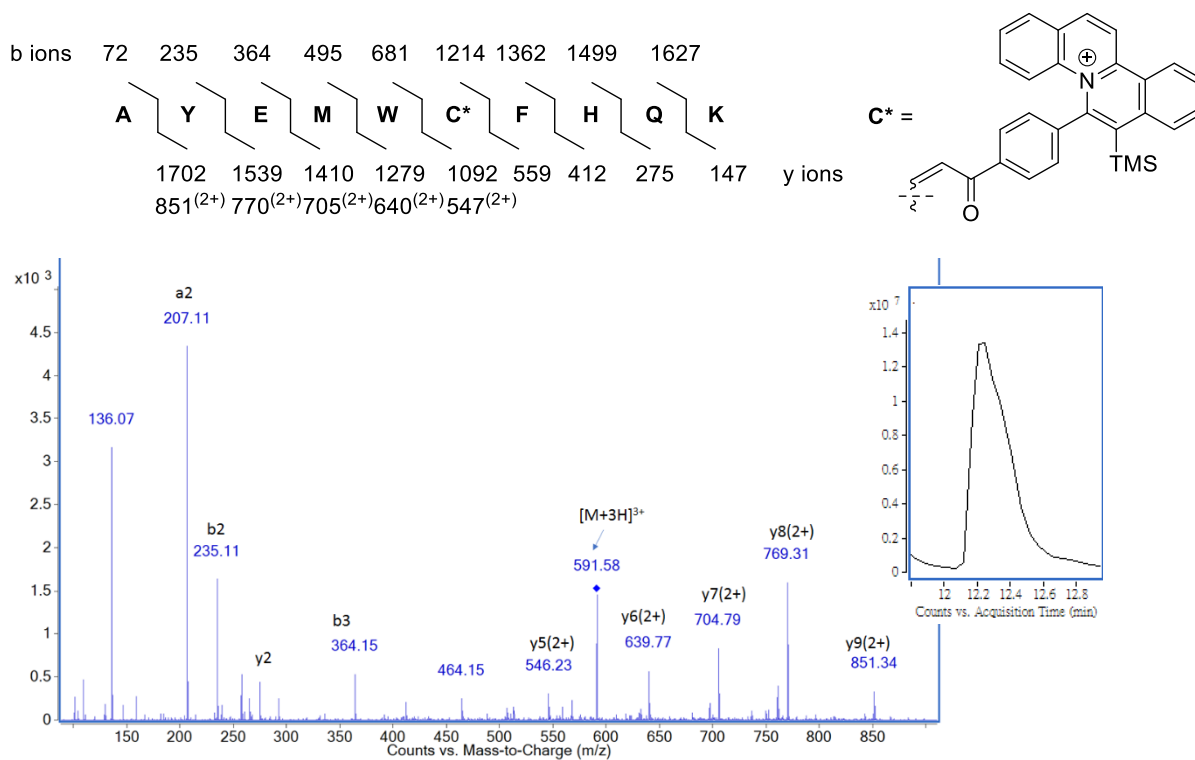


Figure S42. MS/MS spectrum and extracted ion chromatogram (Inset) of **1a**-modified AYEMWCFHQK (ESI source, triply charged ion of m/z 591.58).

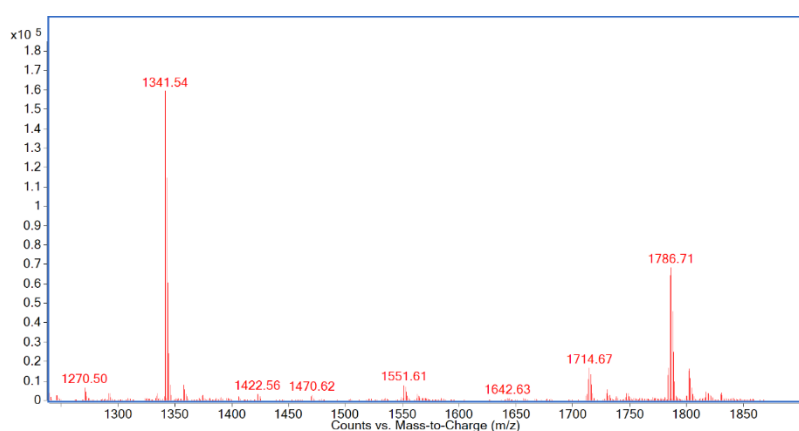
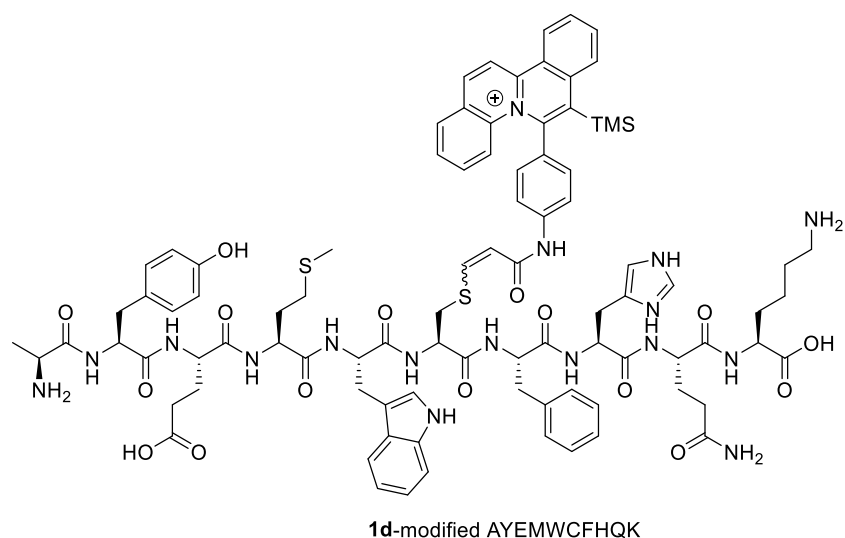


Figure S43. Deconvoluted mass spectrum of **1d**-modified AYEMWCFHQK (m/z 1786.71).

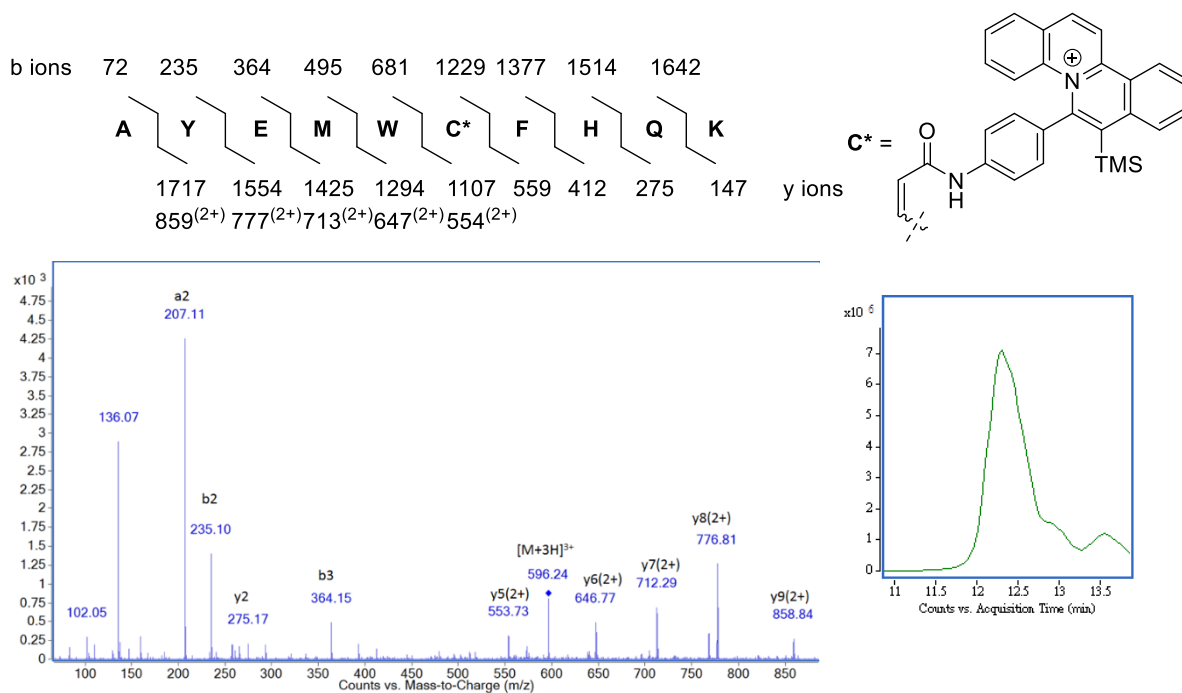


Figure S44. MS/MS spectrum and extracted ion chromatogram (Inset) of **1d**-modified AYEMWCFHQK (ESI source, triply charged ion of m/z 596.24).

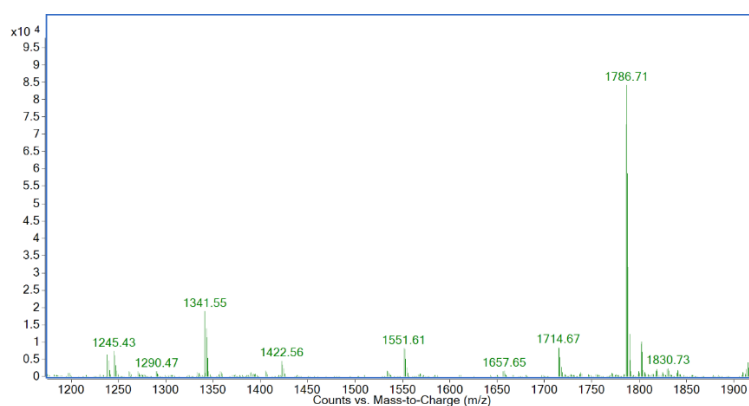
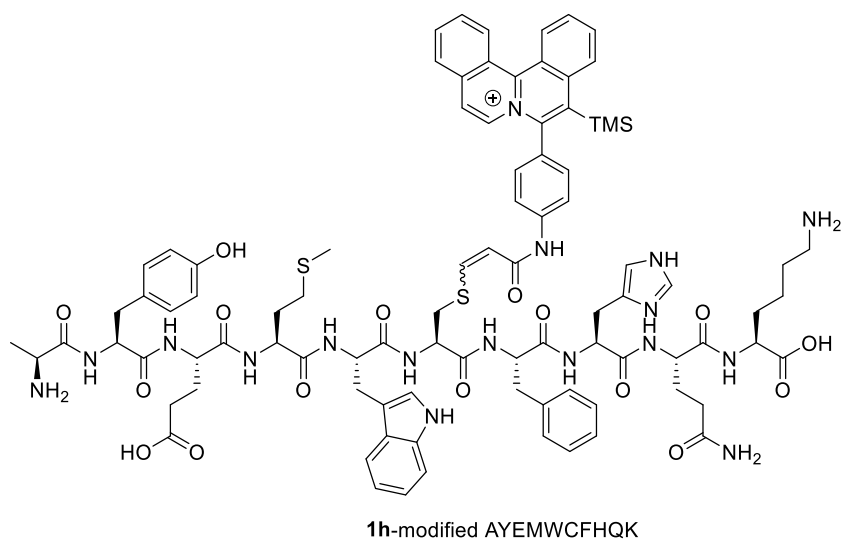


Figure S45. Deconvoluted mass spectrum of **1h**-modified AYEMWCFHQK (m/z 1786.71).

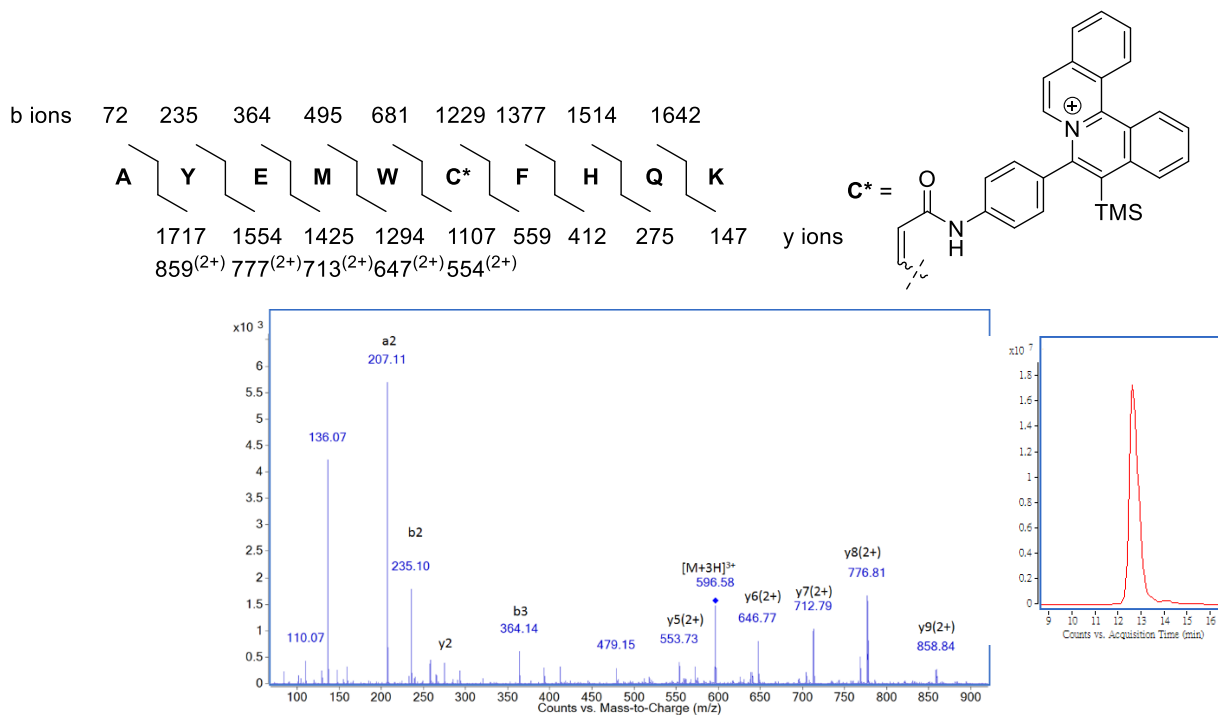


Figure S46. MS/MS spectrum and extracted ion chromatogram (Inset) of **1h**-modified AYEMWCFHQK (ESI source, triply charged ion of m/z 596.58).

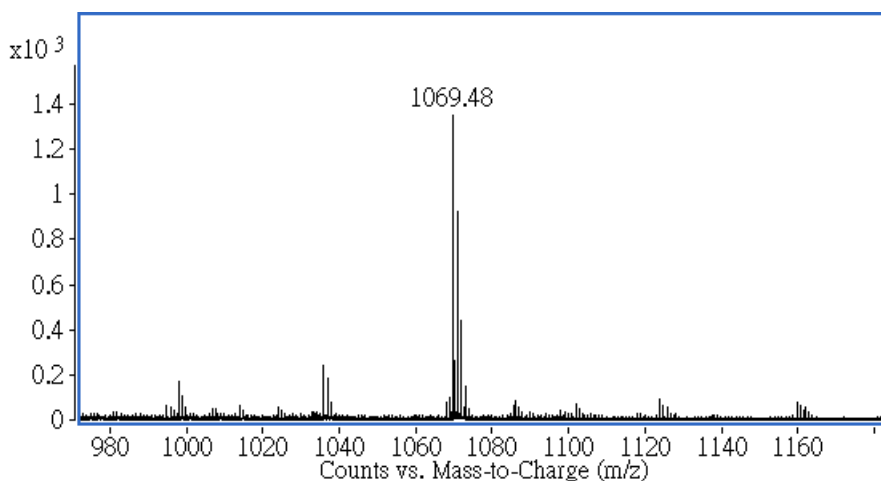
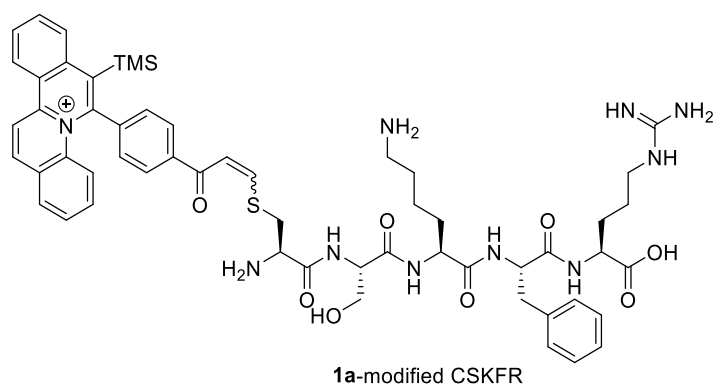


Figure S47. Deconvoluted mass spectrum of **1a-modified CSKFR** (m/z 1069.48).

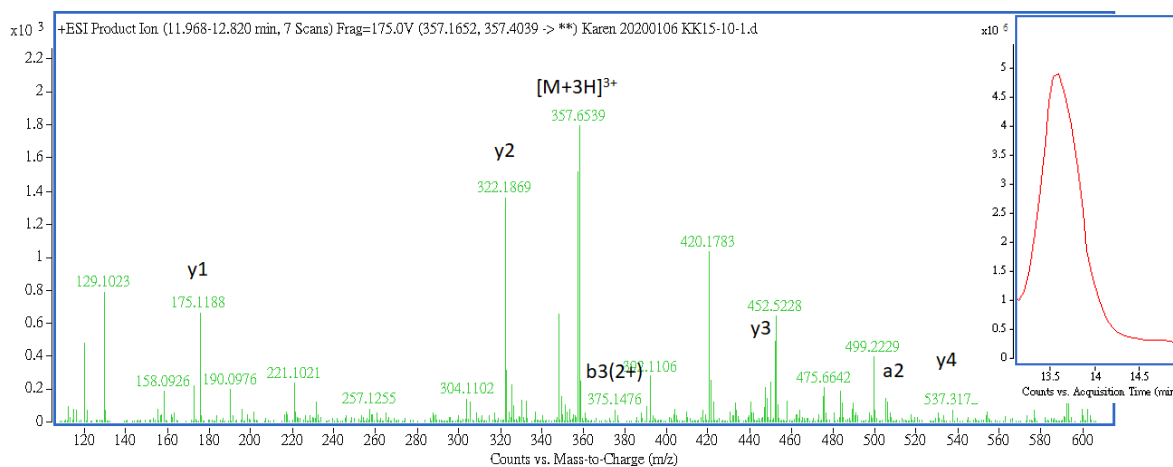
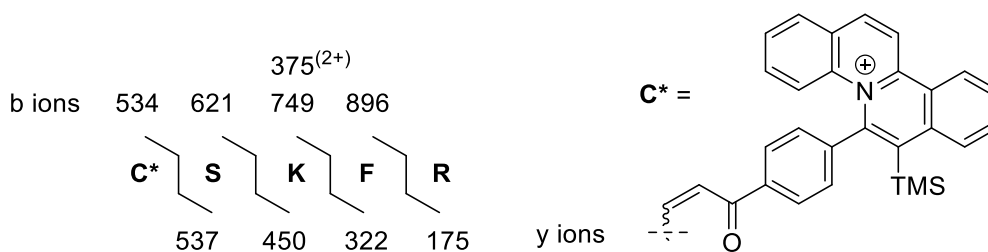


Figure S48. MS/MS spectrum and the extracted ion chromatogram (Inset) of **1a-modified CSKFR** (ESI source, triply charged ion of m/z 357.65).

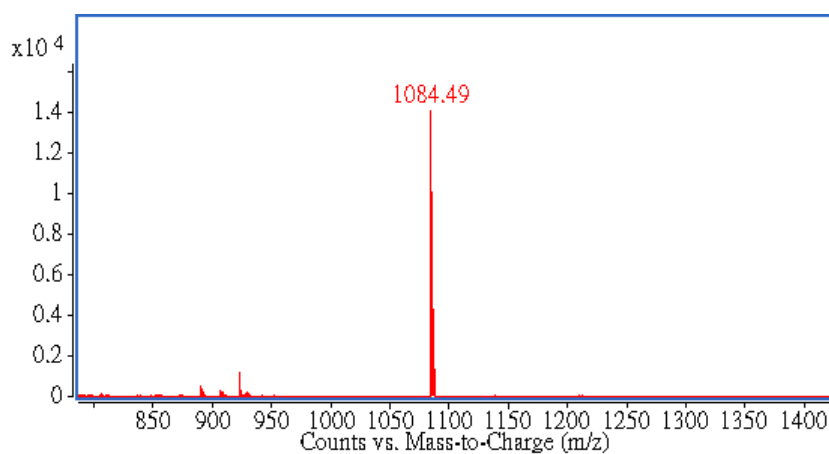
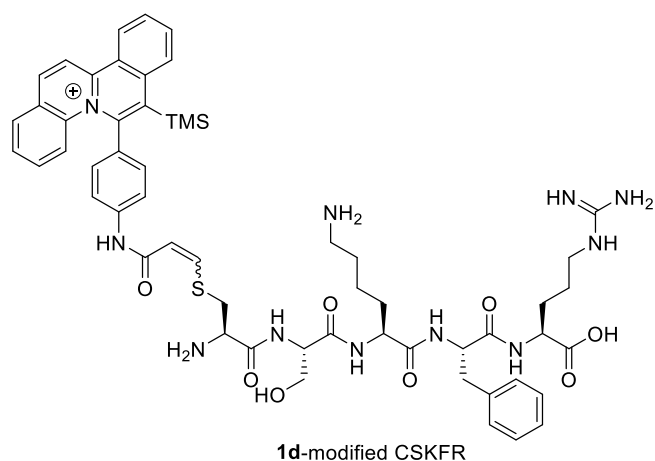


Figure S49. Deconvoluted mass spectrum of **1d**-modified CSKFR (m/z 1084.49).

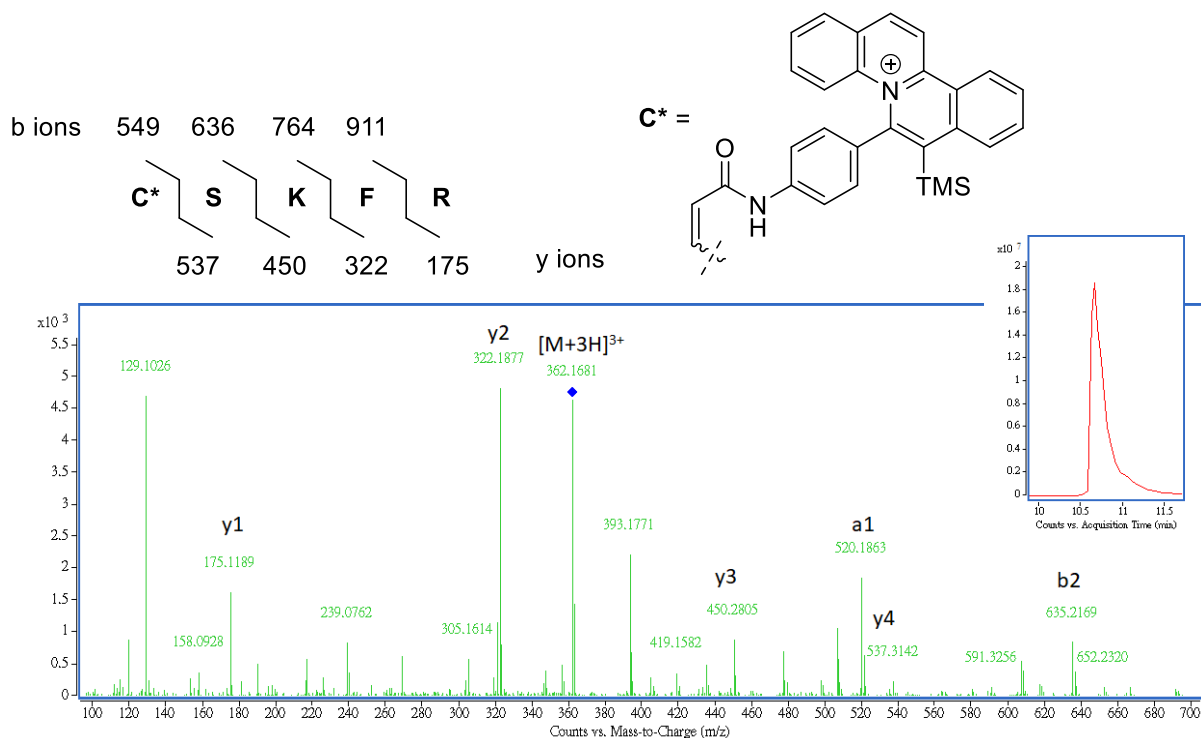


Figure S50. MS/MS spectrum and extracted ion chromatogram (Inset) of **1d**-modified CSKFR (ESI source, triply charged ion of m/z 362.17).

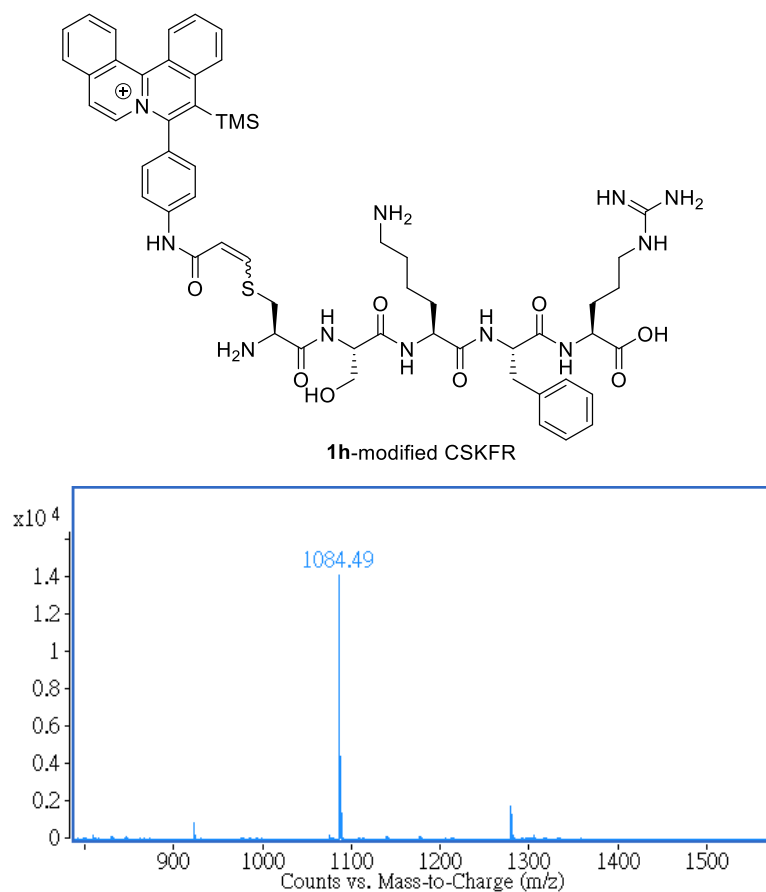


Figure S51. Deconvoluted mass spectrum of **1h**-modified CSKFR (m/z 1084.49).

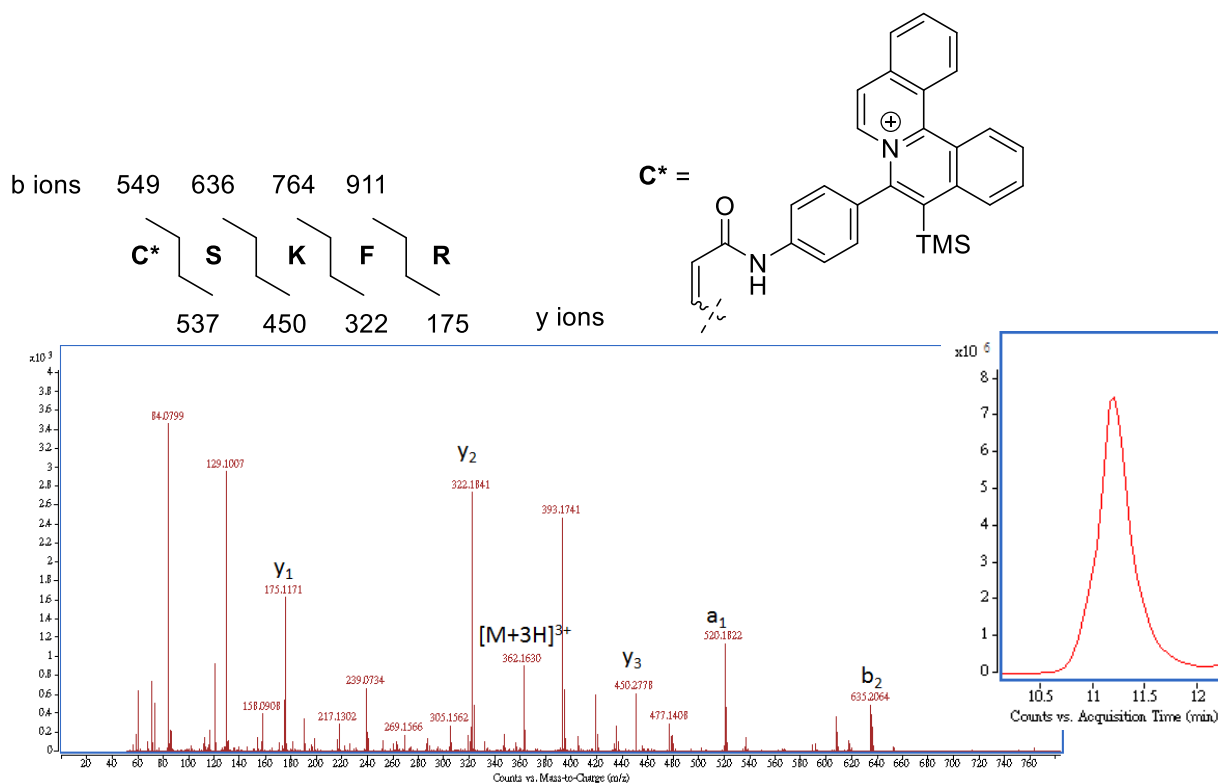


Figure S52. MS/MS spectrum and extracted ion chromatogram (Inset) of **1h**-modified CSKFR (ESI source, triply charged ion of m/z 362.16).

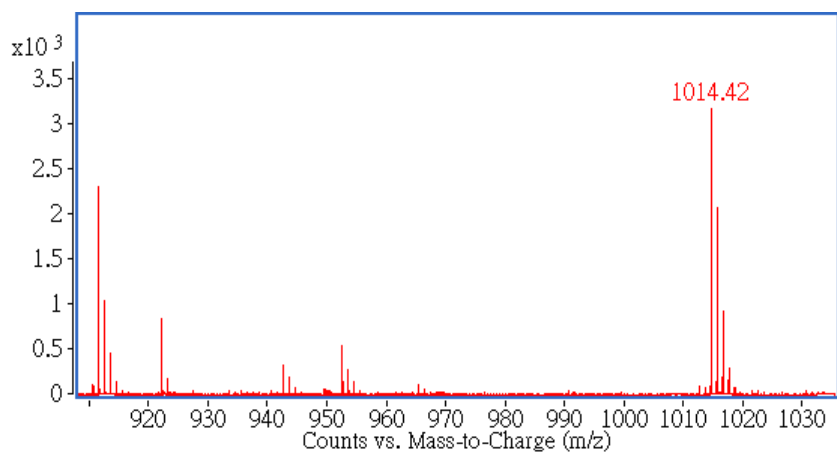
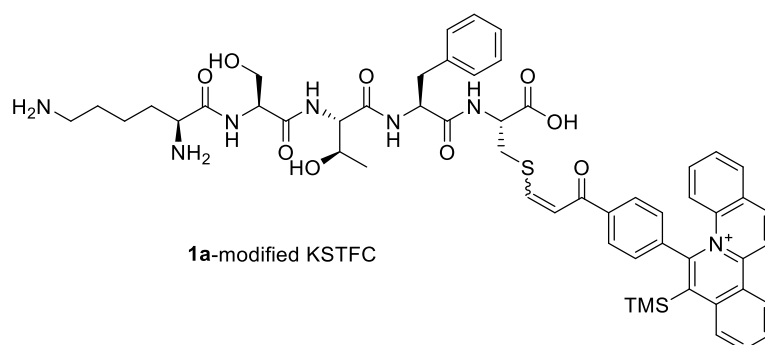


Figure S53. Deconvoluted mass spectrum of **1a-modified KSTFC** (m/z 1014.42).

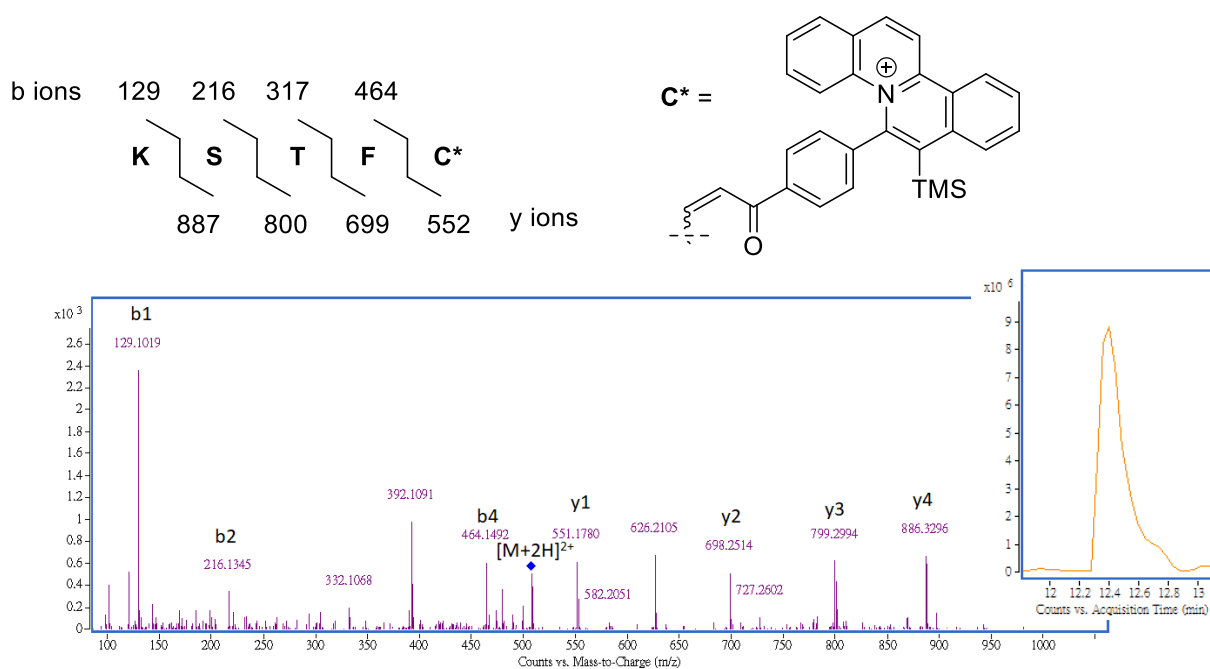


Figure S54. MS/MS spectrum and extracted ion chromatogram (Inset) of **1a-modified KSTFC** (ESI source, doubly charged ion of m/z 508.14).

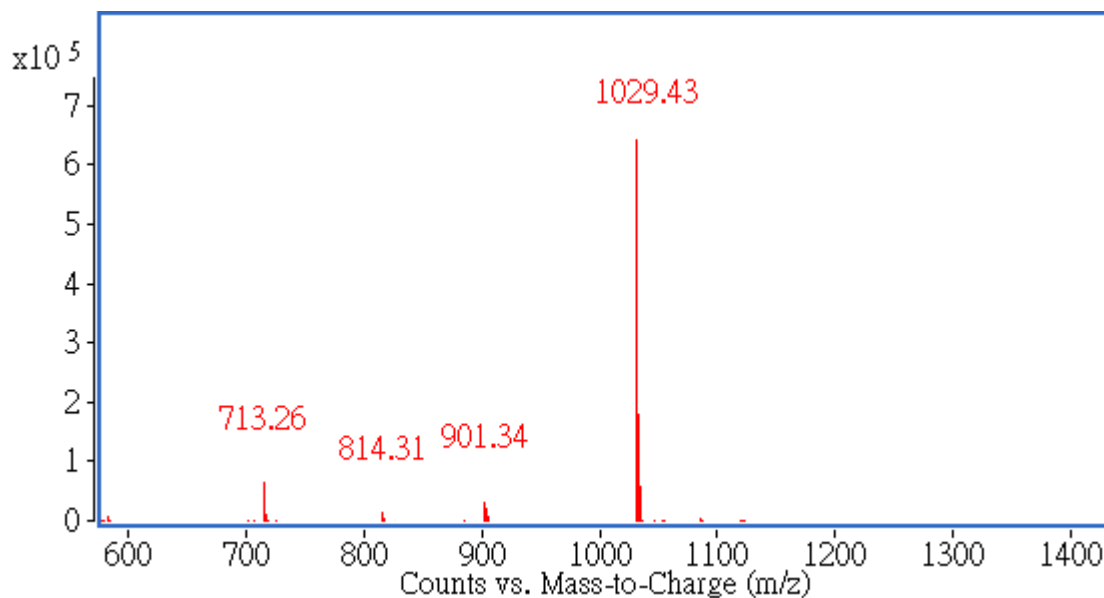
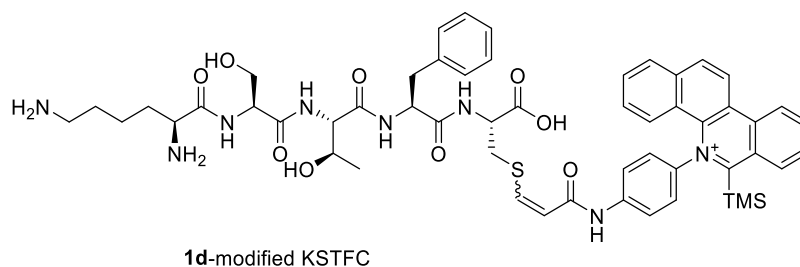


Figure S55. Deconvoluted mass spectrum of **1d-modified KSTFC** (m/z 1029.43).

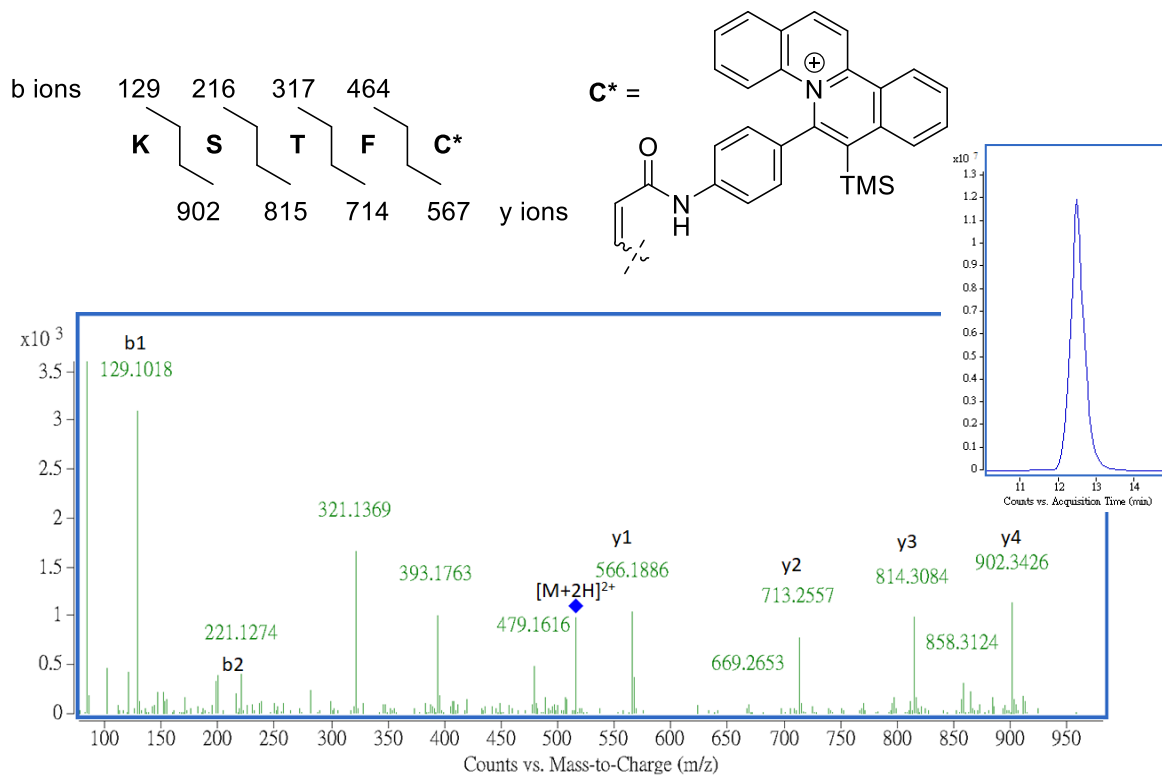


Figure S56. MS/MS spectrum of **1d-modified KSTFC** (ESI source, doubly charged ion of m/z 515.63).

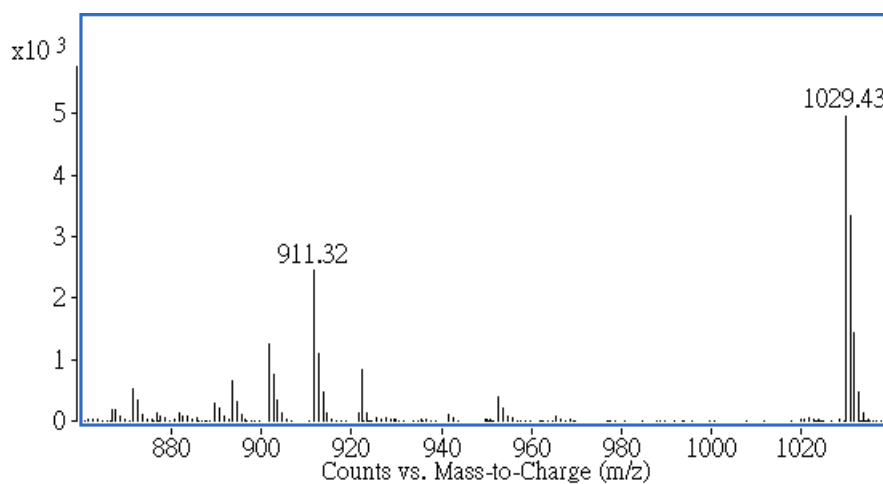
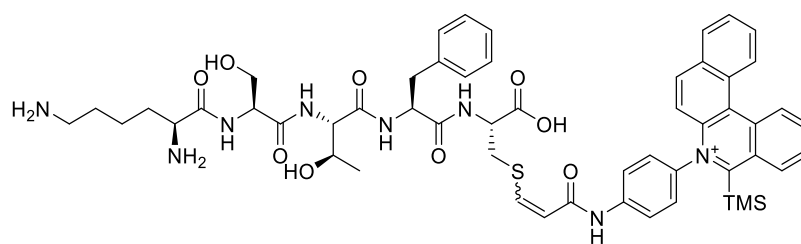


Figure S57. Deconvoluted mass spectrum of **1h**-modified KSTFC (m/z 1029.43).

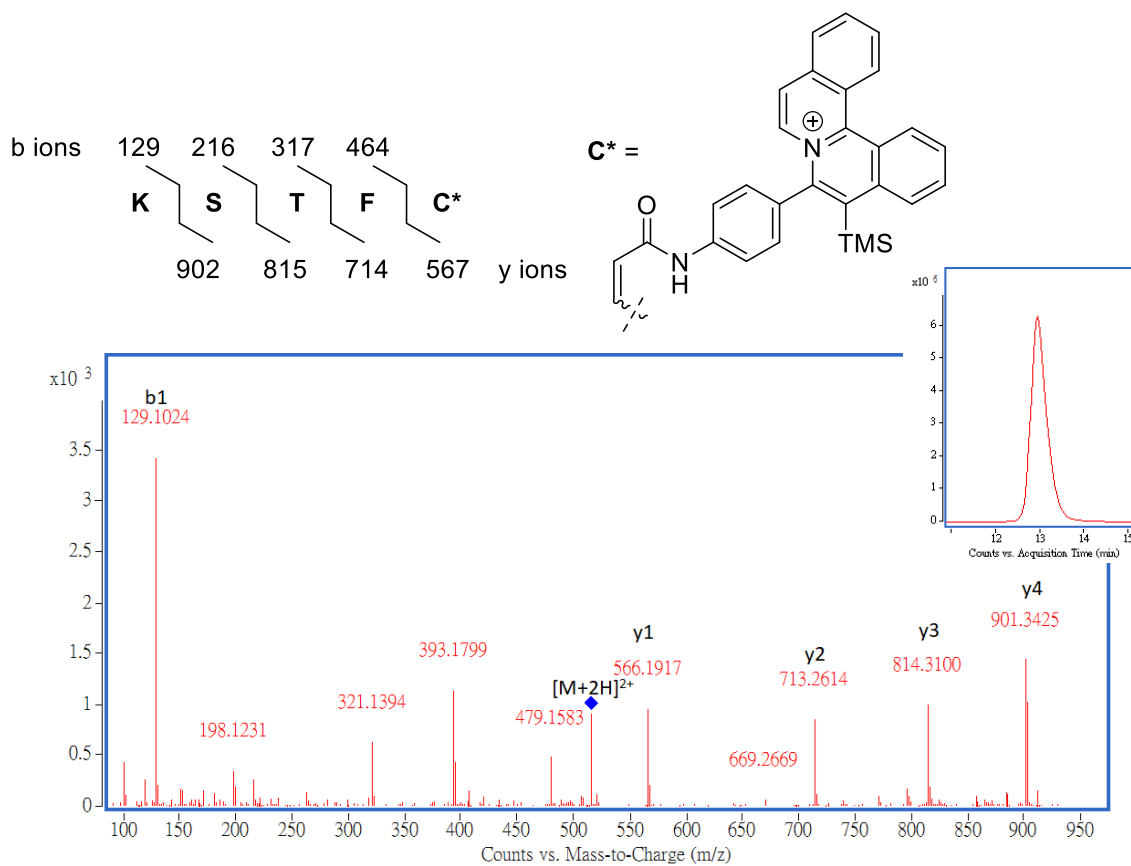


Figure S58. MS/MS spectrum and extracted ion chromatogram (Inset) of **1h**-modified KSTFC (ESI source, doubly charged ion of m/z 515.63).

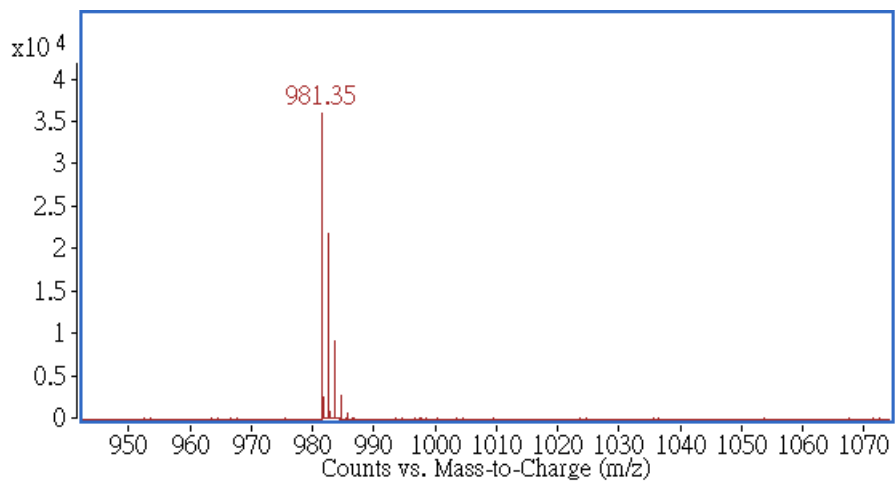
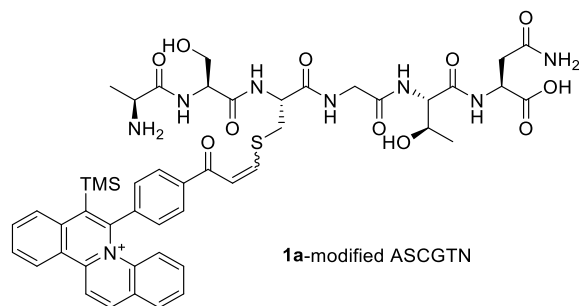


Figure S59. Deconvoluted mass spectrum of **1a**-modified ASCGTN (m/z 981.35).

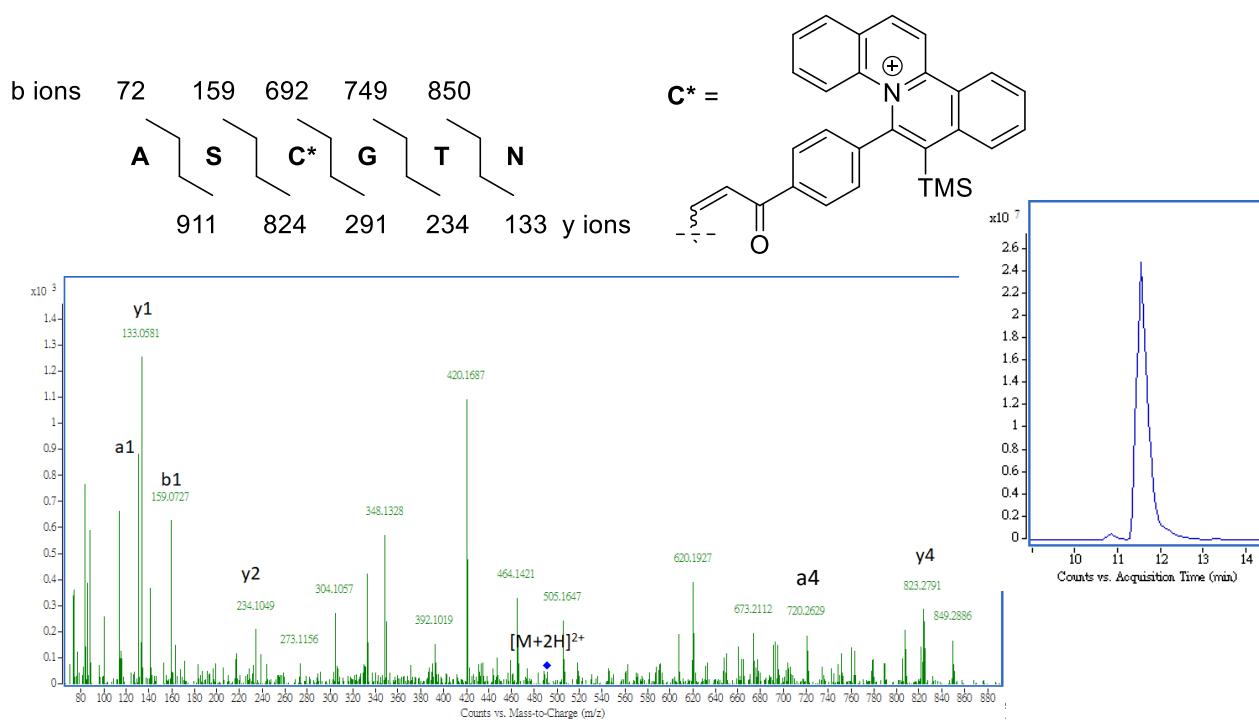


Figure S60. MS/MS spectrum and extracted ion chromatogram (Inset) of **1a**-modified ASCGTN (ESI source, doubly charged ion of m/z 491.60).

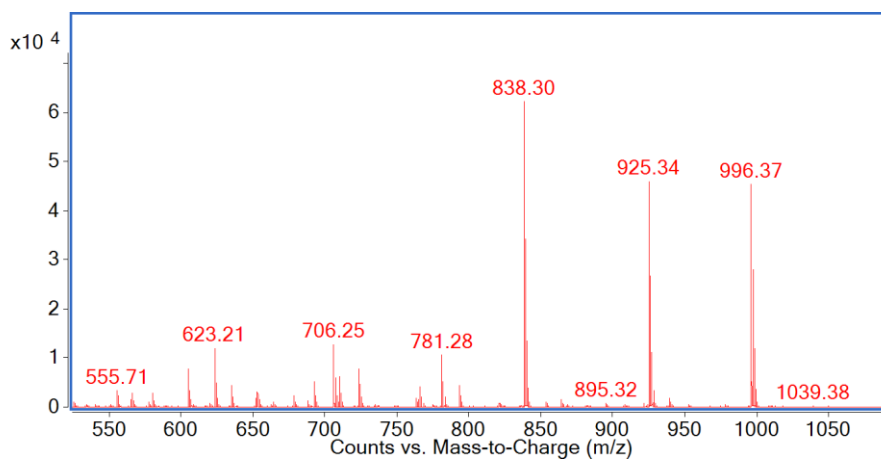
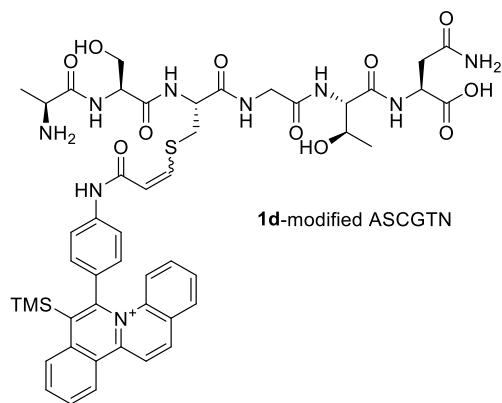


Figure S61. Deconvoluted mass spectrum of **1d**-modified ASCGTN (m/z 996.37).

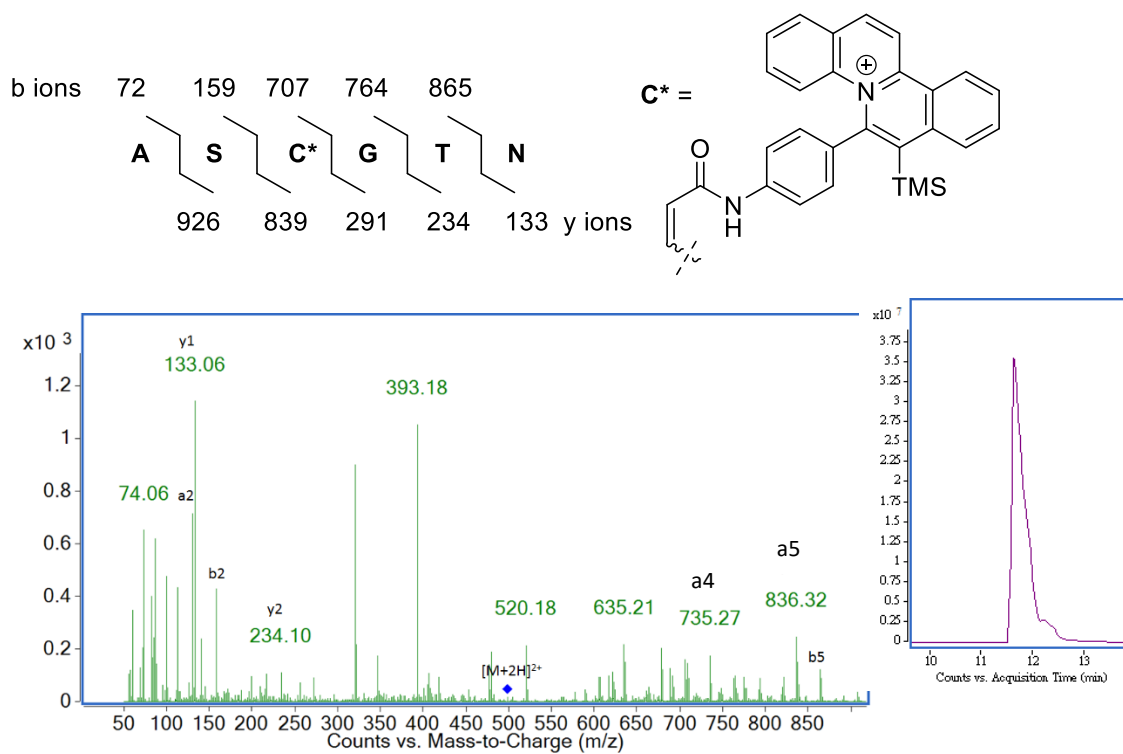


Figure S62. MS/MS spectrum and extracted ion chromatogram (Inset) of **1d**-modified ASCGTN (ESI source, doubly charged ion of m/z 499.11).

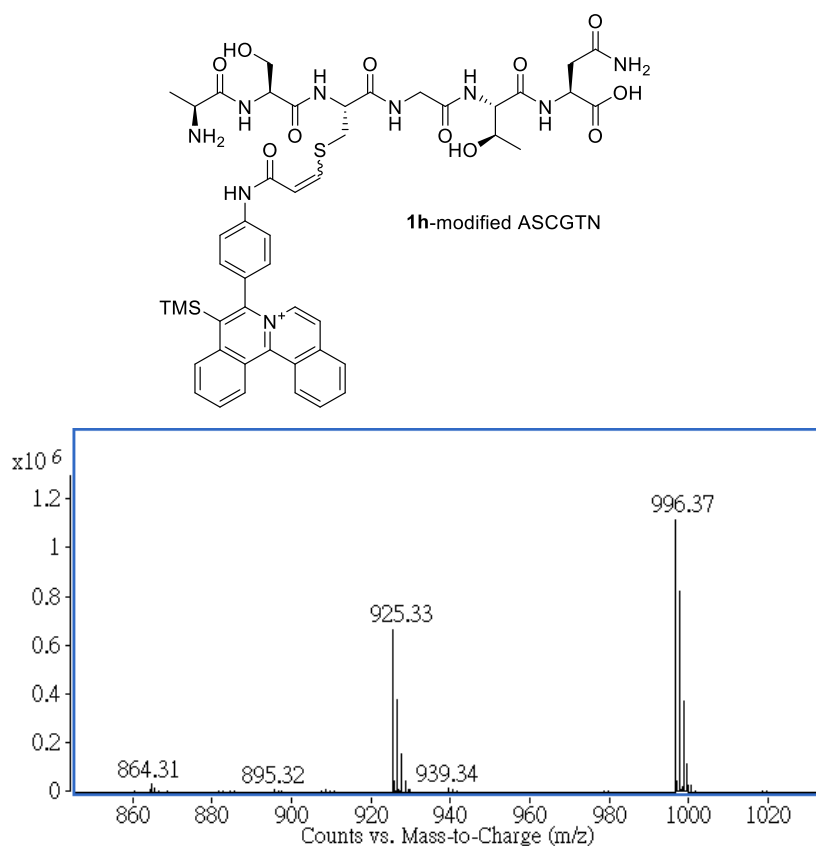


Figure S63. Deconvoluted mass spectrum of **1h**-modified ASCGTN (m/z 996.37).

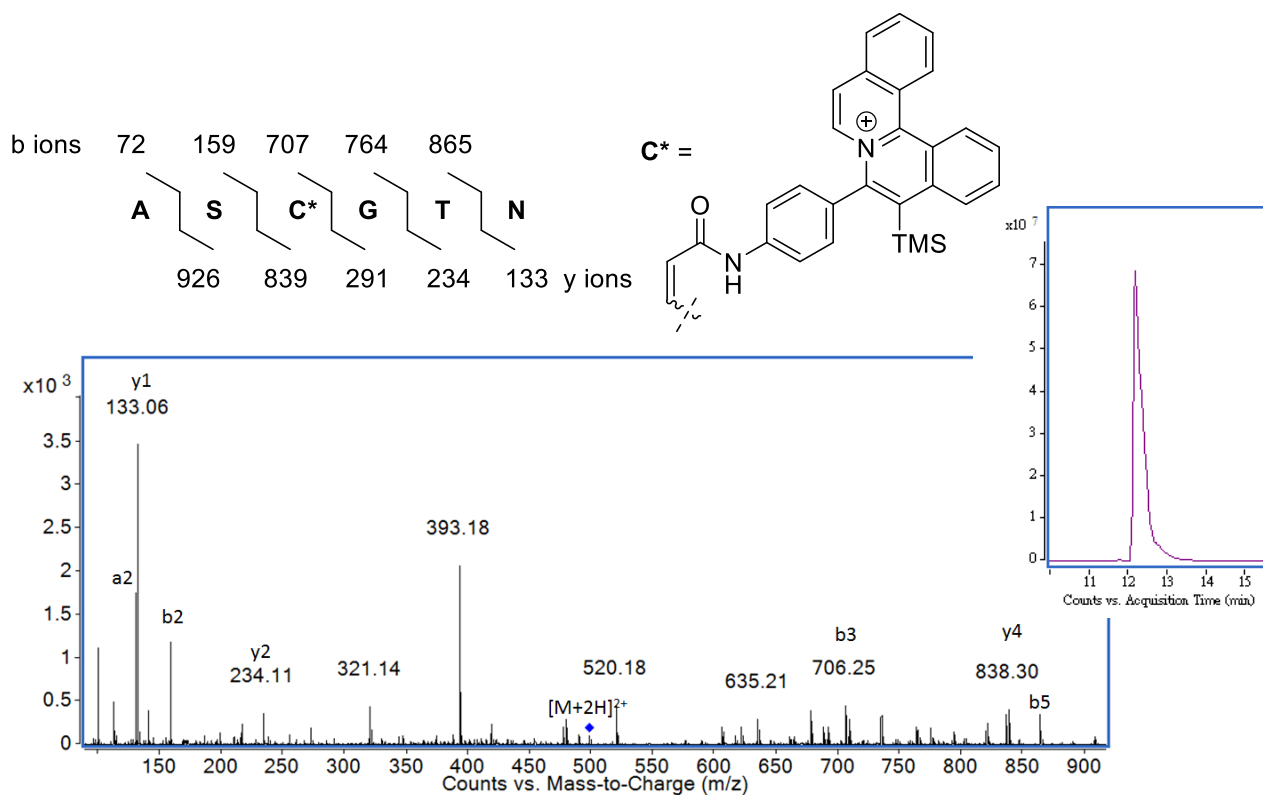


Figure S64. MS/MS spectrum and extracted ion chromatogram (Inset) of **1h**-modified ASCGTN (ESI source, doubly charged ion of m/z 499.11).

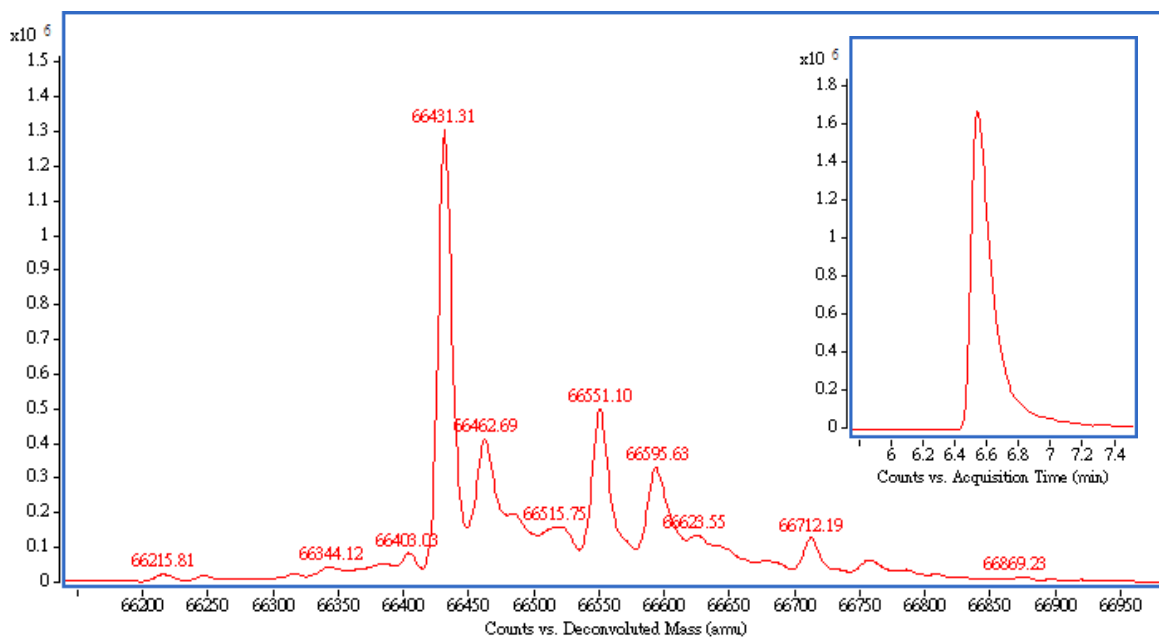


Figure S65. Deconvolution mass spectrum and extracted ion chromatogram (Inset) of native BSA (PDB: 4F5S) (ESI source, the charged ion of m/z 1385.00).

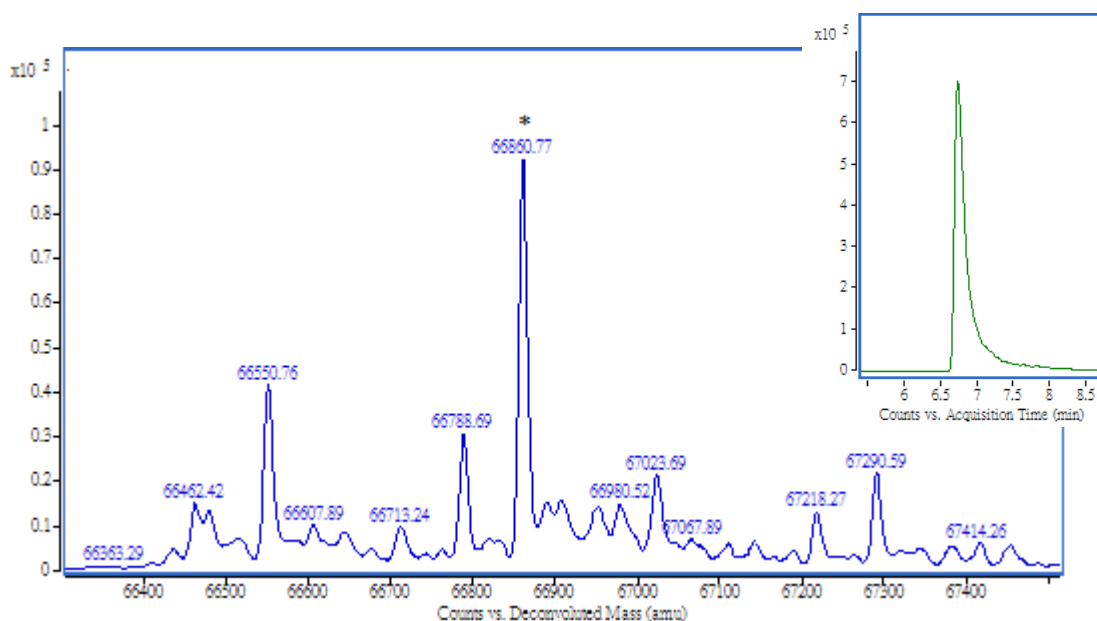


Figure S66. Deconvolution spectrum and extracted ion chromatogram (Inset) of **1a**-modified BSA (1 equiv. of **1a** used) in 50 mM PBS (pH 7.4)/DMSO (95:5) (ESI source, the charged ion of m/z 1393.94).

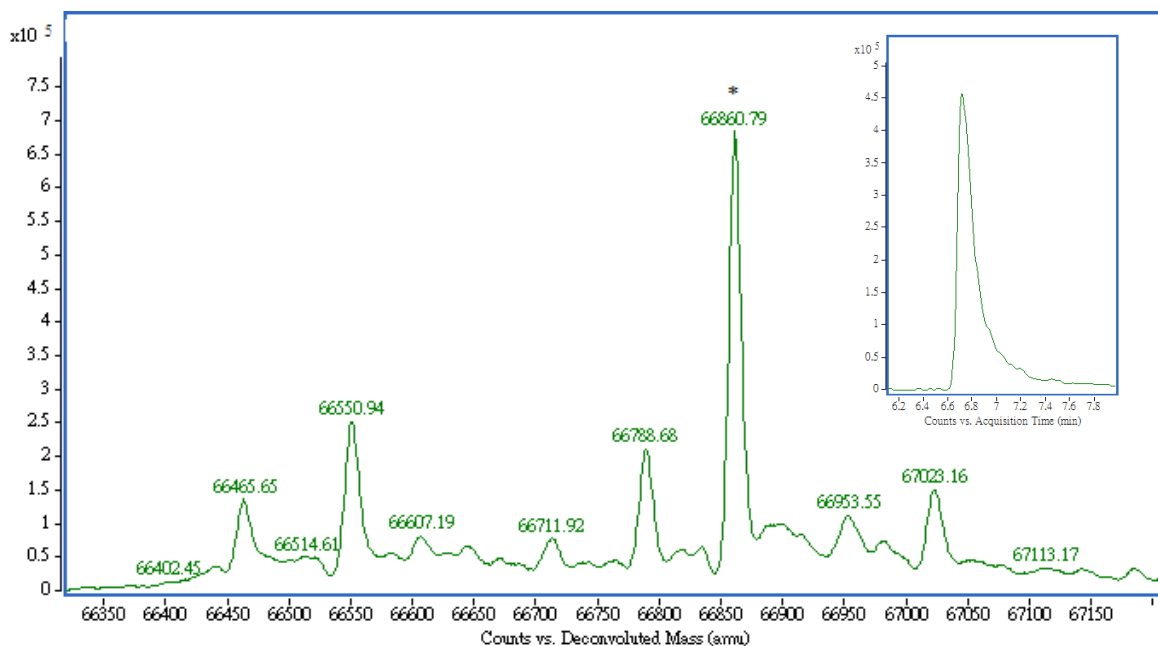


Figure S67. Deconvolution mass spectrum and extracted ion chromatogram (Inset) of **1a**-modified BSA (2 equiv. of **1a** used) in 50 mM PBS (pH 7.4)/DMSO (95:5) (ESI source, the charged ion of m/z 1393.95).

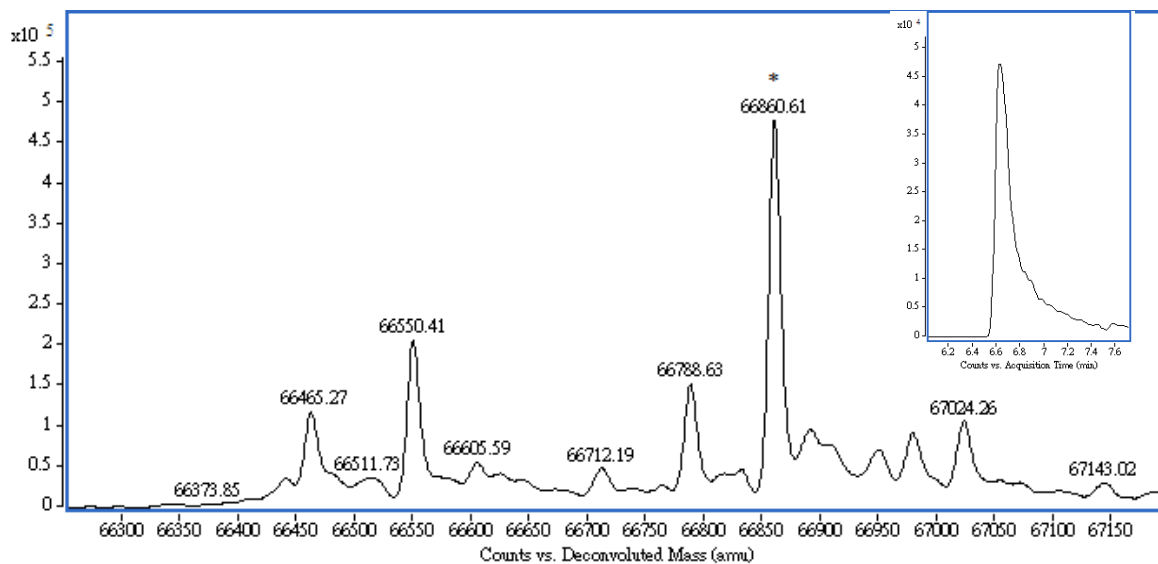


Figure S68. Deconvolution mass spectrum and extracted ion chromatogram (Inset) of **1a**-modified BSA (2 equiv. of **1a** used) in 50 mM Tris-HCl (pH 7.4)/DMSO (95:5) (ESI source, the charged ion of m/z 1393.95).

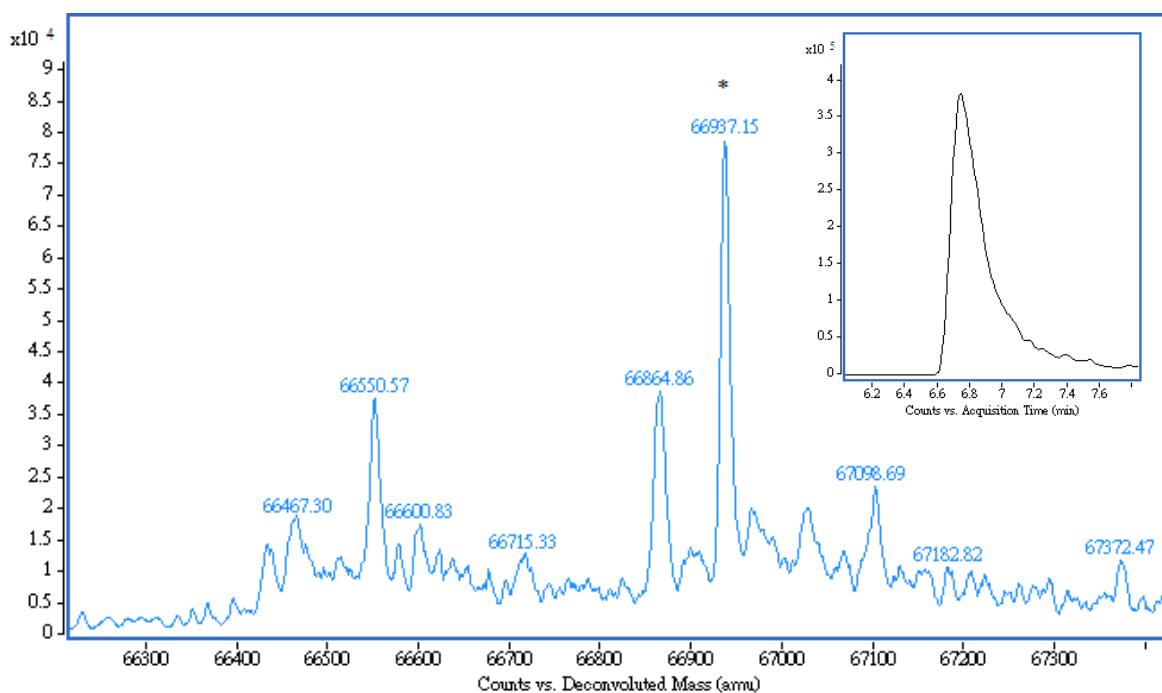


Figure S69. Deconvolution spectrum and extracted ion chromatogram (Inset) of **1b**-modified BSA (2 equiv. of **1b** used) in 50 mM PBS (pH 7.4)/DMSO (95:5) (ESI source, the charged ion of m/z 1395.53).

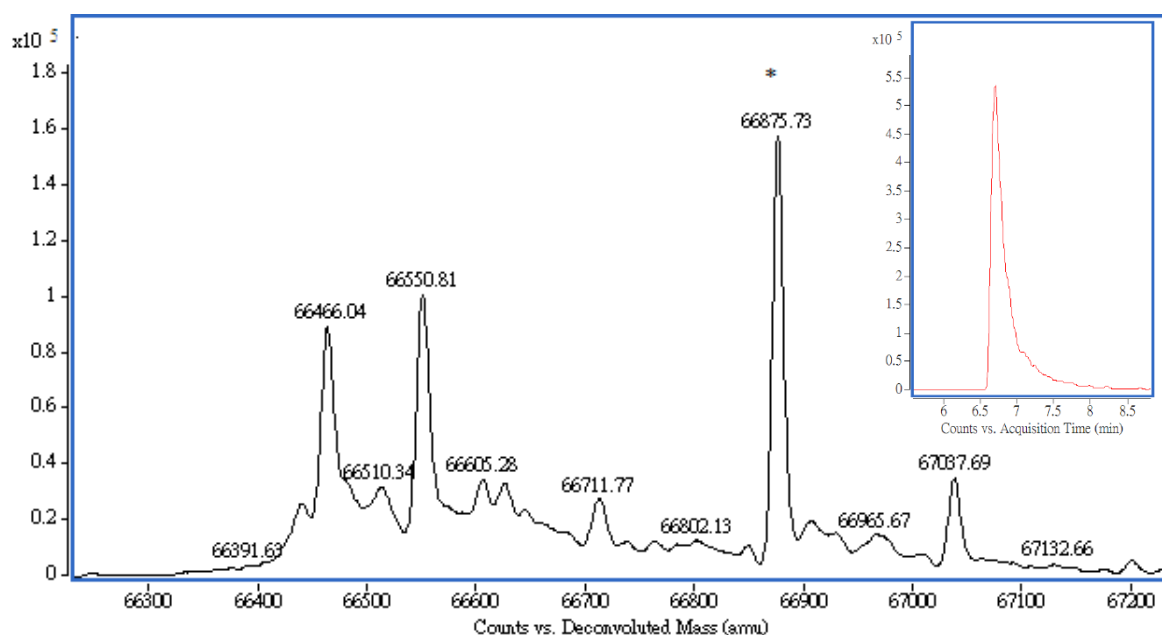


Figure S70. Deconvolution spectrum and extracted ion chromatogram (Inset) of **1d**-modified BSA (2 equiv. of **1d** used) in 50 mM PBS (pH 7.4)/DMSO (95:5) (ESI source, the charged ion of m/z 1394.24).

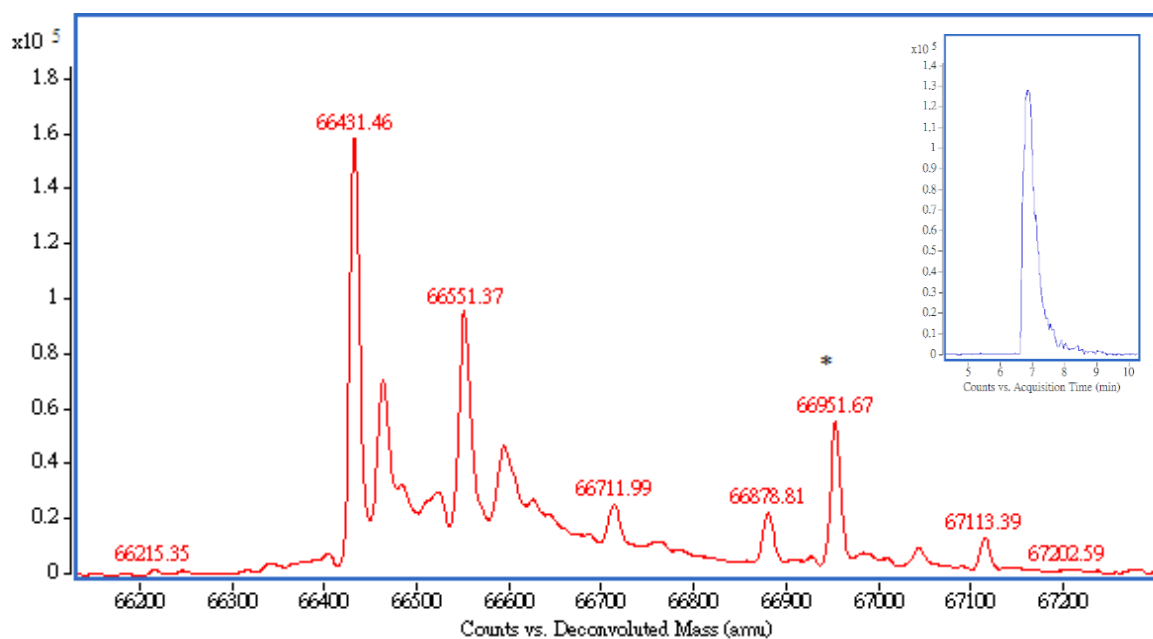


Figure S71. Deconvolution spectrum and extracted ion chromatogram (Inset) of **1e**-modified BSA (2 equiv. of **1e** used) in 50 mM PBS (pH 7.4)/DMSO (95:5) (ESI source, the charged ion of m/z 1394.21).

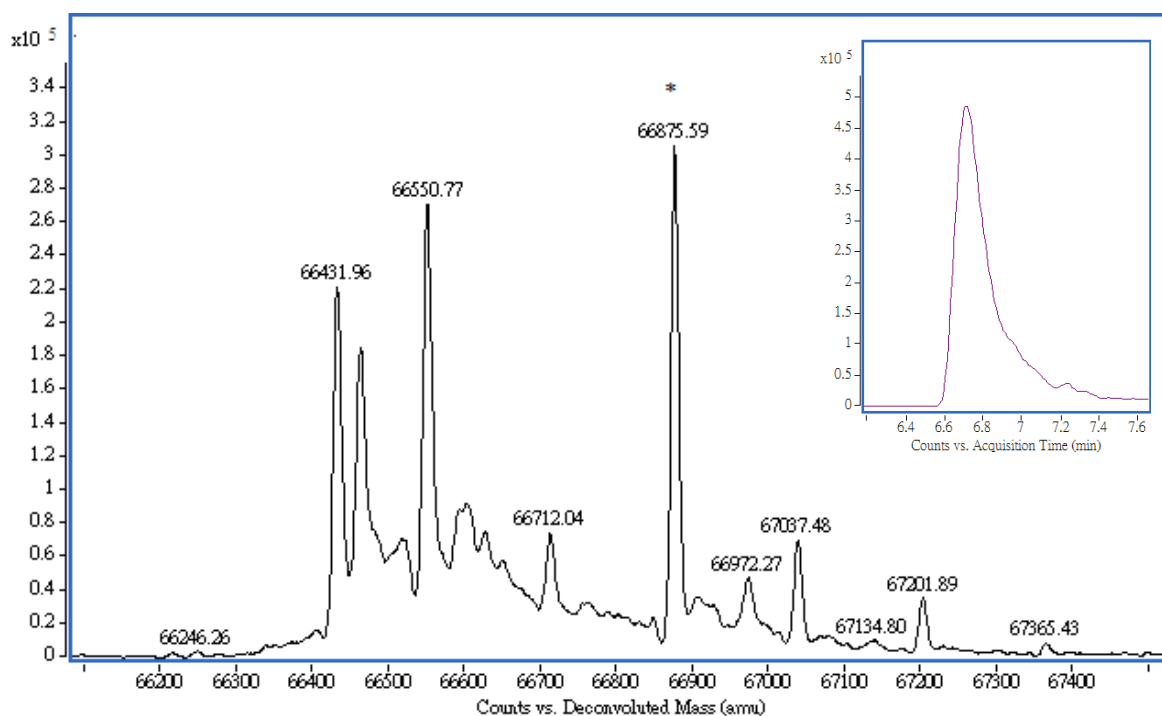


Figure S72. Deconvolution spectrum and extracted ion chromatogram (Inset) of **1h**-modified BSA (2 equiv. of **1h** used) in 50 mM PBS (pH 7.4)/DMSO (95:5) (ESI source, the charged ion of m/z 1394.25).

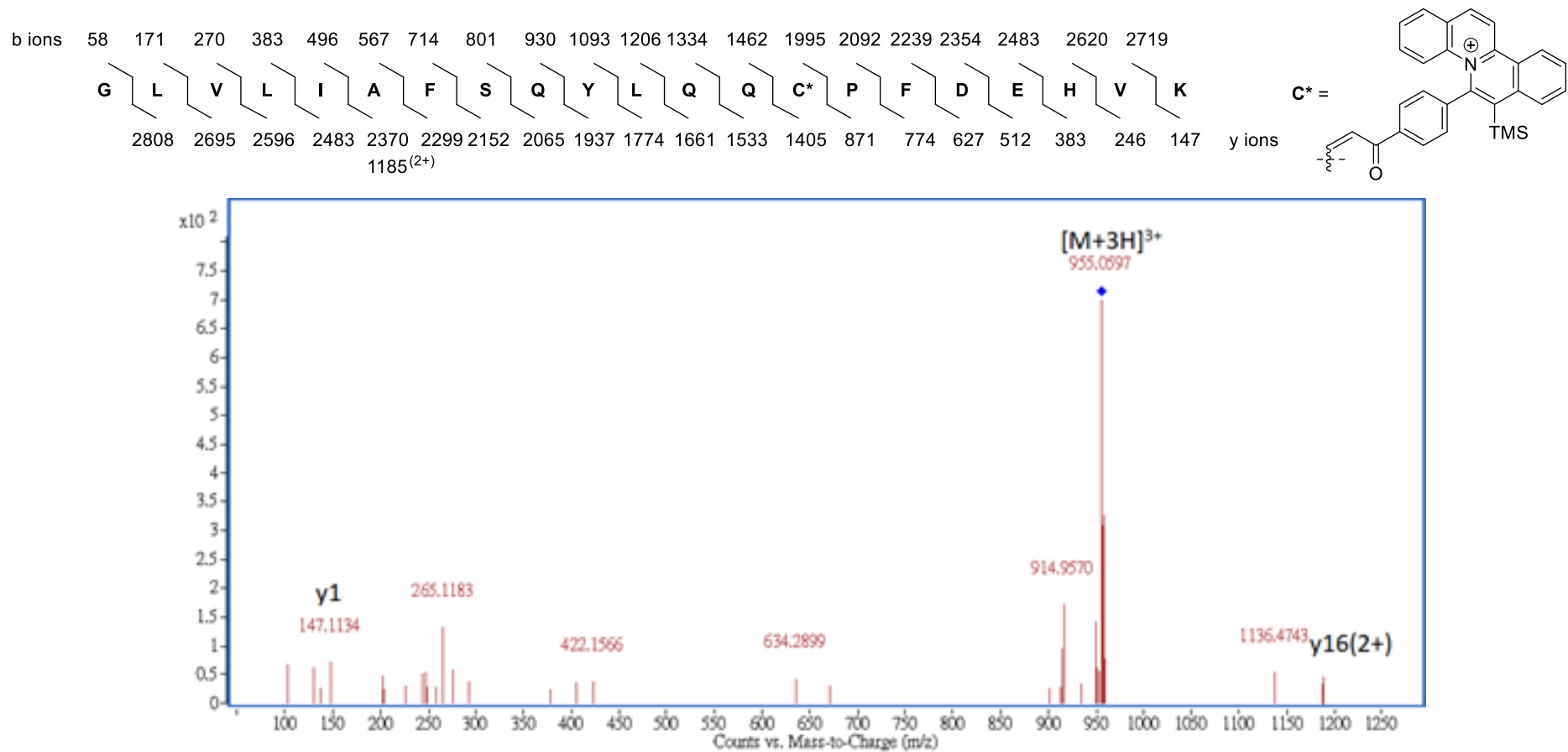


Figure S73. MS/MS spectrum of **1a**-modified GLVLIAFSQYLQQCPFDEHVK with quarterly charged ion of m/z 955.7988 after trypsin digestion of **1a**-modified BSA (2 equiv. of **1a** used) in 50 mM PBS (pH 7.4)/DMSO (95:5).

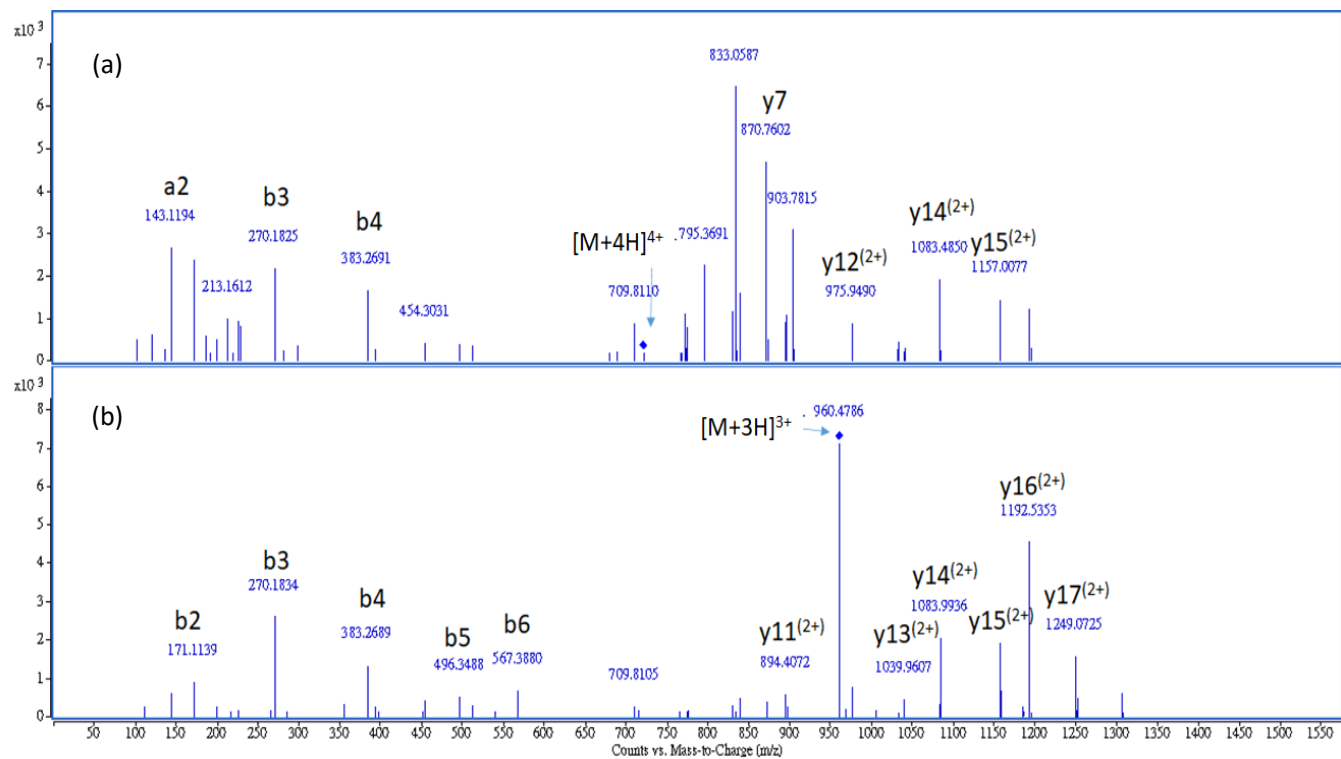
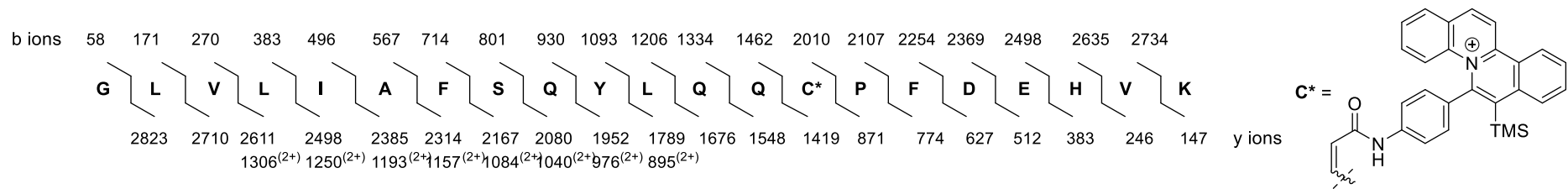


Figure S74. MS/MS spectrum of **1d**-modified GLVLIAFSQYLQQPFDEHVK with (a) quadruply charged ion, m/z 720.62 and (b) triply charged ion, m/z 960.48 after trypsin digestion of **1d**-modified BSA (2 equiv. of **1d** used) in 50 mM PBS (pH 7.4)/DMSO (95:5).

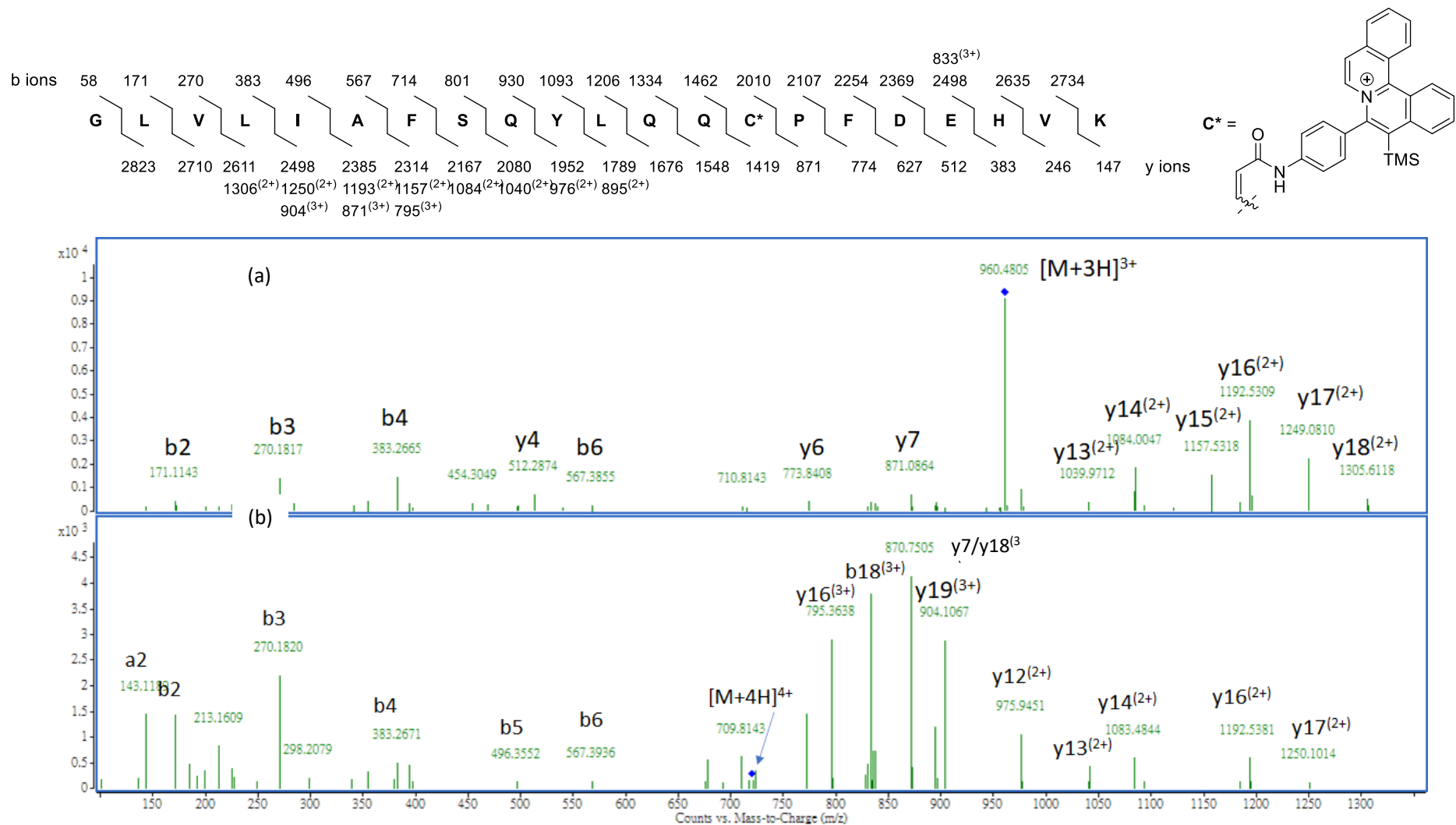


Figure S75. MS/MS spectrum of **1h**-modified GLVLIAFSQYLQPCFDEHVK with (a) triply charged ion of m/z 960.48 and (b) quarterly charged ion of m/z 720.61 after trypsin digestion of **1h**-modified BSA (2 equiv. of **1h** used) in 50 mM PBS (pH 7.4)/DMSO (95:5).

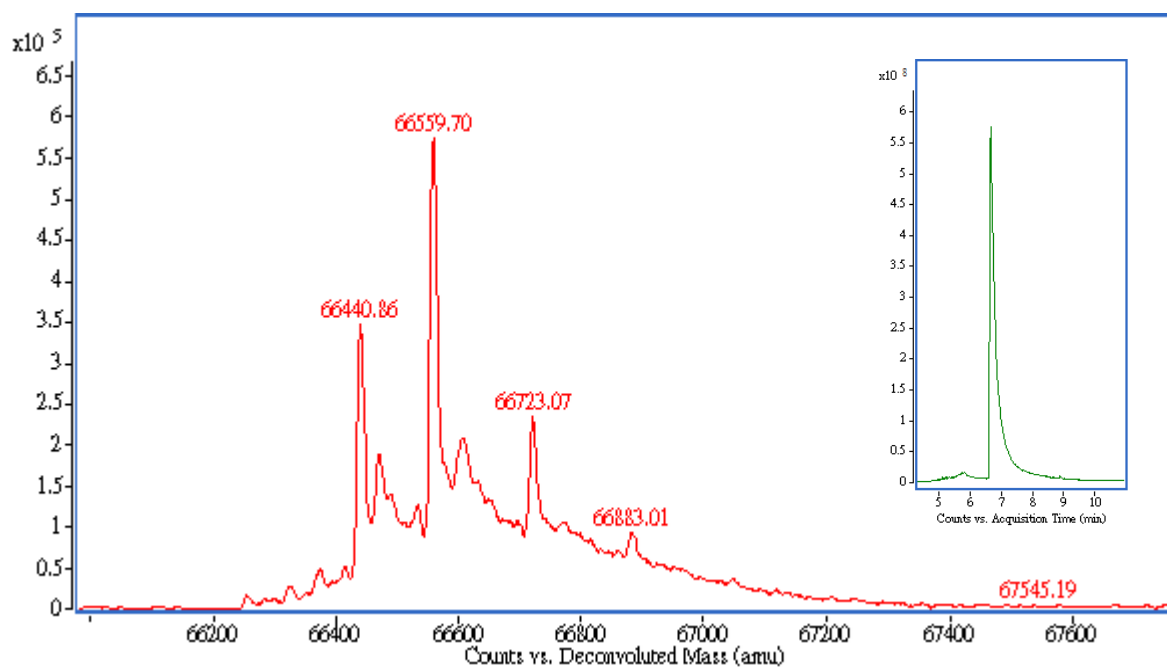


Figure S76. Deconvolution spectrum and extracted ion chromatogram (Inset) of native HSA (PDB: 1AO6) (ESI source, the charged ion of m/z 1445.34).

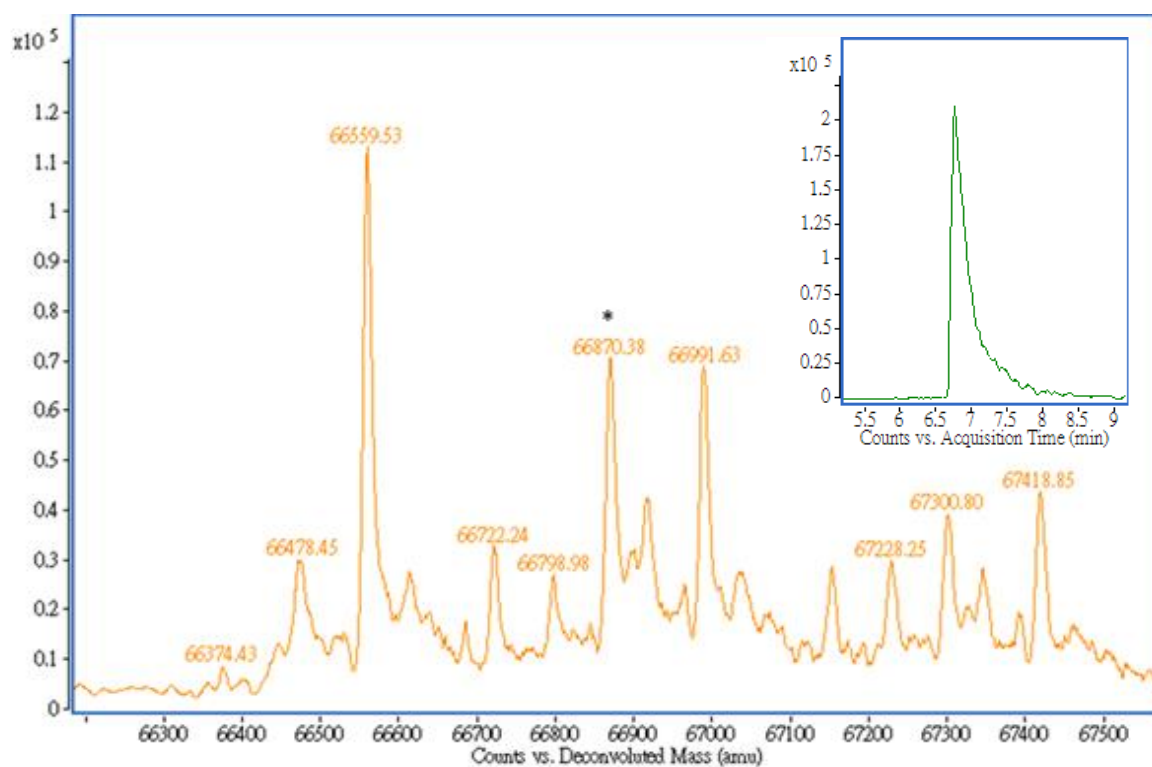


Figure S77. Deconvolution spectrum and extracted ion chromatogram (Inset) of **1a**-modified HSA (2 equiv. of **1a** used) in 50 mM PBS (pH 7.4)/DMSO (95:5) (ESI source, the charged ion of m/z 1454.85).

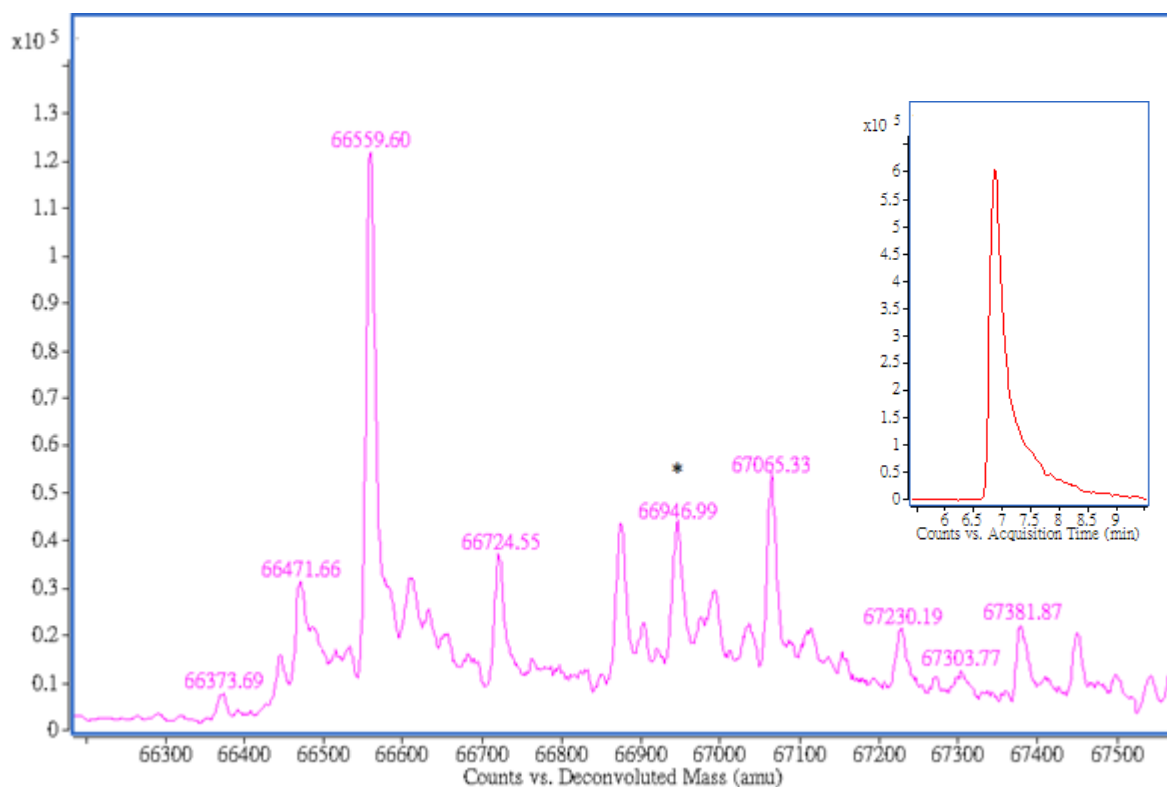


Figure S78. Deconvolution spectrum and extracted ion chromatogram (Inset) of **1b**-modified HSA (2 equiv. of **1b** used) in 50 mM PBS (pH 7.4)/DMSO (95:5) (ESI source, the charged ion of m/z 1456.43).

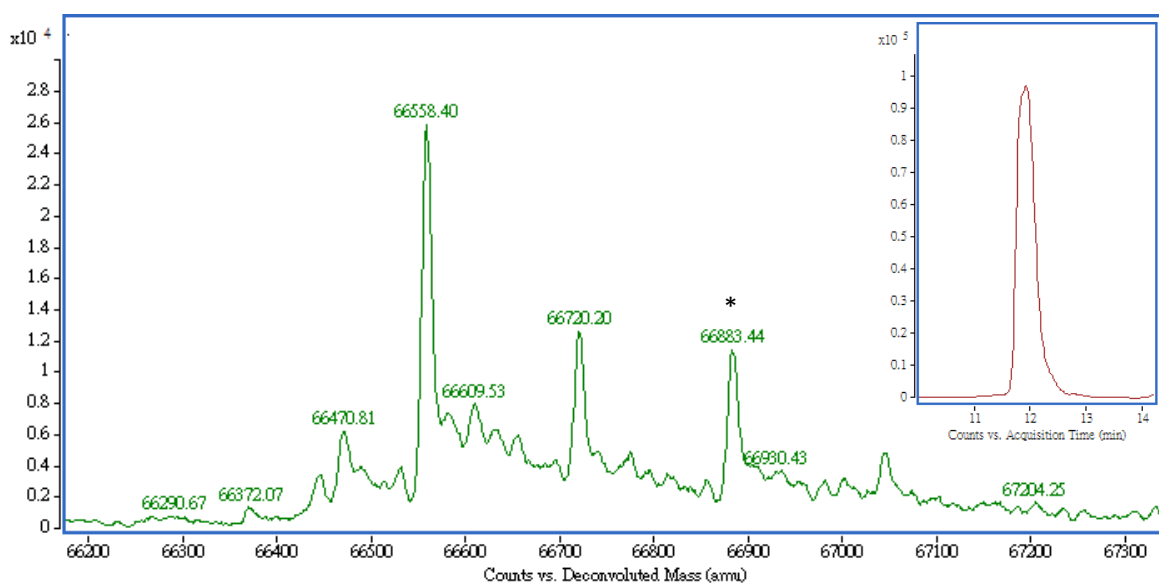


Figure S79. Deconvolution spectrum and extracted ion chromatogram (Inset) of **1d**-modified HSA (2 equiv. of **1d** used) in 50 mM PBS (pH 7.4)/DMSO (95:5) (ESI source, the charged ion of m/z 1455.02).

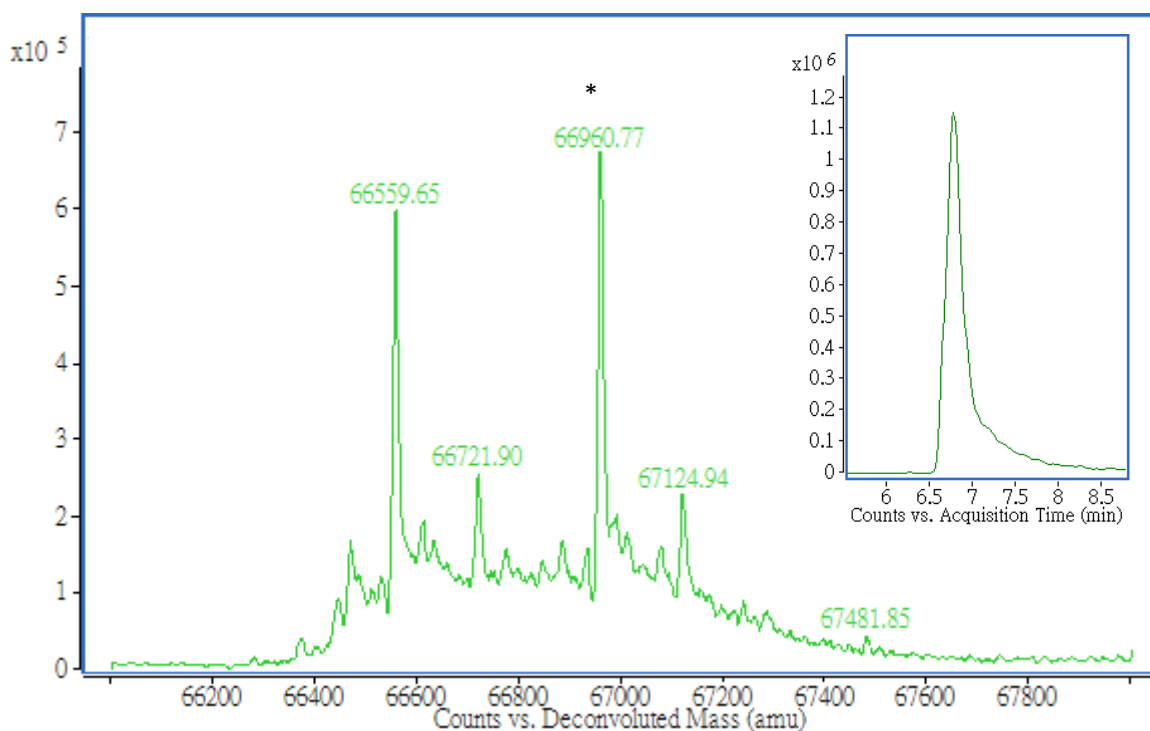


Figure S80. Deconvolution spectrum and extracted ion chromatogram (Inset) of **1e**-modified HSA (2 equiv. of **1e** used) in 50 mM PBS (pH 7.4)/DMSO (95:5) (ESI source, the charged ion of m/z 1456.68).

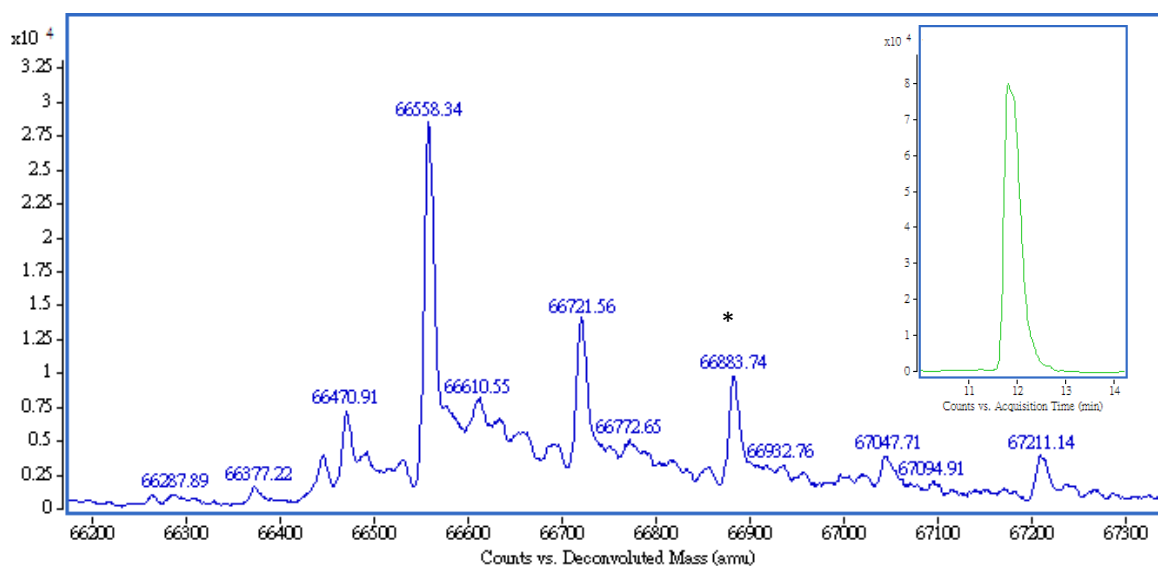


Figure S81. Deconvolution spectrum and extracted ion chromatogram (Inset) of **1h**-modified HSA (2 equiv. of **1h** used) in 50 mM PBS (pH 7.4)/DMSO (95:5) (ESI source, the charged ion of m/z 1455.02).

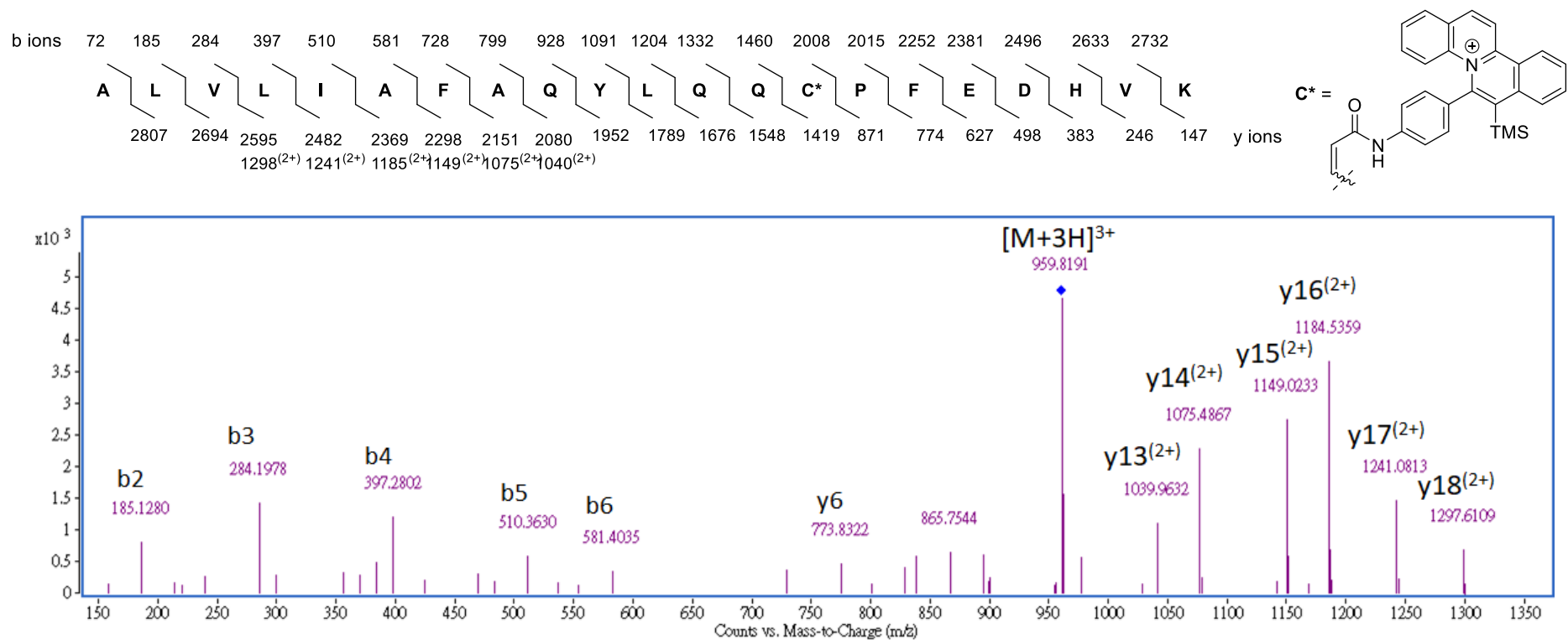


Figure S82. MS/MS spectrum of **1d**-modified ALVLI AFAQYLQQCPFEDHVK with triply charged ion of m/z 959.82 after trypsin digestion of **1d**-modified HSA (2 equiv. of **1d** used) in 50 mM PBS (pH 7.4)/DMSO (95:5).

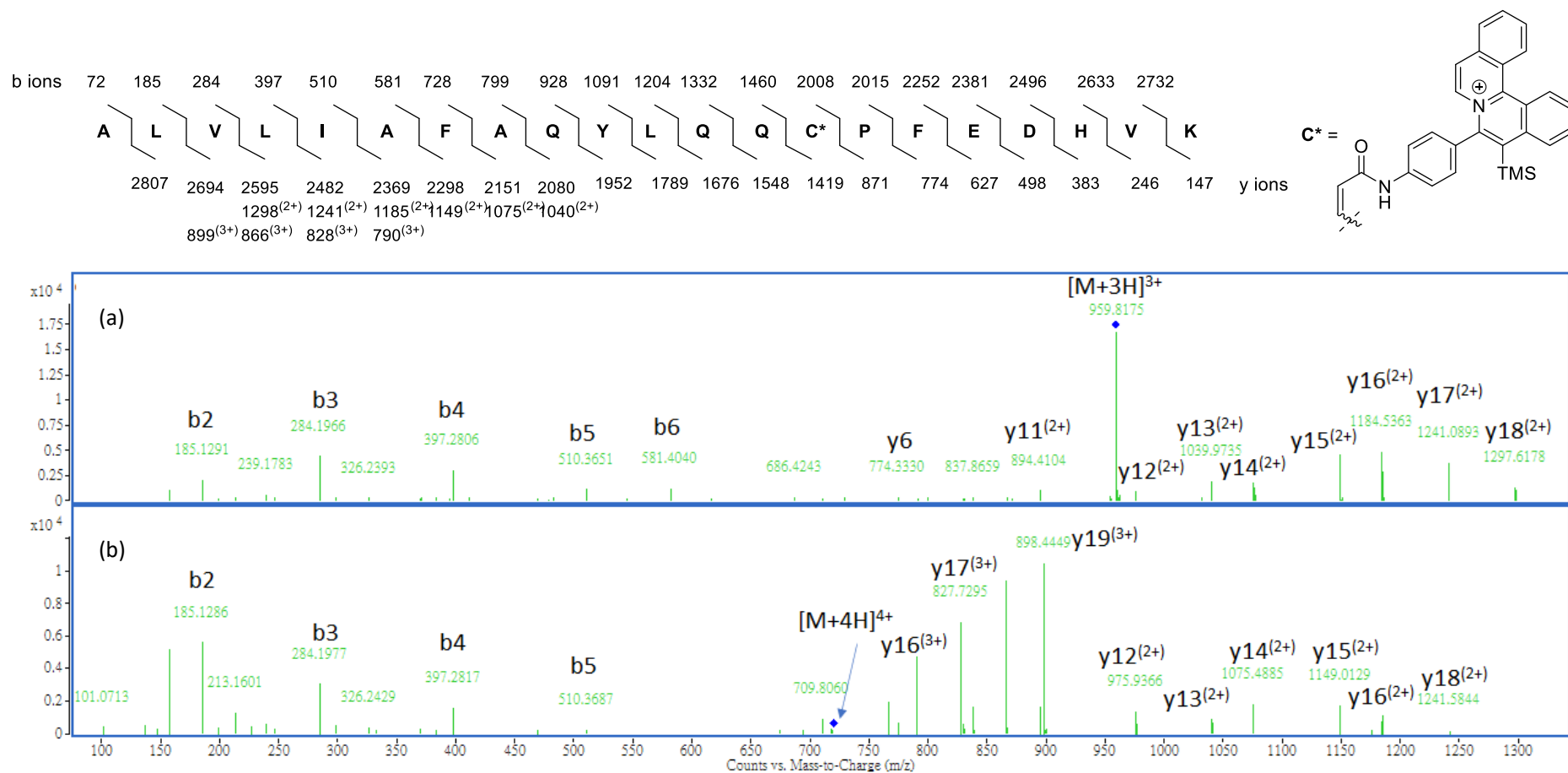


Figure S83. MS/MS spectrum of **1h**-modified ALVLI AFAQYLQQCPFEDHVK with (a) triply charged ion of m/z 959.82 and (b) quarterly charged ion of m/z 721.12 after trypsin digestion of **1h**-modified HSA (2 equiv. of **1h** used) in 50 mM PBS (pH 7.4)/DMSO (95:5).

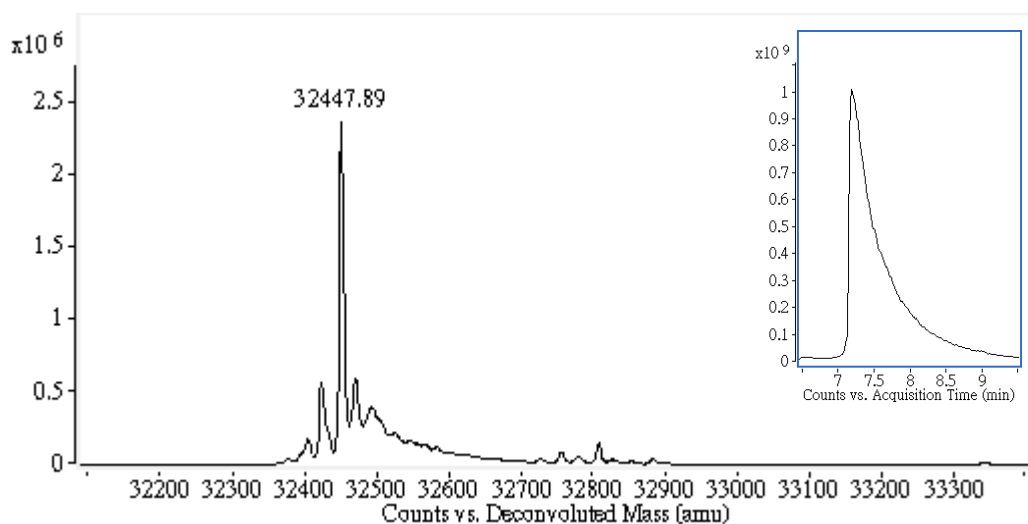


Figure S84. Deconvolution spectrum and extracted ion chromatogram (Inset) of the BCArg mutant (ESI source, the charged ion of m/z 984.25).

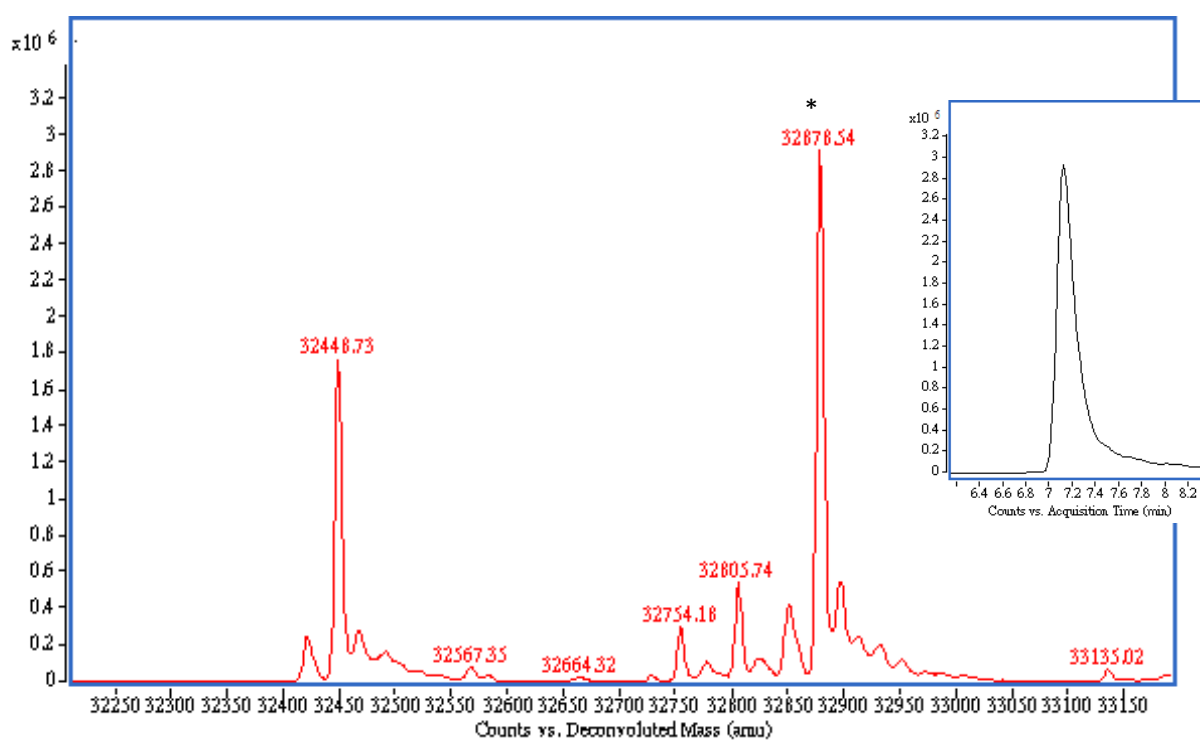


Figure S85. Deconvolution spectrum and extracted ion chromatogram (Inset) of **1a**-modified BCArg mutant (1 equiv. of **1a** used) in 20 mM Tris·HCl (pH 7.4)/DMSO (95:5) (ESI source, the charged ion of m/z 997.29) .

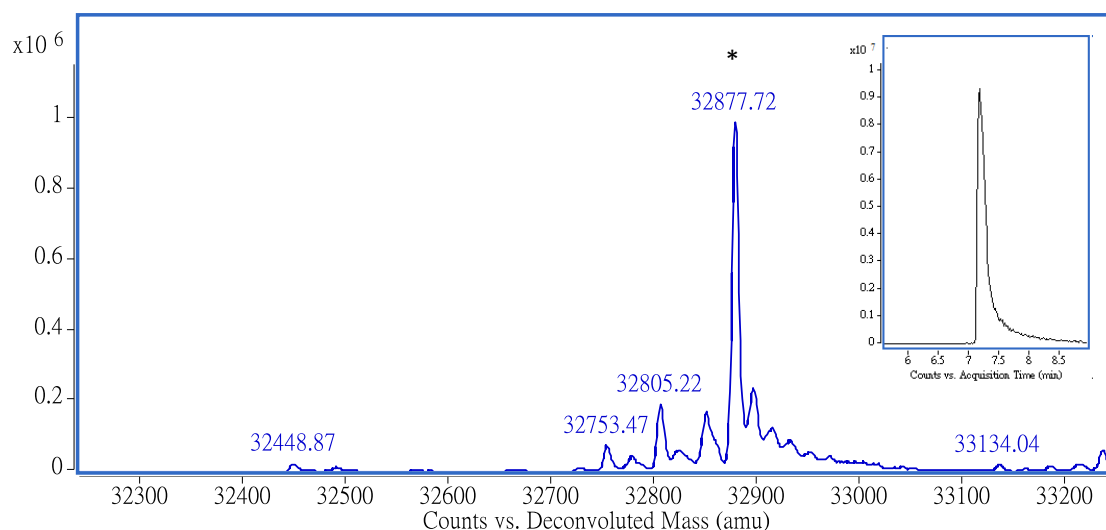


Figure S86. Deconvolution spectrum and extracted ion chromatogram (Inset) of **1a**-modified BCArg mutant (2 equiv. of **1a** used) in 20 mM Tris·HCl (pH 7.4)/DMSO (95:5) (ESI source, the charged ion of m/z 997.29).

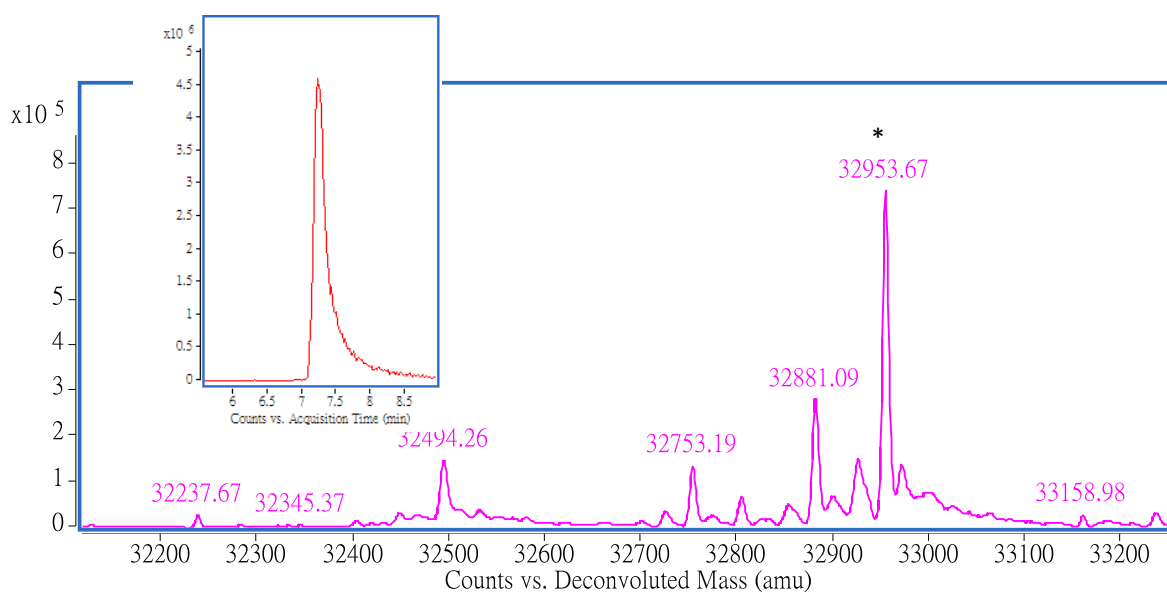


Figure S87. Deconvolution spectrum and extracted ion chromatogram (Inset) of **1b**-modified BCArg mutant (2 equiv. of **1b** used) in 20 mM Tris·HCl (pH 7.4)/DMSO (95:5) (ESI source, the charged ion of m/z 999.60).

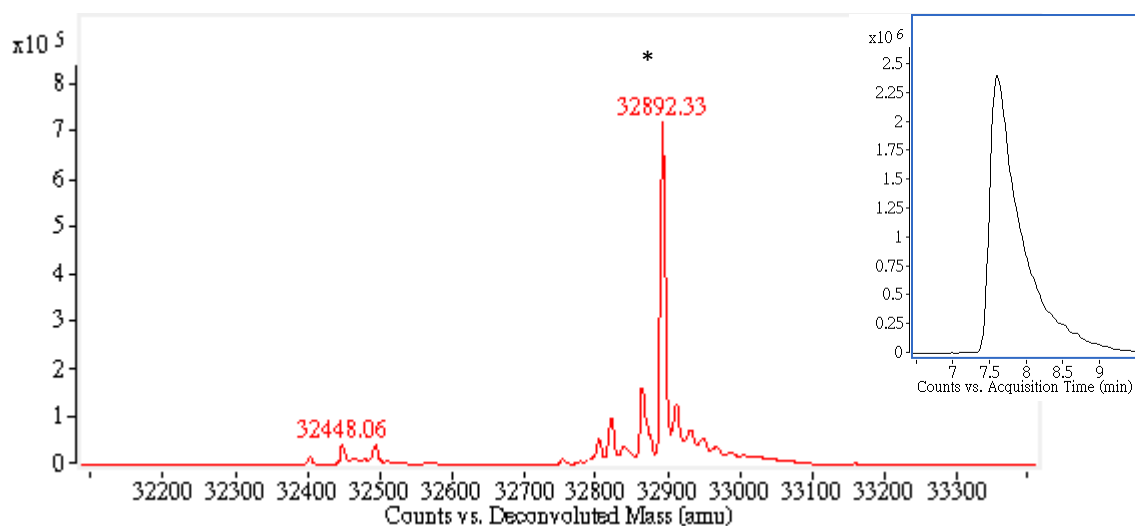


Figure S88. Deconvolution spectrum and extracted ion chromatogram (Inset) of **1d**-modified BCArg mutant (2 equiv. of **1d** used) in 20 mM Tris·HCl (pH 7.4)/DMSO (95:5) (ESI source, the charged ion of m/z 997.74).

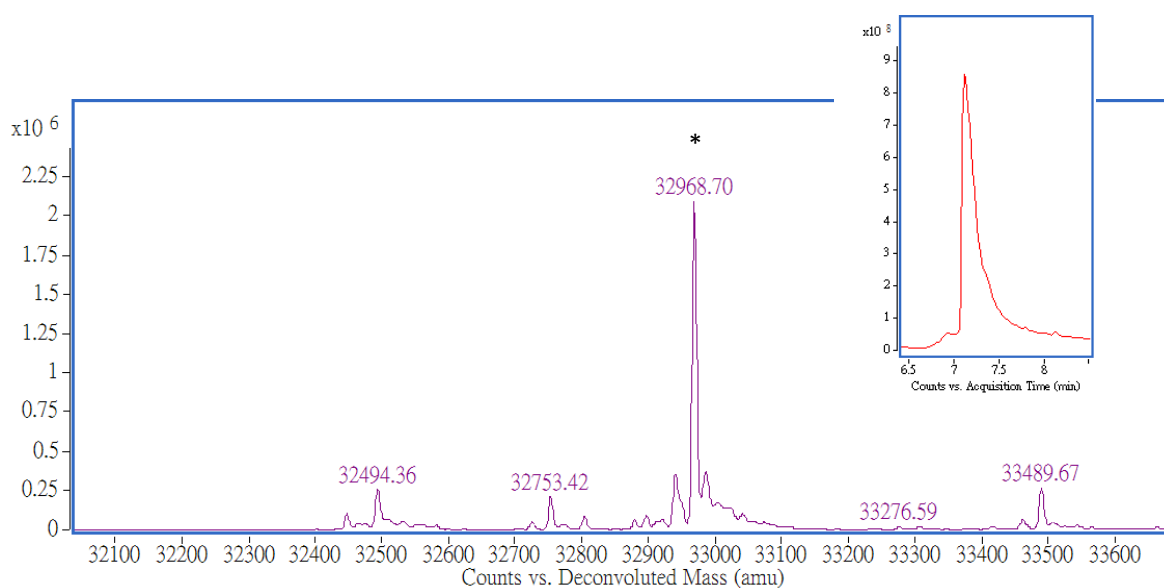


Figure S89. Deconvolution spectrum and extracted ion chromatogram (Inset) of **1e**-modified BCArg mutant (2 equiv. of **1e** used) in 20 mM Tris·HCl (pH 7.4)/DMSO (95:5) (ESI source, the charged ion of m/z 1000.04).

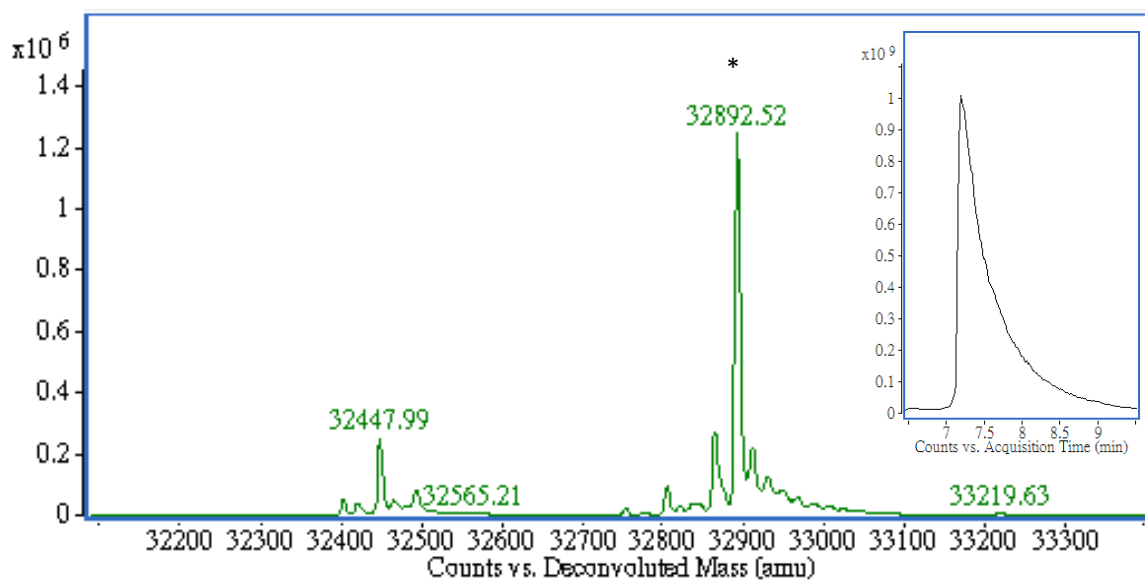


Figure S90. Deconvolution spectrum and extracted ion chromatogram (Inset) of **1h**-modified BCArg mutant (2 equiv. of **1h** used) in 20 mM Tris·HCl (pH 7.4)/DMSO (95:5) (ESI source, the charged ion of m/z 997.74).

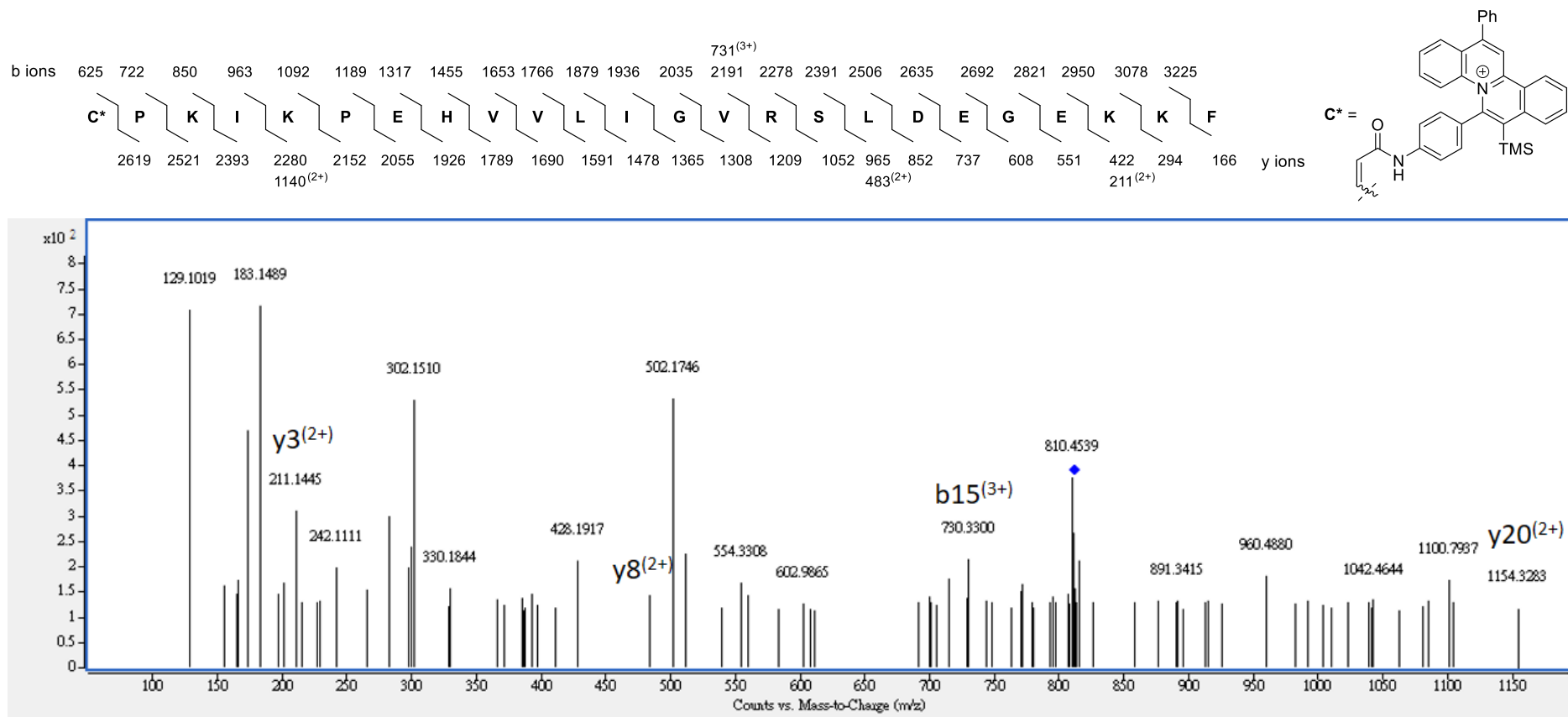


Figure S91. MS/MS spectrum of **1e**-modified CPKIKPEHVVLIGVRSLEGEKKF with quadruply charged ion, m/z 812.45 after trypsin digestion of **1e**-modified BCArg mutant.

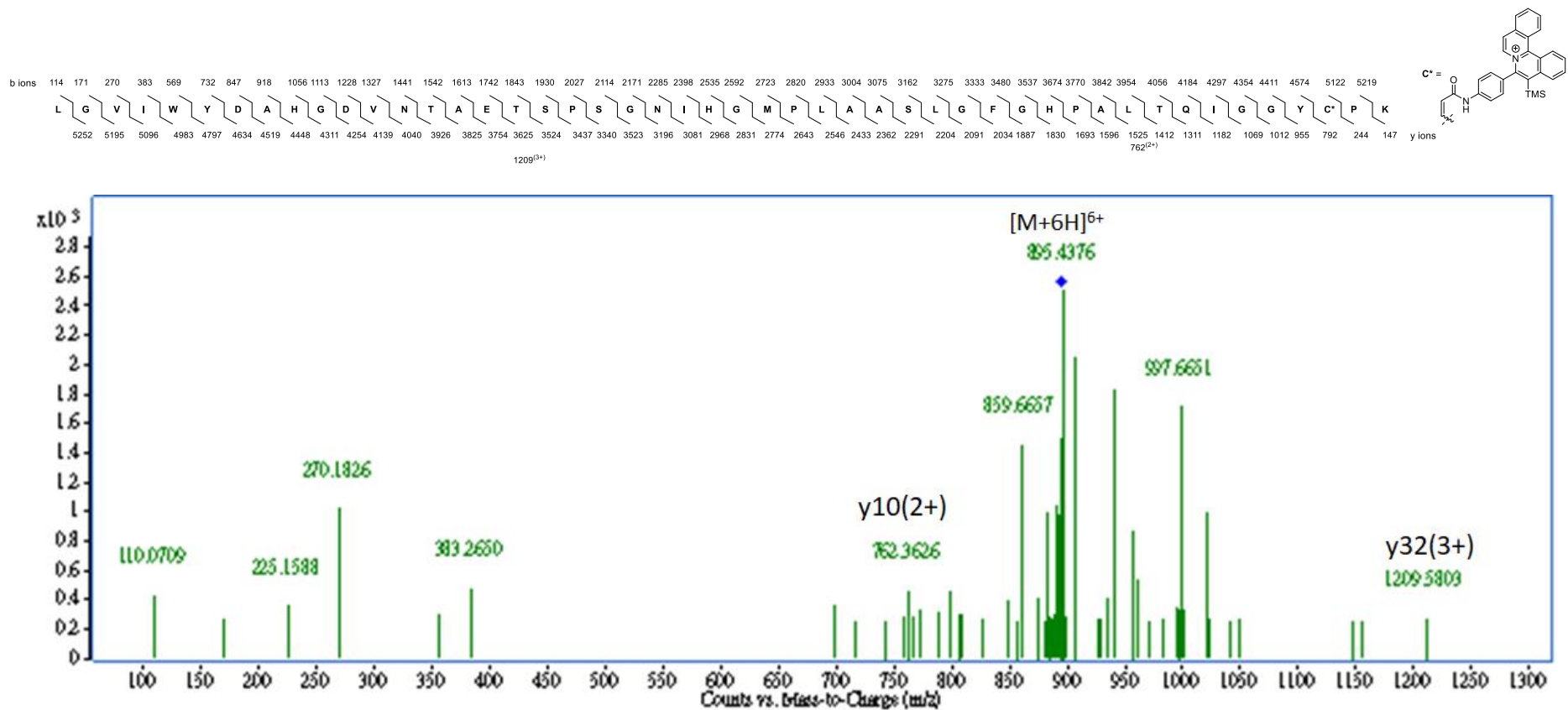


Figure S92. MS/MS spectrum of **1h**-modified LGVIWYDAHGVDVNTAETSPSGNIHGMPLAASLGFGHPALTQIGGYCPK with sextuply charged ion, m/z 895.44 after trypsin digestion of **1h**-modified BCArg mutant.

UV/Visible Absorption Spectra of Quinolizinium Compounds

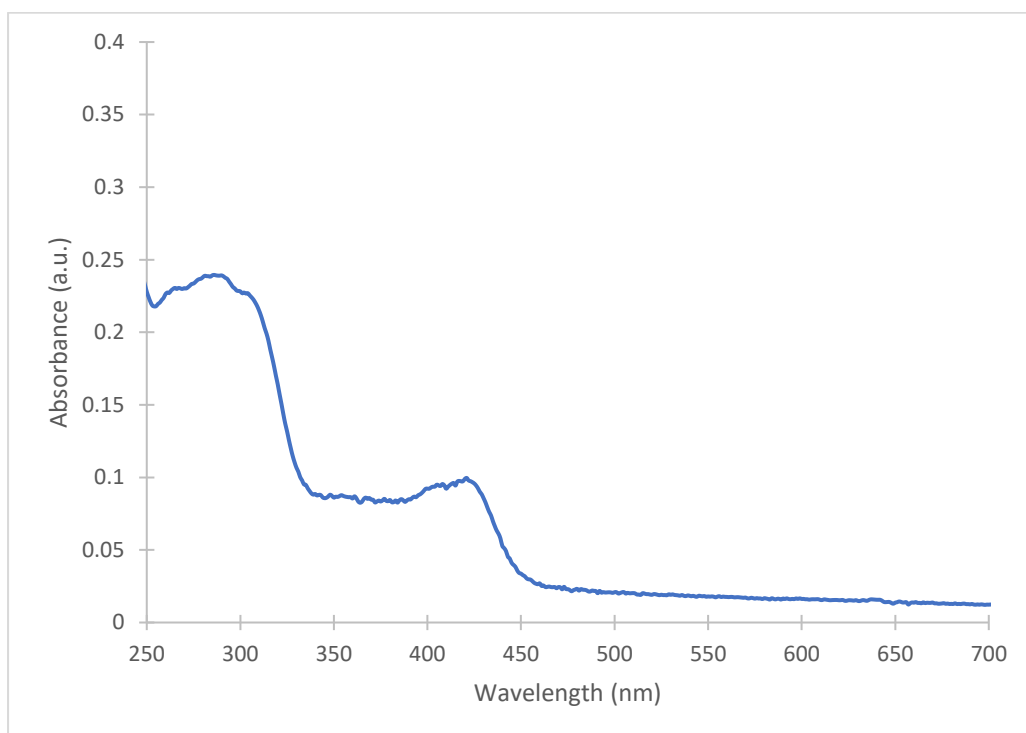


Figure S93. Absorption spectrum of compound **1a**.

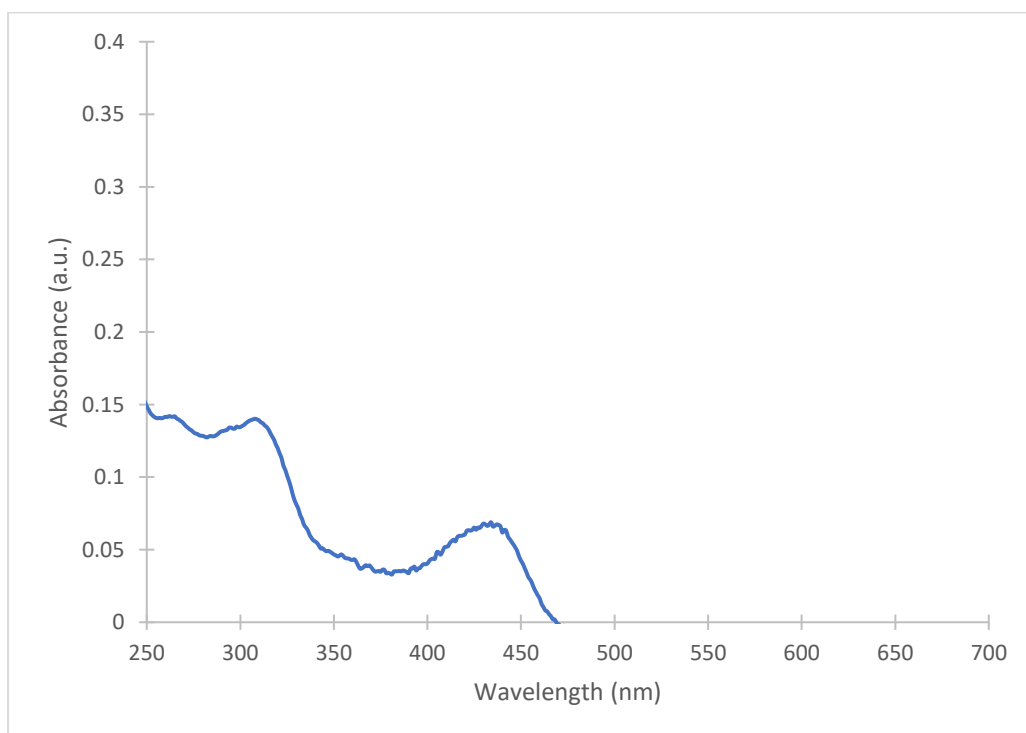


Figure S94. Absorption spectrum of compound **1b**.

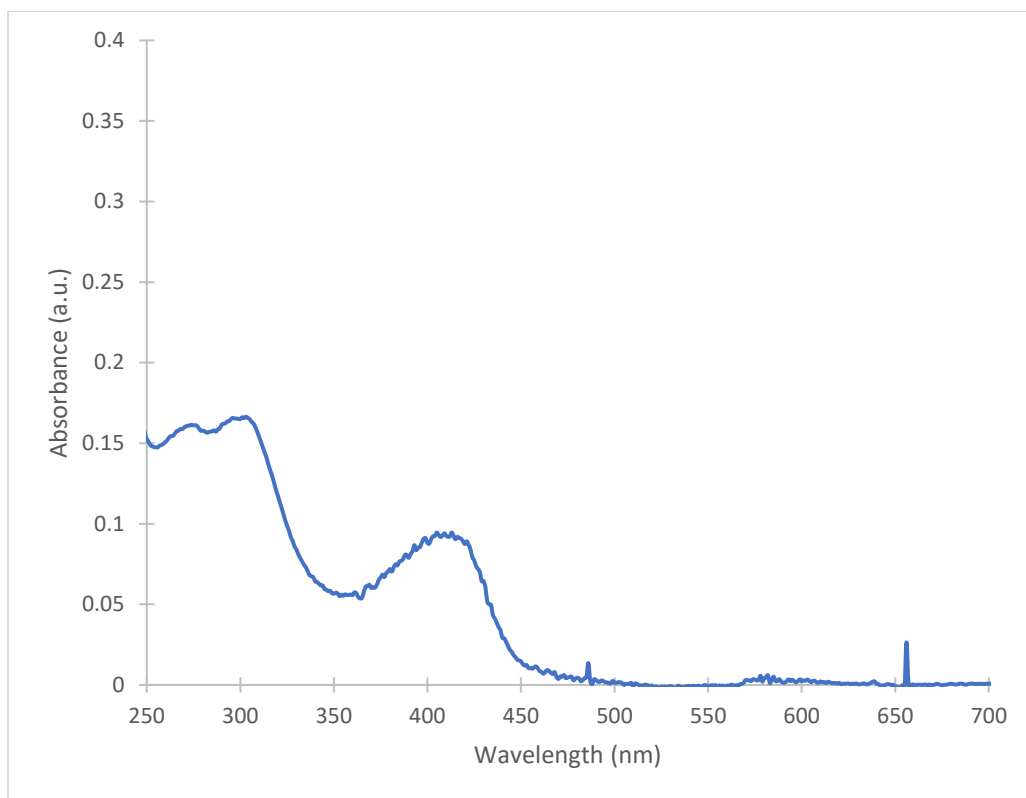


Figure S95. Absorption spectrum of compound **1c**.

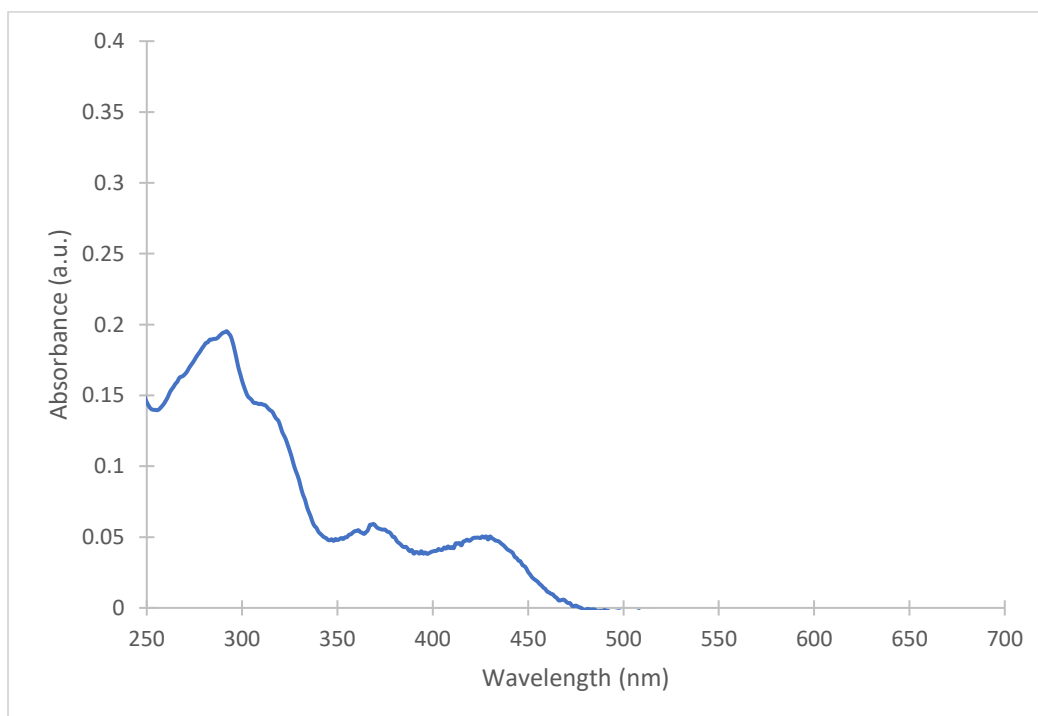


Figure S96. Absorption spectrum of compound **1d**.

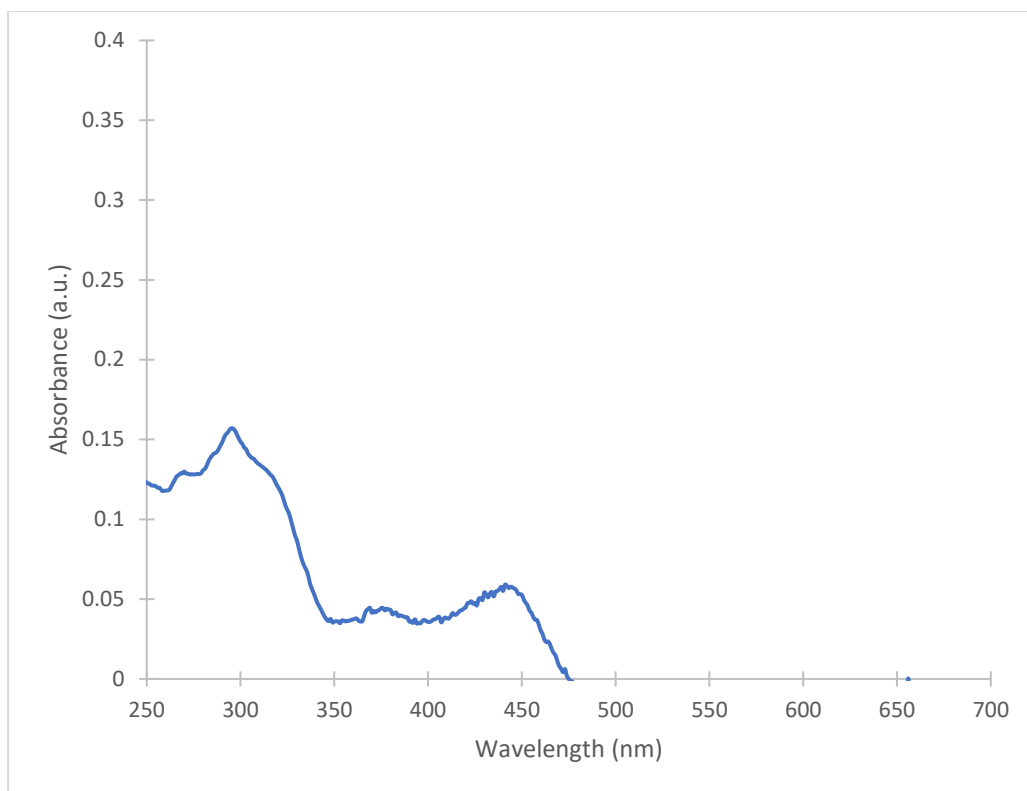


Figure S97. Absorption spectrum of compound **1e**.

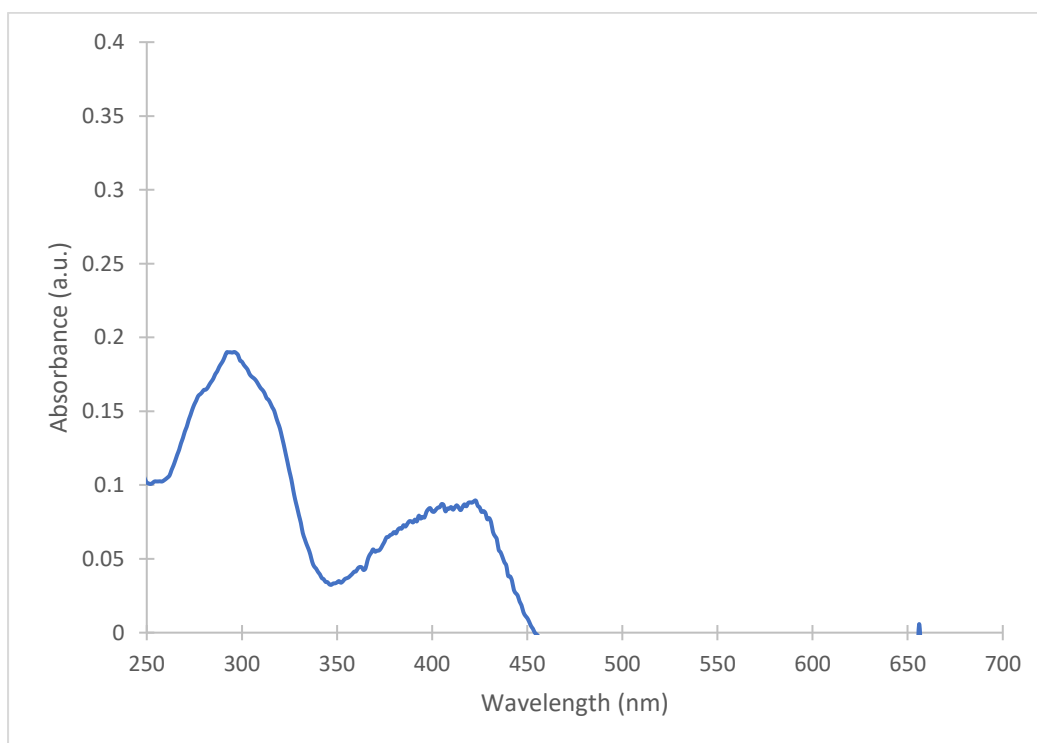


Figure S98. Absorption spectrum of compound **1f**.

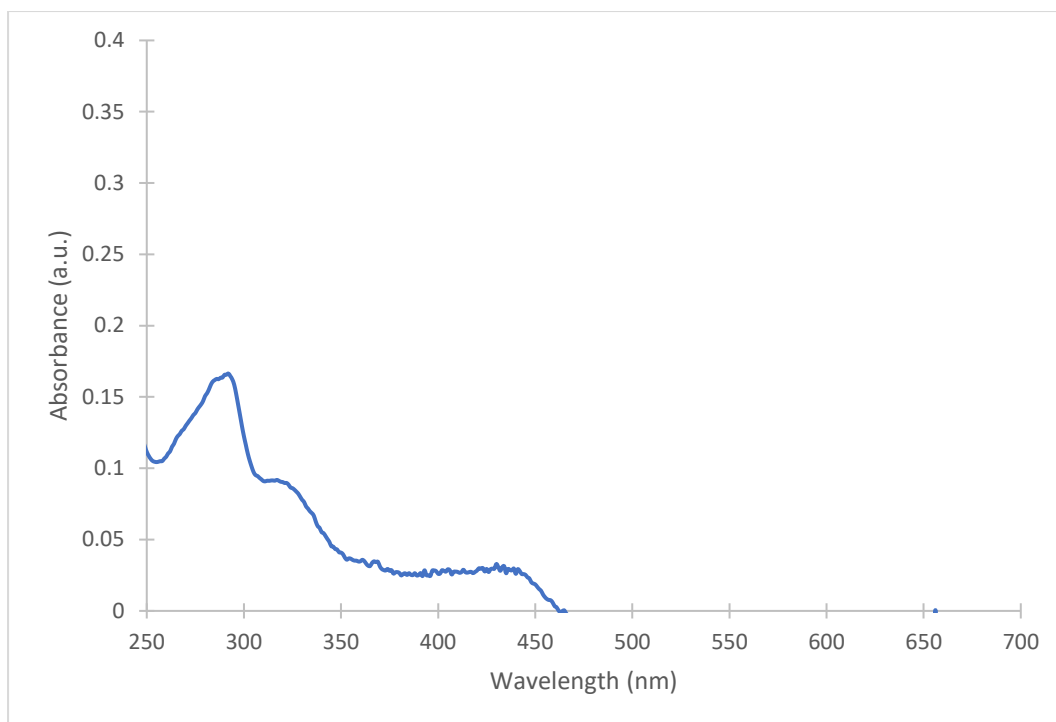


Figure S99. Absorption spectrum of compound **1g**.

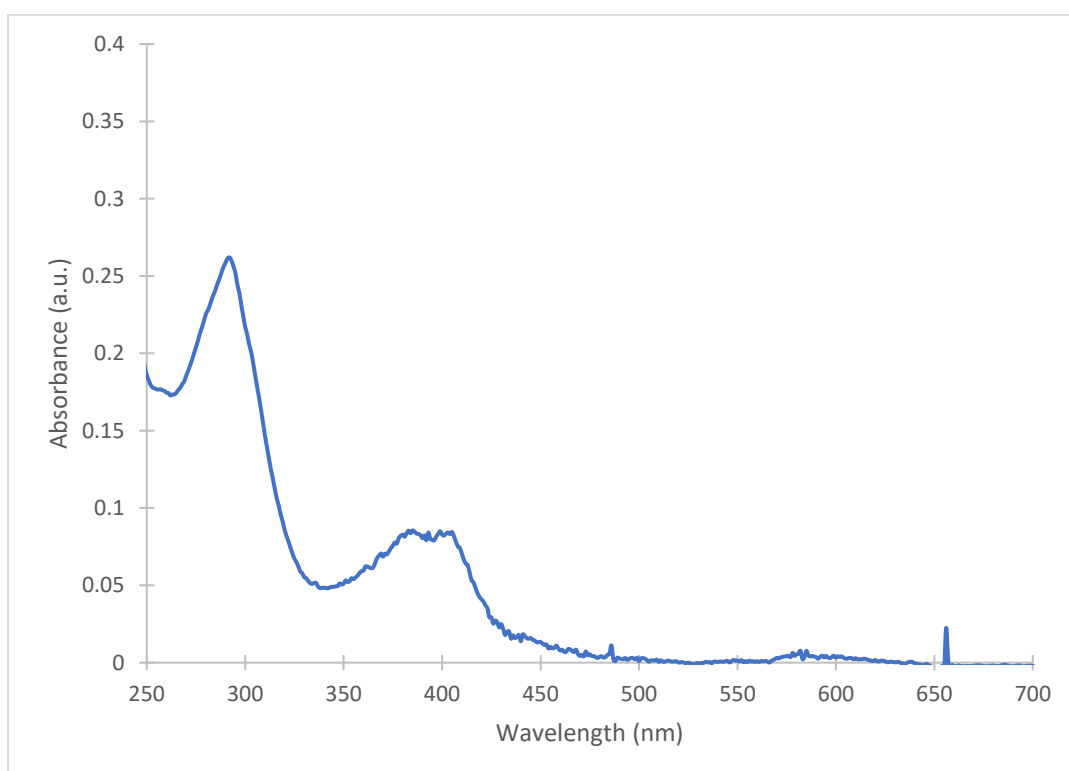


Figure S100. Absorption spectrum of compound **1h**.

Emission spectrum of quinolizinium compounds

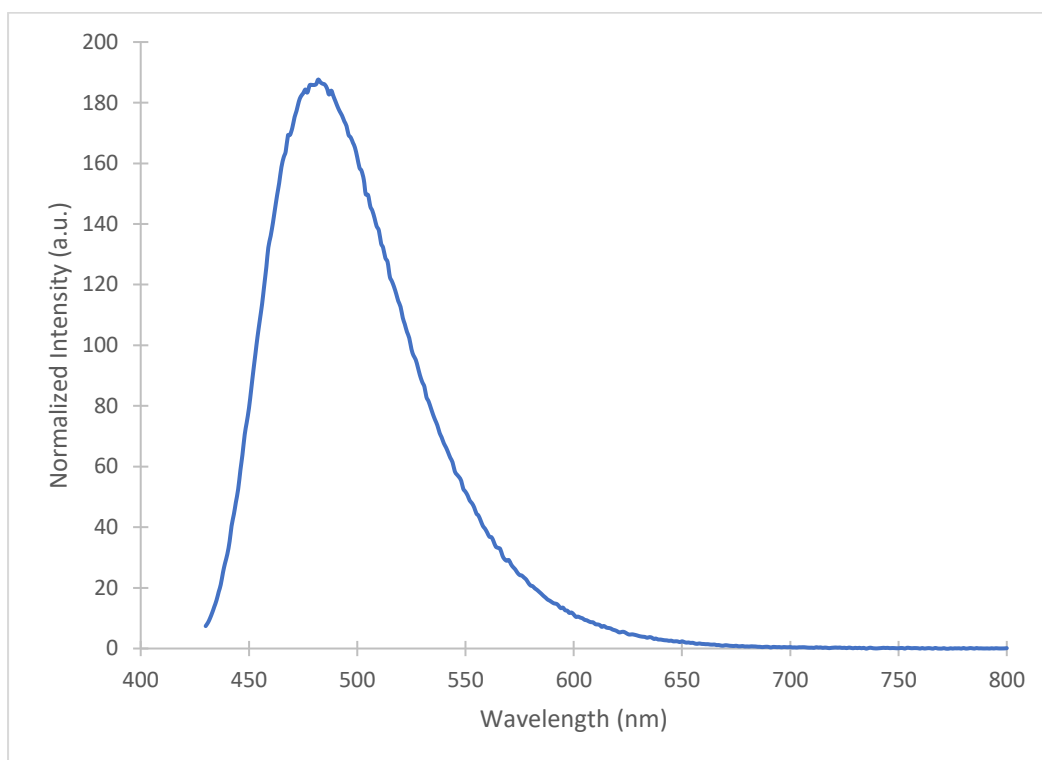


Figure S101. Emission spectrum of compound **1a**.

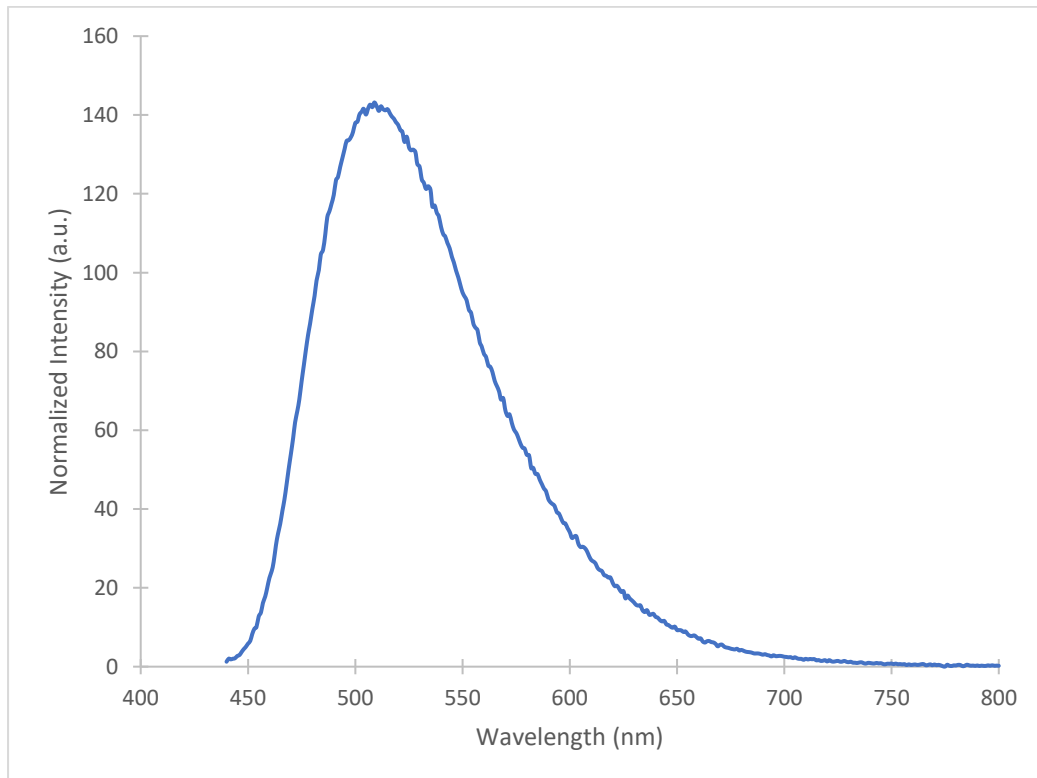


Figure S102. Emission spectrum of compound **1b**.

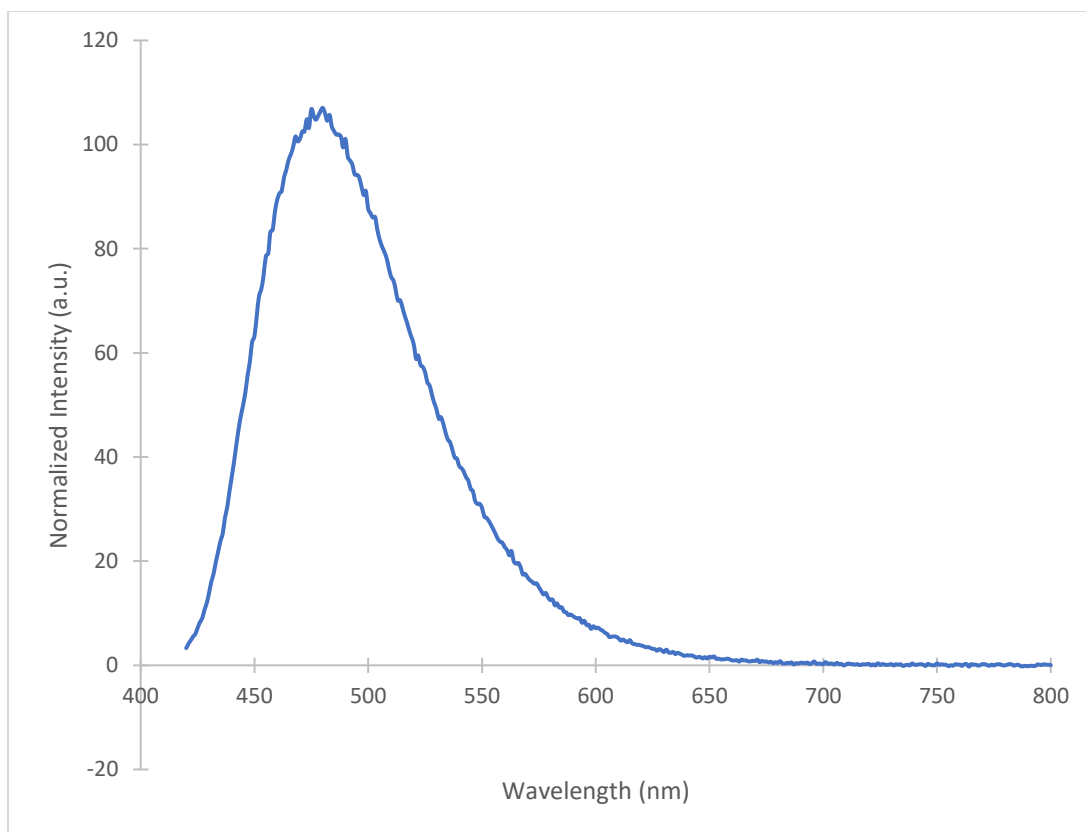


Figure S103. Emission spectrum of compound 1c.

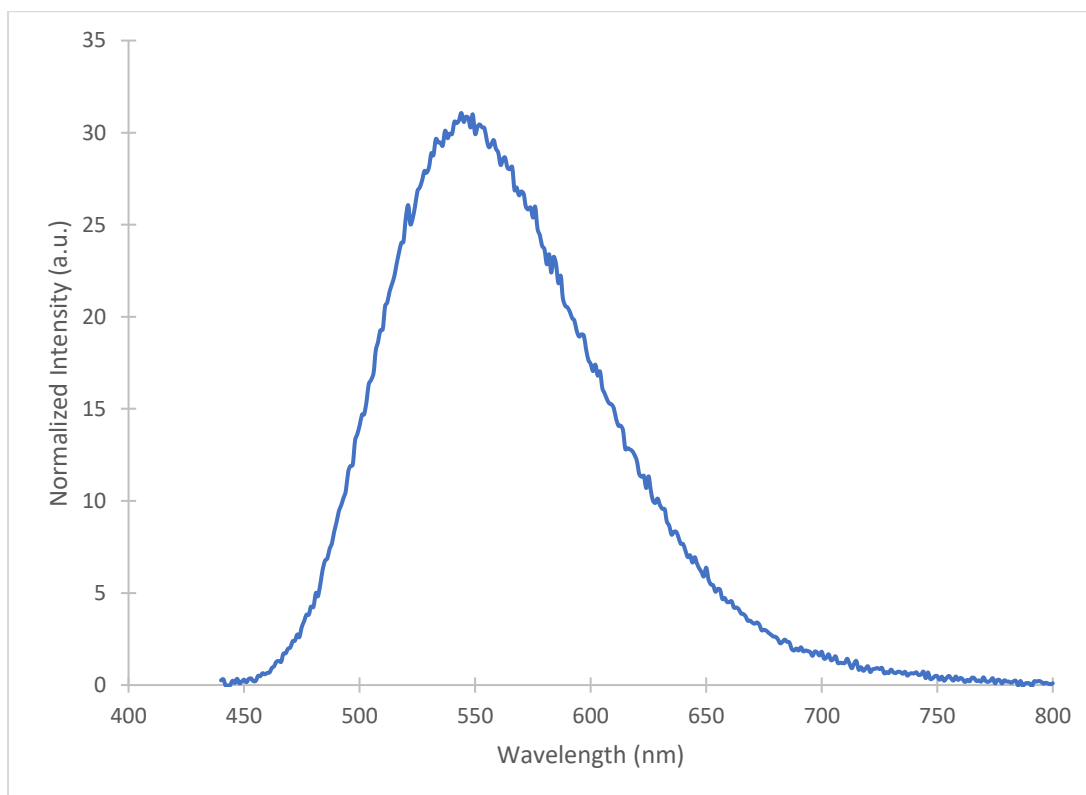


Figure S104. Emission spectrum of compound 1d.

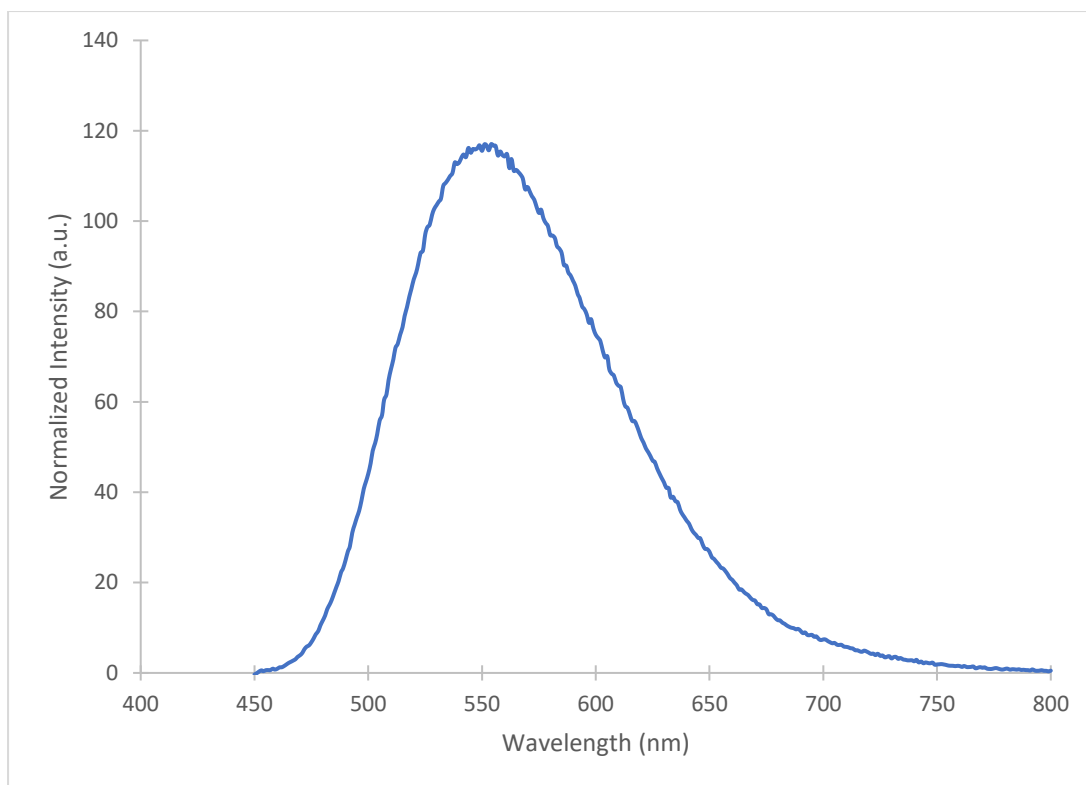


Figure S105. Emission spectrum of compound **1e**.

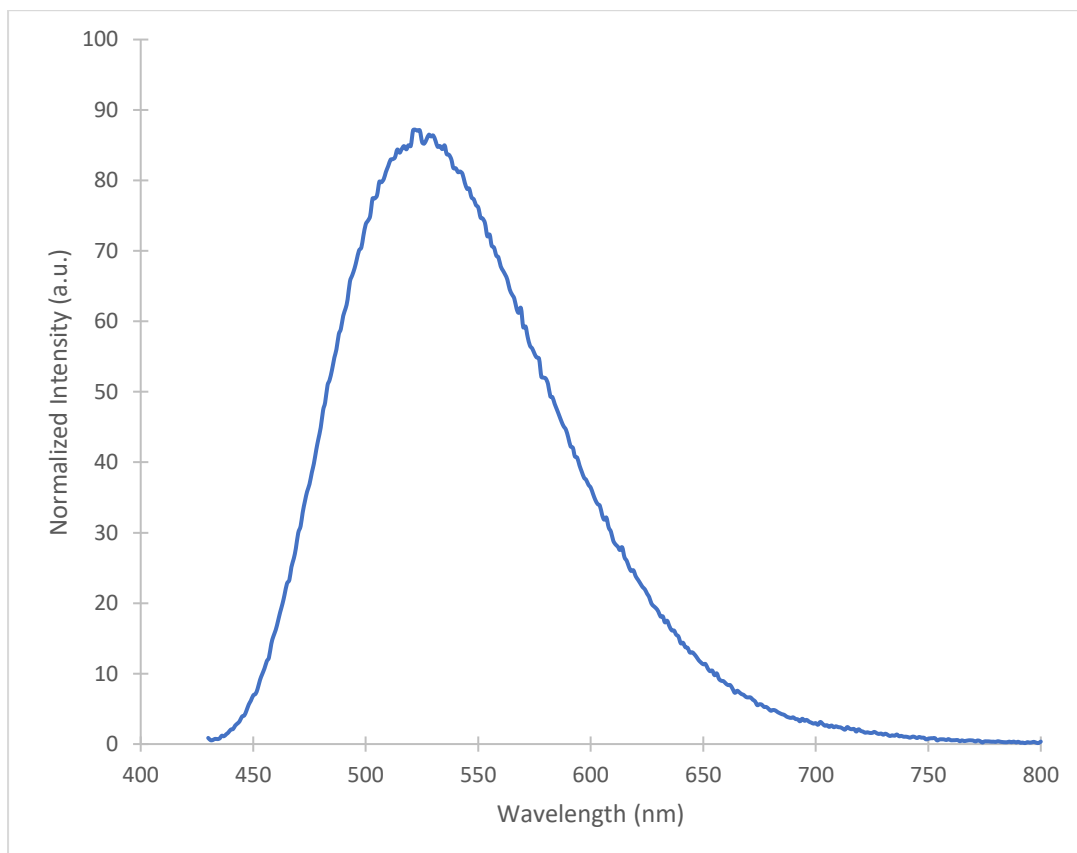


Figure S106. Emission spectrum of compound **1f**.

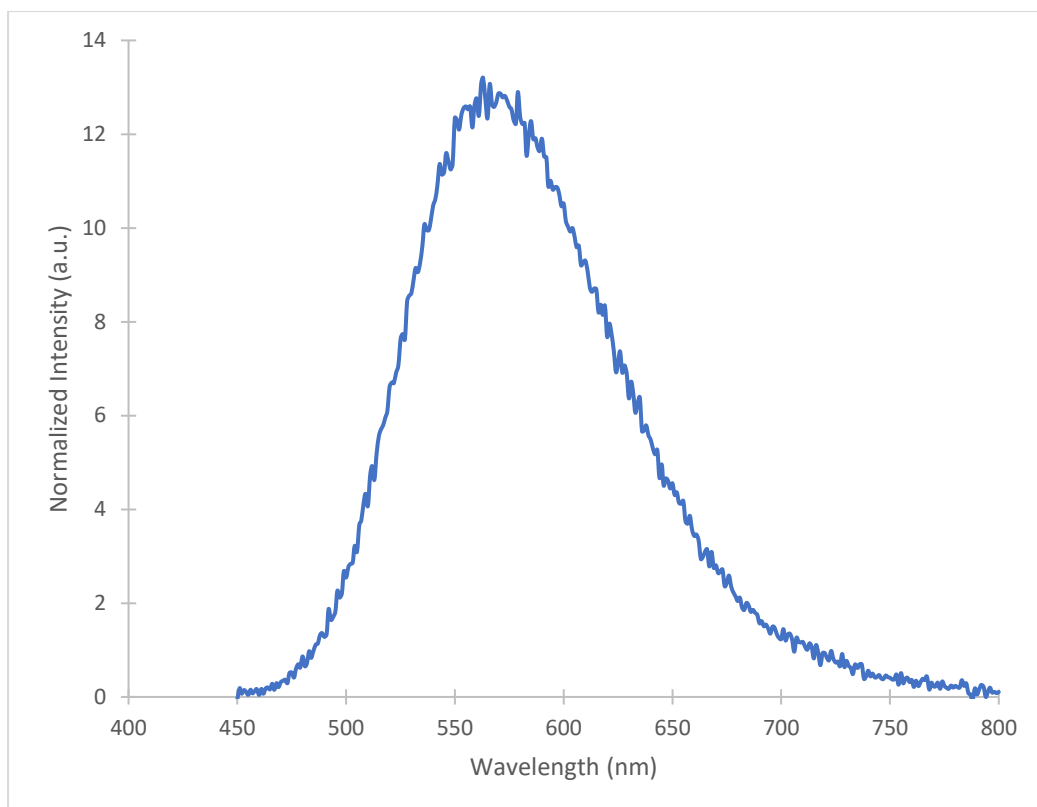


Figure S107. Emission spectrum of compound **1g**.

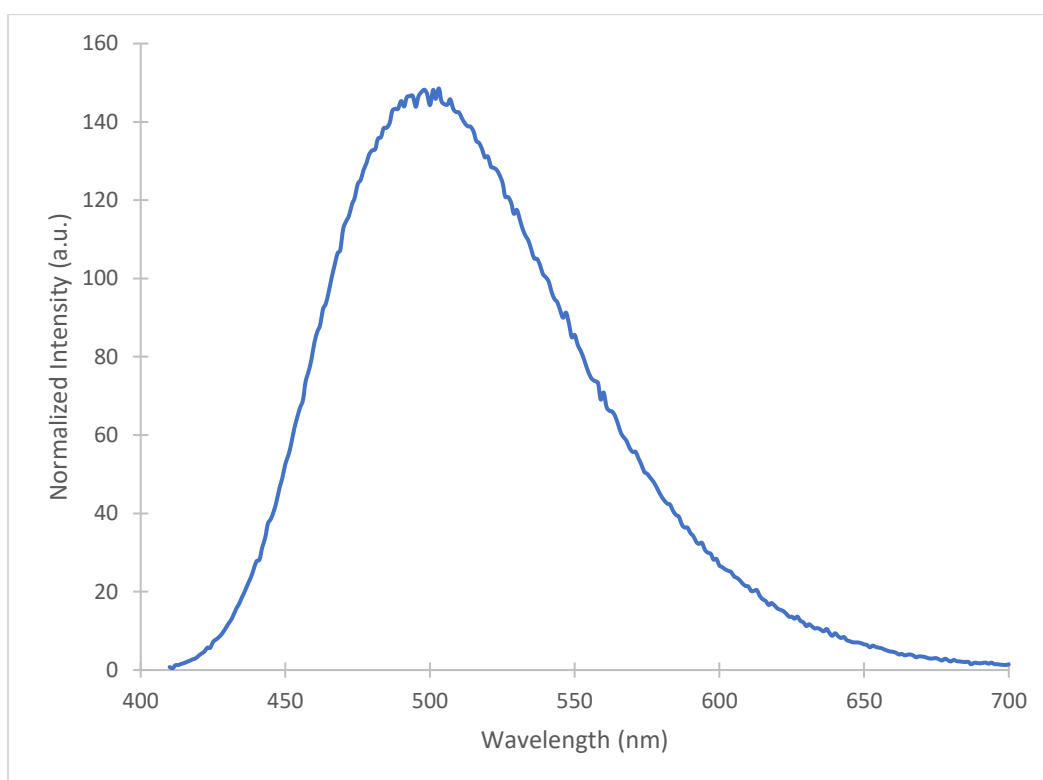


Figure S108. Emission spectrum of compound **1h**.

Supplementary References

1. J.-R. Deng, W.-C. Chan, N. Chun-Him Lai, B. Yang, C.-S. Tsang, B. Chi-Bun Ko, S. Lai-Fung Chan and M.-K. Wong, *Chem. Sci.*, 2017, **8**, 7537-7544.
2. For selected examples, see (a) L. Purushottam, S. R. Adusumalli, U. Singh, V. B. Unnikrishnan, D. G. Rawale, M. Gujrati, *et al. Nat. Commun.*, 2019, **10**, 2539. (b) J. Willwacher, R. Raj, S. Mohammed and B. G. Davis, *J. Am. Chem. Soc.*, 2016, **138**, 8678-8681. (c) P. Dai, C. Zhang, M. Welborn, J. J. Shepherd, T. Zhu, T. Van Voorhis, *et al. ACS Cent. Sci.*, 2016, **2**, 637-646. (d) Y. A. Lin, J. M. Chalker and B. G. Davis, *J. Am. Chem. Soc.*, 2010, **132**, 16805-16811.
3. K. Rurack and M. Spieles, *Anal. Chem.*, 2011, **83**, 1232-1242.
4. (a) M. Kleinova, O. Belgacem, K. Pock, A. Rizzi, A. Buchacher and G. Allmaier, *Rapid Commun. Mass Spectrom.* 2005, **19**, 2965–2973; (b) A. Pratesi, D. Cirri, D. Fregona, G. Ferraro, A. Giorgio, A. Merlino and L. Messori, *Inorg. Chem.*, 2019, **58**, 10616–10619.
5. Y. C. Leung, W. Lo, Site-directed pegylation of arginases and the use thereof as anti-cancer and anti-viral agents, U.S. Patent 8507245B2, Aug 13, 2013.
6. S.-F. Chung, C.-F. Kim, S.-Y. Tam, M.-C. Choi, P.-K. So, K.-Y. Wong, Y.-C. Leung and W.-H. Lo, *Appl. Microbiol. Biotechnol.*, 2020, **104**, 3921-3934.